Shape Optimization Design of Arch Type Dams under Uncertainties

DISSERTATION

Zur Erlangung des akademischen Grades eines
Doktor-Ingenieur
an der Fakultät Bauingenieurwesen
der Bauhaus-Universität Weimar

vorgelegt von

Tan, Fengjie

aus Gansu, V.R. China

Mentor: Prof. Dr. rer. nat. Tom Lahmer

Weimar, October 2018

This is dedicated to my parents, who love me, believe in me, inspire me and have supported me every step of the way.

Acknowledgements

I am grateful to my supervisor, Prof. Dr. rer. nat. Tom Lahmer and from Institute of Structure Mechanics (ISM), Bauhaus-Universität Weimar for giving me a valuable opportunity to work with him and to gain broad experience through the four years researching, and for his valuable support , encouraging advice and patience throughout the program. I consider myself fortunate to work under his supervision. Also I 'd like to thank Prof. Witt and Prof. Zhuang for their kind help on the reporting.

I have been so fortunate to have my parents, and deeply grateful for their unchanging love, support, and encouragement. I want to express my deep thanks to them.

Thanks are also due to many colleagues in our institute throughout the program for their valuable company and help.

I also want to acknowledge the financial support through all years for my studies and researches from „China Scholarship Council“ .

Finally, I would like to express my gratitude to all my friends for all the help and cares bringing me back from the edge of breaking down.

Abstract

Due to an increased need for hydro-electricity, water storage, and flood protection, it is assumed that a series of new dams will be built throughout the world. Comparing existing design methodologies for arch-type dams, model-based shape optimization can effectively reduce construction costs and leverage the properties of construction materials. To apply the means of shape optimization, suitable variables need to be chosen to formulate the objective function, which is the volume of the arch dam here. In order to increase the consistency with practical conditions, a great number of geometrical and behavioral constraints are included in the mathematical model. An optimization method, namely Genetic Algorithm is adopted which allows a global search.

Traditional optimization techniques are realized based on a deterministic approach, which means that the material properties and loading conditions are assumed to be fixed values. As a result, the real-world structures that are optimized by these approaches suffer from uncertainties that one needs to be aware of. Hence, in any optimization process for arch dams, it is necessary to find a methodology that is capable of considering the influences of uncertainties and generating a solution which is robust enough against the uncertainties.

The focus of this thesis is the formulation and the numerical method for the optimization of the arch dam under the uncertainties. The two main models, the probabilistic model, and non-probabilistic models are introduced and discussed. Classic procedures of probabilistic approaches under uncertainties, such as RDO (robust design optimization) and RBDO (reliability-based design optimization), are in general computationally expensive and rely on estimates of the system's response variance and failure probabilities. Instead, the robust optimization (RO) method which is based on the non-probabilistic model, will not follow a full probabilistic approach but works with pre-defined confidence levels. This leads to a bi-level optimization program where the volume of the dam is optimized under the worst combination of the uncertain parameters. By this, robust and reliable designs are obtained and the result is independent of any assumptions on stochastic properties of the random variables in the model.

The optimization of an arch-type dam is realized here by a robust optimization method under load uncertainty, where hydraulic and thermal loads are considered. The load uncertainty is modeled as an ellipsoidal expression. Comparing with any traditional deterministic optimization (DO) method, which only concerns the minimum objective value and offers a solution candidate close to limit-states, the RO method provides a robust solution against uncertainties.

All the above mentioned methods are applied to the optimization of the arch dam to compare with the optimal design with DO methods. The results are compared and analyzed to discuss the advantages and drawbacks of each method.

In order to reduce the computational cost, a ranking strategy and an approximation model are further involved to do a preliminary screening. By means of these, the robust design can generate an improved arch dam structure which ensures both safety and serviceability during its lifetime.

Zusammenfassung

Aufgrund des erhöhten Bedarfs an Wasserkraft, Wasserspeicherung und Hochwasserschutz wird davon ausgegangen, dass weltweit eine Reihe neuer Staudämme gebaut werden. Vergleicht man bestehende Entwurfsmethoden für Staudämme vom Bogentyp, kann die modellbasierte Formoptimierung effektiv die Konstruktionskosten reduzieren und besser die Eigenschaften von Baumaterialien nutzen. Um die Algorithmen der Formoptimierung anzuwenden, müssen geeignete Variablen gewählt werden, um einerseits eine Zielfunktion zu formulieren, hier das Volumen der Bogenstaumauer, andererseits Parameter gefunden werden, die eine flexible Beschreibung der Bauform zulassen.

Um die Übereinstimmung mit den praktischen Bedingungen zu erhöhen, sind ferner im mathematischen Modell und der Optimierung eine große Anzahl von geometrischen und Verhaltensbeschränkungen enthalten. Für das resultierende nicht-lineare, nicht-konvexe und restringierte Optimierungsproblem wird eine globale Optimierungs-methode (ein genetischer Algorithmus) vorgeschlagen.

Herkömmliche Optimierungstechniken werden auf der Grundlage eines deterministischen Ansatzes realisiert, was bedeutet, dass die Materialeigenschaften und die Belastungsbedingungen als feste und bekannte Werte angenommen werden. Infolgedessen leiden die realen Strukturen, die durch diese Ansätze optimiert werden, unter Effekten von Unsicherheiten, welches impliziert, dass die strukturelle Zuverlässigkeit mitunter nicht garantiert ist. Daher ist es bei jedem Optimierungsprozess für Bogenstaumauern notwendig, eine Methodik zu finden, die in der Lage ist, die Einflüsse von Unsicherheiten zu berücksichtigen und eine Lösung zu entwickeln, die robust gegen natürliche Streuungen in Lasten sowie Materialkennwerten ist.

Der Schwerpunkt dieser Arbeit liegt daher in der Formulierung und der numerischen Optimierung einer Bogenstaumauer unter Unsicherheiten. Verschiedene Ansätze, mit den Unsicherheiten umzugehen, werden dabei vorgestellt, analysiert und miteinander verglichen. Die beiden Hauptmodelle, ein probabilistisches Modell und ein nicht-probabilistisches Modell werden vorgestellt und diskutiert. Klassische Verfahren der probabilistischen Optimierungen unter Unsicherheiten wie RDO (Robust-Design-Optimierung) und RBDO (Zuverlässigkeits-basierte Designoptimierung)

sind im Allgemeinen rechenintensiv und beruhen auf Schätzungen der Antwortvarianz und Ausfallwahrscheinlichkeiten des Systems. Stattdessen wird als Alternative die robuste Optimierungsmethode (RO), die auf einem nicht-probabilistischen Konzept basiert und mit vordefinierten Konfidenzniveaus arbeitet, vorgeschlagen. Dies führt zu einem zweistufigen Optimierungsprogramm, bei dem das Volumen der Staumauer unter der ungünstigsten Kombination der unsicheren Parameter optimiert wird. Dadurch werden robuste und zuverlässige Designs erhalten, und das Ergebnis ist unabhängig bezüglich zu treffender Annahmen über stochastische Eigenschaften der Zufallsvariablen im Modell. Die Optimierung eines bogenförmigen Staudamms wird hier durch eine robuste Optimierungsmethode unter Lastunsicherheit, bei der hydraulische und thermische Belastungen berücksichtigt werden, realisiert.

Im Vergleich zu einer traditionellen deterministischen Optimierungsmethode (DO), die nur den minimalen Zielwert betrifft und einen Lösungskandidaten in der Nähe von Grenzzuständen bietet, liefern die RDO, die RBDO und RO-Methode robuste Lösung bezüglich Unsicherheiten.

Obwohl alle drei unsicherheits-orientierten Methoden zunächst ein Ziel haben, die Zuverlässigkeit der Strukturen zu erhöhen, ergeben sich in den Wegen zu den finalen Designs und den berechneten Formen Unterschiede, die in der Arbeit verglichen und analysiert werden, um die Vor- und Nachteile jeder Methode herauszuarbeiten.

Um den Rechenaufwand zu reduzieren, sind eine Rangfolgestrategie und ein Approximationsmodell erforderlich. Dadurch kann die robuste Konstruktion effizient eine verbesserte Bogenstaumauer erzeugen, die während ihrer Lebensdauer sowohl Sicherheit als auch eine höhere Wartungsfreundlichkeit gewährleistet.

Contents

List of Figures

LIST OF FIGURES

List of Tables

Nomenclature

Symbol	Description
α, β_1, β_2	Coefficients to decide the shape of dam's vertical section
t_1, t_2, t_3	The thickness of dam's central vertical section
ϕ	Central angle of arch dam
a	Coefficient to decide the dam's horizontal arc curves
$g_i(x)$	Constraints
s	Overhang degree
K_i	Sliding resistance
$(x_g, y_g, z_g)^T$	Global coordinates for Isoparametric solid elements
$(\xi_l, \eta_l, \zeta_l)^T$	Local coordinates for Isoparametric solid elements
σ	Stress
ε	Strain
u	Nodal displacements vector
$[N]$	Shape matrix
$[B]$	Transform matrix
$[k_g]$	Elemental stiffness
$[K_g]$	Global structural stiffness
$[J]$	Jaccobi matrix
$[D]$	Elastic matrix
$\{P_g\}$	Nodal force vector
q_x, q_y, q_z	The heat flow through the unit area
k_{xx}, k_{yy}, k_{zz}	Thermal conductivity
T	Temperature
ρ_s	Density of material
c	Specific heat
Q_{in}	Inner heat generation
S_1	Dirichlet boundary
S_2	Thermal boundary between dam surface and air
$\{n_x, n_y, n_z\}$	Outward normal vector of boundary surface
β_{T_c}	Convection coefficient
γ_j	Coefficient to decide the trend type of Kriging metalmodel
$Z(\mu(x), R(x, x^{'}, \theta)$	A stochastic process with zero mean
μ	Mean value
$R(x, x^{'}, \theta)$	Correlation function for the stochastic process
θ	Correlation length
F_X	Cumulative distribution function
f_X	Probability density function
ρ_{XY}	Correlation coefficient between random variables X and Y

$COV[X,Y]$	The co-variance of random variables X and Y
I_1	The first invariant of the Cauchy stress
J_2	The second invariant of the Cauchy stress
J_3	The third invariant of the Cauchy stress
β_r	Reliability index
P_f	Failure probability
$\Phi(\cdot)$	Standard normal cumulative distribution function
$[H]$	Hessian matrix
MMP	The most probable point
G	The vector contains the limit function responses corresponding to experimental design
α_w	Weighting factor
ξ	Uncertain parameters (only used in chapter 4)
κ	A parameter having the definition that $0 \leq \kappa \leq 1$
r	Radius for Euclidean ball
x_c	The center point of the Euclidean ball
$[P]$	The matrix determines the distance between ellipsoid's boundary and the center x_c
$\mathbf{U}$	Uncertain data set
$\mathbf{C}$	Convex set
S_+^n	Symmetric positive semi-definite matrix
S^n	Symmetric matrix
B_h	The shape matrix of the ellipsoid
$L(\cdot)$	Lagrange duality
$g_X(x)$	Limit Function
μ_X	Mean value of random variables vector X
σ_X	Standard deviation of random variables vector X
ε	Random experimental error assumed to have zero mean
$I_g(x)$	An indicator function which is equal to 1 if $g_X(x) \leq 0$ and other wise equal to 0
p_0	The nominal value of applied load vector

Chapter 1

Introduction

1.1 Motivation

The historical development of arch dams progressed through the following five periods: the Roman arch dams (1st centuries BC and AD), the Mongol dams (14 and 15th centuries), some advanced masonry dams in the early 19th century, the Austrailan concrete arch dams (1880-1896) and the modern arch dams at the beginning of the 20th century ([4]). Generally, the modern arch dam is made of concrete and placed in a "V"-shaped valley. To efficiently carry the loads, arch dams are shaped to carry the loads in a relatively smooth and uniform manner consisting of smooth upstream and downstream curves without corners. The shape of arch dams has changed from shapes that look more like thin gravity dams with straight segments for the upstream and downstream faces to curved upstream and downstream faces to minimize cantilever tensile stresses.

The structure of the arch dam utilizes the upstream curvature to transfer the water pressure to both sides of the valley. At the same time, the water pressure presses against the arch, compressing and strengthening the structure. These particular characteristics make the arch dam thinner than any other type of dam, and more economically and practically fit for those projects with high demands on a dam's height. Consequently, choosing an appropriate dam design has significant influence on the economy and safety of the arch dam.

Traditionally, the design of an arch dam is realized by trial and error. To obtain a better shape, the designer should select several alternative schemes with various patterns and modify them to obtain a number of feasible shapes. The best shape, satisfying the demands of the design specifications, is selected as a final design. The results, however, are not necessarily optimal even after a long time of analysis and calculation. A

huge advancement came with the invention of shape optimization techniques. These techniques not only provide a more accurate design with improved efficiency but also substantially reduce the amount of construction material required.

The use of efficient optimization tools leads to a higher quality of product and improved functionality. Most of the design results are realized through deterministic optimization techniques. However, it is known that uncertainties exist in engineering systems due to variations which cannot be determined. The task of identifying these uncertainties during optimization has increasingly received extensive attention. Compared to conventional deterministic design methods, which only consider the nominal values of parameters neglecting the uncertainties involved in the structural system, the methods considering uncertainties have advantages in prolonging the structural service life and reducing the maintenance costs.

The methods that take the parameter uncertainties into optimization have been developed in the last decades. They are basically classified into two kinds of models: Probabilistic model and non-probabilistic model. For the probabilistic model, the uncertain data are assumed to be random obeying a known or a partially known probability distribution. The corresponding optimization problems concern the generations of the optimized results under the probability constraints evaluated by the reliability analysis,(often referred as the reliability-based optimization (RBDO)) ([5],[6],[7]), or aim at minimizing the variations of structural performance (often known as robust design optimization (RDO)) ([8,9,10]) .

In contrast, the method based on the non-probabilistic model, also named as the robust optimization (RO) ([11],[2]), considers the uncertainty as a parameter within an uncertain data set **U**. The RO method focuses on searching out an optimal design candidate relatively insensible to the uncertainty data set. If the uncertainties existing in the structural system can be well considered, the acquired arch dam design not only reduces the materials required but also increases the lifespan of the structure.

The traditional research dealing with data uncertainty in optimization is sensitivity analysis; Taguchi ([12]) introduced the concept of parameter design which is to reduce variation in performance by reducing the sensitivity of engineering designs to sources of variation rather than controlling the sources. Fiacco ([13]) and Sobieski ([14]) *et al.* provided methods for evaluating sensitivities of optimal objective function and optimal design to changes in design variables and parameters that were kept constant during optimization. Beltracchi and Gabriele ([15]) presented a method based on recursive quadratic programming to estimate sensitivity without having to evaluate the second deviation of the objective function.

In recent years, there is a burst of application of RO into structural optimization, such as Sun *et al.* ([16]) described a design in sheet metal forming using robust optimization, Kanno ([17]) and Guo ([18]) realized a bar truss structure's optimization under uncertainties with RO methods. More works on the applications of the RO method can be found in ([19,20,21]).

1.2 Literature Review

1.2.1 General Optimization of Arch Dams

Extraordinary efforts on arch dam optimization have begun from the late 1960's. There are several reasons for the prosperous application of optimization methods into arch dam design. Firstly, the reduction of weight is essential for arch dam design, and various design conditions can be involved as design constraints during the optimization process. Secondly, the finite element method can be exploited in structural optimization, the analysis of structural performance can be evaluated precisely and efficiently.

In the early research investigation of arch dams ([22]), it mainly focused on dealing with membrane-type solutions only concerning a single, simple loading condition. Based on this assumption, the acquired structure was venerable to resist against the real-world loading environment. Later, Rajan ([23]); Mohr ([24]) *et al.* considerably developed membrane shell theory-based solutions. When Sharpe ([25]) first proposed the mathematical programming of the optimization problems, the Finite Element Method (FEM) ([26,27]) was introduced to analyze the structural stress state, and sequential linear programming method was involved in searching for the optimum shape design of an arch dam under static loads.

In the optimization, the arch dam is described by three-dimensional 8-node isoparametric hyper-elements, the design variables are the geometrical parameters of these elements, and the objective function is the dam volume. Other similar works are mentioned in ([28]) based on the neural network approach to the definition of near-optimal arch dam shape. Nevertheless, one of the most critical investigations in the field of shape optimization of concrete arch dams was carried out by Bofang ([29,30]) *et al.* since the middle 1970's. The geometrical model used by Bofang is a continuous, rational and practical model and thus could draw the interests of many researchers. It is the basis of the majority of later works in the field of shape optimization of arch dams.

Mathematical models for both single curve and multi-curves are developed to find out

the optimum designs of arch dams at the given boundary conditions and constraints. Later, with the development of heuristic algorithms ([31]),such as genetic algorithm (GA) ([32]), particle swarm optimization (PSO) ([33]), Honey-bee mating optimization (HBMO) ([34]) etc., it became popular to use these new methodologies in the optimization of arch dams to obtain the optimum designs ([35,36]). However, heuristic algorithms are computationally less efficient in comparison to the gradient-based methods, which provide the possibility to find global optimum solutions.

1.2.2 Realiability-Based Design Optimization (RBDO) Method

By 1960, the concept of RBDO was applied to structural weight minimization for a specified reliability cost ([37]). The early work of Freudenthal ([38]) and the subsequent development by Ronay and Freudenthal ([39]) provided the reliability bases of structural analysis and design. With these as the foundation, Cornell ([40]) formulated bounds on the reliability of structural systems, and Moses ([41],[42]) *et al.* presented methods for incorporating reliability analysis into the optimization design of a structural system. With the development of computer science, the reliability analysis was applied to optimization methods. Since 1973, the RBDO method becomes matured and is successfully used in many real-life engineering applications ([7,43,44]).

RBDO involves the evaluation of probabilistic constraints using the reliability index or the performance measure. For acquiring the reliability index, many available techniques, such as Monte Carlo Simulation, first- and second-order reliability methods ([45]) can be used. Hasofer ([46]) developed a commonly used procedure for the calculation of the reliability index. The calculation of the reliability index often require large amounts of evaluations of the limit state functions. To solve the computation problem caused by the evaluation amounts, Bucher ([47]) proposed a response surface model (RSM) to represent the system behavior. Based on the theory of response surface, Liu and Mose ([48]) developed a reliability analysis program for aircraft structural systems combined the sequential RSM with Monte Carlo importance sampling. Liaw and Devries ([49]) described a reliability-based optimal design process by integrating reliability and variability analyses with design optimization.

1.2.3 Robust Design Optimization (RDO) Method

The robust design optimization method is to reduce the variability of structural performance caused by regular fluctuations rather than of the safety in the extreme events.

This character makes the design candidates less sensitive to the variation of the design parameters. This method has been succeeded applied to all kinds of structural designs considering uncertainties. With the introduction of the multi-objective function, which is composed of mean and standard deviation of the objective function due to variations ([50]), both objective formulations of robust design and constraints are defined, and the framework is developed.

Modeling the robust design optimization and the application are widely studied, as a consequence of the increased power of computation brought by computers. A lot of successful applications of the RDO methods can be found in the literature from ([8,9,51]). In general, the RDO is an issue related to how to better model a design's performance with stochastic data models when making trade-offs between the mean value and variance attributes.

1.2.4 Robust Optimization (RO) Method

Stochastic problems are often very complicated, requiring overly simplistic assumptions in order to obtain a closed form of solutions. It is particularly true of many engineering problems, where we cannot get enough information to build a precise stochastic model. Hence, the robust optimization based on non-probabilistic models should be developed to satisfy this requirement.

The first work to consider the robust programming goes back to 1970s ([52]). In next subsequent decades, Taguchi ([53]) described the concept of robust design, which is a method for improving the quality of a problem through minimizing the effect of the causes of variation, ignoring the causes. As a non-probabilistic but bounded uncertainty model, Ben-Haim ([54]) established the convex approach. Pantelides and Ganzerli ([55]) applied this method to the robust optimization of a truss structure under stress, displacements, and buckling constraints. Elishakoff ([56]) proposed a methodology for structure optimization under uncertainties but with interval bounded load, and the problem is solved by checking the vertices of the load-uncertainty domain. Lombardi ([57]) used a two-step technique for non-probabilistic robust optimization of truss structures.

Since 2000, the RO area revived the development of theory and applications. Ben-Tal and Nemirovski ([19]) contributed to the development of a unified methodology of the robust counterpart of a broader class of convex optimization problems and applied it to the truss structure. Calafiore ([58]) proposed a method for finding the ellipsoid bound of the solution set of uncertain linear equations. Other efforts on the applications of the RO method could be seen in the works: Sun and Li *et al.* ([16]) described a design

in sheet metal forming using robust optimization, Kanno and Takewaki ([17]) developed a sequential semidefinite program to do robust design of truss structures under load uncertainty, and Guo *et al.* ([18]) realized a bar truss structure's optimization under uncertainties with a proposed confidence formulation, etc.

1.2.5 Techniques Used in Optimization Procedure

1.2.5.1 Metamodel Approach

The simulation for the optimization of arch dams concerning the uncertainties is a computationally expensive program, and it becomes impractical to rely exclusively on simulation codes for design optimization. A superior choice is to use the approximation models, also referred to metamodels, to save the total amount of simulation time by reducing the number of FEM simulations.

Lots of studies have been conducted on the application of various metamodeling techniques. Jin *et al.* ([59]) used multiple modeling criteria and multiple test problems to test the metamodels, Sherali ([7]) and Lee ([60]) provided the proofs that the Kriging metamodeling technique was considered to be a more suitable approximation model. Jin ([59]) applied and compared various metamodels on the application and accuracy for the optimization under uncertainties. The results showed that metamodeling techniques offered a promising method for the optimization under uncertainties.

1.2.5.2 Adaptive Kriging Monte Carlo Simulation (AK-MCS)

For the RBDO method, the reliability analysis is especially crucial during the optimization using this method. According to ([59]), Kriging as metamodeling technique is considered to be a more suitable approximation method than the response surface method since the former methods can provide a more accurate prediction. In this research work, the adaptive built Kriging metamodel combined with Monte Carlo simulation is adopted to complete the reliability analysis ([61]).

This method is known as adaptive Kriging Monte Carlo simulation (AK-MCS) ([62]). The process of AK-MCS is summarized as: Firstly use Kriging metamodel to predict the value of the limit-state function with the experimental design samples. Then, an adaptive experimental design is introduced to increase the accuracy of the surrogate model. Finally, the Monte Carlo method is applied to evaluate the failure probability.

1.3 Objectives of the Dissertation

The goal of the shape optimization of an arch dam is to search for an economical, robust and reliable design. Through the literature survey, it can be seen that limitations and drawbacks are existing in the previous work. Therefore, there is a potential to improve some of them. As mentioned above, the commonly used optimization design is a deterministic optimization procedure without considering the uncertainties existing in the structural analysis system, such as material properties, loading conditions, and construction procedure, *etc*.

Reviewing of the available literatures on the optimization techniques, the goal of this work is to conduct an in-depth analysis of applying existing techniques to the optimization of the arch dams under uncertainties, and compare these methods with deterministic optimization methods through comparing the acquired optimized designs. Through this research, the following objectives are expected as:

1. Reducing the computational cost

    - The optimization procedure is performed based on a large structure with complex mechanical properties. The shape optimization itself for such a big project is a computationally expensive challenge. If the uncertainties are involved in the optimization procedure, even higher demand for computational cost is required. It is because the evaluations of both the objective function and constraints are more costly under uncertain conditions. An appropriate and efficient technique for coping with uncertainties in the optimization procedure should, therefore, be used.

    - A ranking strategy and approximation model are involved in the shape optimization procedure to do a preliminary screening. The Kriging Metamodel will be adapted to approximate the volume of the arch dam and the tensile stress at the point in the structure where possibly suffered the maximum tensile stresses.

2. The optimization under uncertainties with probabilistic model

- One optimization approach of the probabilistic model under uncertainties used in this work is the RBDO method with predefined distributions of uncertainties, and the realization procedure will be proposed. The reliability index is involved as a constraint to offer a good judgment on both the prediction and evaluation of the arch dam's safety.

- The success of reliability analyses relies on the accuracy of the modeling. The traditional Monte Carlo simulation can offer a proper evaluation, but it requires a large number of samples to reduce the error of simulation. The Adaptive Kriging Monte Carlo simulation (AK-MCS) will be used to do the reliability analysis.

- The uncertainty is described by probabilistic distribution functions, and the corresponding optimization problem can also be expressed towards minimizing the mean value of the objective function and the variance of the structural responses (Robust design and optimization (RDO). It is also attractive to be a framework for searching out the robust arch dam design candidate.

- The structural responses of both the objective function and implicit constraints must be evaluated by running a computationally expensive FEM calculation. In order to acquire the converge of the optimization algorithm, large numbers of FEM simulations must be performed. Therefore, an efficient methodology should be developed to reduce the costs from FEM simulations.

3. Robust optimization

- The robust optimization method under an unknown-but-bounded uncertainty set uses the framework called worst-case design and optimization. The purpose of the RO method is to minimize the cost of the design while ensuring the safety of the structure under the worst combination of uncertain parameters.

- The traditional approach for the solution of the RO problems cannot guarantee a feasible and global optimal design. A confidence formulation for the robust optimization proposed by Guo *et al.* ([18]) will be adopted to solve the robust optimization of an arch dam.

4. Finally, the comparison of tensile stresses, displacements, and von Mises stresses among DO-, RBDO-, RDO- and RO-model would be performed to see the differences in the optimization considering the uncertainty factors. Also, through the comparison of these optimized arch dam models, we need to know about the advantages and disadvantages of RBDO-, RDO- and RO-model when solving the problems under uncertainties.

1.4 Dissertation Organization

From the previous sections, some key issues that will be addressed in this research are identified through an introduction to the structural optimization under uncertainyies, and the objectives of this work are clarified. The following parts of the dissertation are divided into four chapters.

Chapter 2 begins with the description of the geometry of the arch dam. The shape of an arch dam is determined by central vertical section and the horizontal sections at selected elevations. Altogether with the describing functions of these sections, the design variables are determined. Combined with the FE analysis method, an improved optimization procedure involving ranking strategy and approximation model is formed and applied to do a general shape optimization of an arch dam, which is also called as deterministic optimization of an arch dam.

Chapter 3 realizes the optimization under uncertainties with probabilistic model. There are two kinds of approaches: one is the RBDO method, and the other one is the RDO method. The mathematical models of RBDO and RDO would be introduced first and followed by simple examples to clarify the ideas and differences to solve the optimization problem considering uncertainties with these two different methods. Then, the shape optimal design candidates of the arch dam are acquired through the RBDO and RDO methods, respectively.

Chapter 4 provides a non-probabilistic approach for searching out the feasible optimal design suffering from the uncertainties. Generally, this method is called robust optimization (RO). A confidence semi-defined programming formulation with an unknown-but-bounded uncertainty data set is adopted as a framework to solve the shape optimization of an arch dam under uncertainties. Similar to Chapter 3, a simple mechanical example is tested to show the working procedure of the RO method before the application into searching out the feasible design candidate of an arch dam.

In Chapter 5, the differences of the DO-, RBDO-, RDO-and RO- model are compared to see the influence of uncertainties on arch dam design. A discussion on these different

approaches for the shape optimization of arch dam under uncertainties is given, and the advantages and shortcomings of these approaches are reviewed. Then, the work that has been presented in this dissertation is summarized, and the main contributions of this research are outlined. Finally, some recommendations for future work in this field are suggested.

Chapter 2

General Description of the Shape Optimization of Arch Dams

2.1 Introduction

Shape optimization of an arch dam is a challenging problem due to the nonlinear properties of both objective function and constraints during the optimization process. It is well known that the design of shape has a significant influence on the economy and safety of an arch dam. Traditionally, the design of arch dams is based on engineering experiences and code guidelines. Generally, arch dams are designed by trial and error, that is, an initial shape is given and then analyzed. To get a feasible and better shape, several forms are proposed and analyzed, from which one is selected. The results, however, are not necessarily optimal even after a long time of analysis and calculation.

To improve the efficiency and accuracy of the arch dam design, optimization methods are introduced to find the design candidate. Some progressed achievements have been made in the past years, and methods of shape optimization have been applied with success to many practical arch dams, mainly due to the developments of sophisticated computing techniques and the extensive applications of finite element method.

In this study, the shape optimization problem is studied for an asymmetric arch dam. The Section 2.2.2 gives the description of the shape of the arch dam, then, the Section 2.2.3 and 2.2.1 define the constraints and objective function. The analysis method is the Finite Element (FE) method which is described in Section 2.2.4. In order to improve the optimization efficiency and reduce the computation cost, the approximation model is discussed in Section 2.2.5.1, and then, the optimization procedure is concluded. For demonstration, in Section 2.3, an arch dam model is optimized to see the difference brought by the optimization method to arch dam design.

2.2 General Description of Methods and Models

2.2.1 Objective Function

The purpose of the optimal design is to search out safe, reliable, economical and reasonable shapes of arch dams. In this study, there is no purpose to take all the factors affecting the economics into consideration. The following factors are assumed to be fixed; the height of the dam and the construction material. Now, the objective is to minimize the concrete volume, which will lead to the minimization of excavation cost and concrete material cost.

The objective function of this problem can be expressed as the calculation of the dam's volume with a series of constraints. The corresponding optimization problem can be formulated as follows:

$$\begin{aligned} &\text{minimize:} && f(\mathbf{x}), \quad \mathbf{x} \in \mathbf{R}^n \\ &\text{subject to:} && g_i(\mathbf{x}) \leq 0 \quad (i = 1,2,3,4,\ldots), \\ & && \mathbf{lb} \preceq \mathbf{x} \preceq \mathbf{ub}, \end{aligned} \tag{2.1}$$

where $f(\mathbf{x})$ is the cost function, $g_i(\mathbf{x})$ is the ith constraint, **lb**,**ub** are respectively lower and upper boundaries of $\mathbf{x}$. The vector $\mathbf{x}$ is the design variable vector.

Generally, the objective function of the shape optimization is either defined to ensure minimum stresses of the structure or to ensure the minimum volume of the dam body. In this case, for the shape optimization, the objective function is determined by the minimum volume of the dam. In the coordinate (x,y,z), the function can be written as:

$$f(\mathbf{x}) = \text{Vol}(\mathbf{x}) = \int\int |y_u(x,z) - y_d(x,z)|\, dxdz. \tag{2.2}$$

To tackle the current problem which involves nonlinear constraints and nonlinear objective function, the application of penalty-function method appears to be suitable since it reduces the constrained optimal problem to a simple and convenient unconstrained problem.

Using an exterior penalty formulation, the new unconstrained objective function $\tilde{f}$ reads as follows:

$$\tilde{f}(\mathbf{x}) = f(\mathbf{x}) + \delta_k \sum_{i=1}^{m} [\max 0, g_i(\mathbf{x})]^2. \tag{2.3}$$

Where δ_k is a penalty factor, which can be written as ascending series by increasing iteration number k, and m is the number of constraints.

2.2.2 Design Variables for the Arch Dam

Many factors are influencing the shape of an arch dam, e.g., the mechanical properties of construction materials, the loads acting on the structure or the shape of the valley, where the dam is built. These factors undoubtedly affect the shape of the arch dam and its structural strength and stability. Therefore, proper variables need to be determined to parameterize the dam's shape and to allow a flexible and efficient description of the dam's form.

The shape of the arch dam is determined by the central vertical section and the horizontal sections at selected elevations. There are different ways, such as ([14,22,36]), *etc*., to define the shape of the vertical and horizontal sections: (1) Determine the functions of the upstream and downstream curves; (2) Determine the curves of the upstream boundary and its sectional thickness; (3) Determine the curve function of the central line and the corresponding sectional thickness. In this study, the vertical section is determined by the curve of upstream and the thickness of the section; and the horizontal sections are described by central curves and their thickness at selected elevations. The parameters which determine the shapes are called design variables.

The upstream curve of the vertical section (seen in Fig.2.1(a)) can be determined by a smooth function where polynomials of n-order along the height direction (z coordinate direction as shown in Fig.2.1(a)) has been proven to be a good choice. Polynomials provide a flexible way to represent the shape with a very limited number of variables. The curve for the upstream side can be written setting $n = 3$ by a cubic polynomial $y(z_i) = a_0 + a_1 z_i + a_2 z_i^2 + a_3 z_i^3$ for different heights z_i. Fig.2.1(a) shows few relationships between the height, the upstream curve and resulting coefficients for the structure. According to these relationships, the parameters of the upstream curve can be found by regarding the following equations:

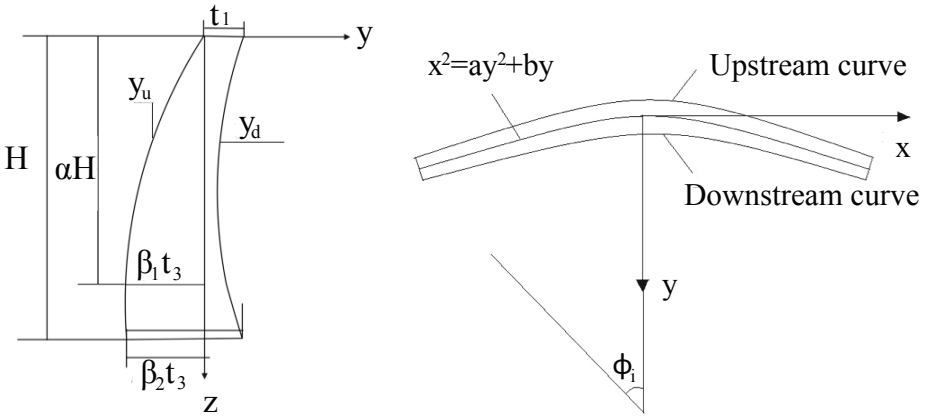

(a) The Central Vertical Section . (b) The Horizontal Section .

Figure 2.1: Description of the Shape of Arch Type Dam.

$$\begin{aligned} y(z_1 = 0) &= 0, \\ y(z_2 = \alpha H) &= -\beta_1 t_3, \\ y(z_3 = H) &= -\beta_2 t_3, \\ \frac{dy}{dz}(z_2 = \alpha H) &= 0. \end{aligned} \tag{2.4}$$

Here t_3 is the bottom thickness of the dams central vertical section; α, β_1, β_2 are coefficients obtained according to the designers' experience, and with these values, the cubic polynomial description of the upstream curve can be acquired. In the same way, the function of the thickness of the central vertical section can be described by $t_c(z_i) = b_0 + b_1 z_i + b2 z_i^2 + b_3 z_i^3$, where parameters are linked as follows:

$$\begin{aligned} t_c(z_1 = 0) &= t_1, \\ t_c(z_2 = \frac{1}{2}H) &= t_2, \\ t_c(z_3 = H) &= t_3, \end{aligned} \tag{2.5}$$

in which, t_1, t_2, t_3 are the thickness of the dam at different heights, here are $0, \frac{1}{2}H, H$.

Generally, the horizontal arch section can be described by upstream and downstream horizontal curves which are expressed respectively in the form of quadratic polynomials. For the sake of simplicity, the center quadratic curve and the dam thickness along

the horizontal direction are used to describe these curves (Fig.2.1(b)). Any quadratic function can be written in the following form:

$$x^2 = ay^2 + by, \tag{2.6}$$
$$\tan\phi = \frac{dy}{dx} = \frac{2x}{\sqrt{4ax^2+b^2}}, \tag{2.7}$$

where the parameter a and central angle ϕ are obtained from the quadratic functions of coordinate z:

$$a_i = \sum_{j=0}^{2} c_j z_i^j \quad i = 1,2,3, \tag{2.8}$$
$$\phi_i = \sum_{j=0}^{2} \gamma_j z_i^j \quad i = 1,2,3. \tag{2.9}$$

The coefficients $c_j, \gamma_j (i = 1,2,3)$ can be derived according to the values of $a_i, \phi_i (i = 1,2,3)$ at control points $(z_1 = 0, z_2 = \frac{1}{2}H, z_3 = H)$.
Based on the above, the design variables are selected and listed in the following vector:

$$\mathbf{x} = [\alpha, \beta_1, \beta_2, t_1, t_2, t_3, \phi_1, \phi_2, \phi_3, a_1, a_2, a_3]^T. \tag{2.10}$$

2.2.3 Constraints

The common causes of failure of arch dams as described in literature and design guidelines are;

1. ultimate stress exceeds allowable strength in structure;
2. overhanging of the structure;
3. sliding of the whole dam section or a monolith;

These factors are of major importance in dam design and must be identified in the design of arch dams to guarantee the structural safety, serviceability, and construction requirements. Hence, the corresponding requirements for these factors are treated as constraints introduced in the design of arch dams, and they are stability constraints, stress constraints, and geometric constraints respectively. According to the article ([30]), the selected constraints $g_i(x)$ used in these research papers are shown as below:

1. **Stress constraint**
   For the assurance of safety condition during lifetime, the maximum stress of an arch dam must be less than the prescribed maximal allowable stress. The stress constraints can be expressed as follows:

$$g_1 = \frac{\sigma_1}{[\sigma_1]} \leq 1, \tag{2.11}$$
$$g_2 = \frac{\sigma_3}{[\sigma_3]} \leq 1. \tag{2.12}$$

   In Eq.2.11 and Eq.2.12, g_i are the constraints, $[\sigma_1], [\sigma_3]$ are respectively the maximum allowable tensile stress and the maximum allowable compressive stress.

2. **Geometric constraint**
   For a conventional construction, the geometrical constraint is generally expressed as the overhang degrees of upstream and downstream, which is represented by s. The principle overhang degree$[s]$ is equal to 0.3 ([30]), and depending on that, the geometrical constraint is written as:

$$g_3 = \frac{s}{[s]} \leq 1, \tag{2.13}$$

   where $[s]$ is the maximum allowable overhang degree.

3. **Slope stability constraint**
   The design for an arch dam must fulfill the requirement of the slope's stability. Consequently, the stability against sliding must be taken into consideration by introducing the coefficients of sliding resistance, which is given by the sliding resistance K_i. The constraint with respect to sliding can be written as:

$$g_4 = \frac{[K_i]}{K_i} \leq 1, \tag{2.14}$$

   where the $[K_i]$ is the minimum allowable value of sliding resistance for the ith point, and K_i is the coefficient of sliding resistance of ith point.

2.2.4 Finite Element (FE) Analysis

2.2.4.1 Finite Element Mesh and Loadings

As illustrated in Fig.2.2, only the dam and foundation meshes are used. The foundation mesh extension in horizontal directions is about the dam height at crest elevation, whereas at the dam bottom it is extended 1.5 times of the dam height. The isoparametric element is selected, and the element used in the analysis is defined by 20 nodes having three degrees of freedom per node. It can tolerate irregular shapes without as much loss of accuracy and have compatible displacement shapes which are well suited to curved model boundaries.

Considering the mesh size has a great influence on the stress responses. Consequently, a series of mesh sizes were tested to find the most useful size with accuracy, but without costing more time by generating too many elements. The von Mises stress variation tendency (Fig.2.3), which was acquired by calculating the maximum and minimum stresses of an arch dam model under mechanical state, shows that the reasonable mesh size for this study of dam models is to divide the dam body into 1536 elements.

Certain loads are accurately predetermined with regard to their distribution and mode of action. In this study, the loads are focused on the dead load and thermal load.

1. **Dead Load**
   The shell structure of a dam body is subjected to the gravity loads, and the action of the water pressure on the upstream face also referred to as the reservoir hydrostatic pressure, is the main destabilizing force acting on the arch dam.

   Another kind of dead loads is the uplift pressure generated from the headwater and tailwater exists through cross sections within the dam at the interface between the dam and foundation. These loads, shown in Fig.2.4, are unavoidable and should be identified as universally applicable and prime importance to all types of dams.

2. **Thermal Load**
   Thermal load is an internal load generated by temperature differences associated with changes in ambient conditions. The cyclic variation of air temperature and solar radiation on the downstream face and the reservoir water temperature on the upstream face affect the distribution of the temperature throughout the dam body, leading to the variations in degrees of expansion. Due to this expansion,

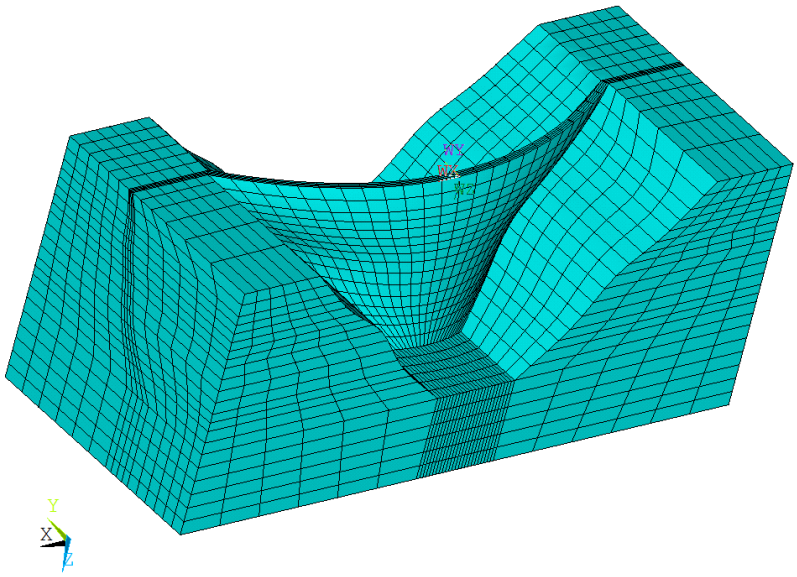

Figure 2.2: Finite Element Mesh Model of the Arch Dam under Study.

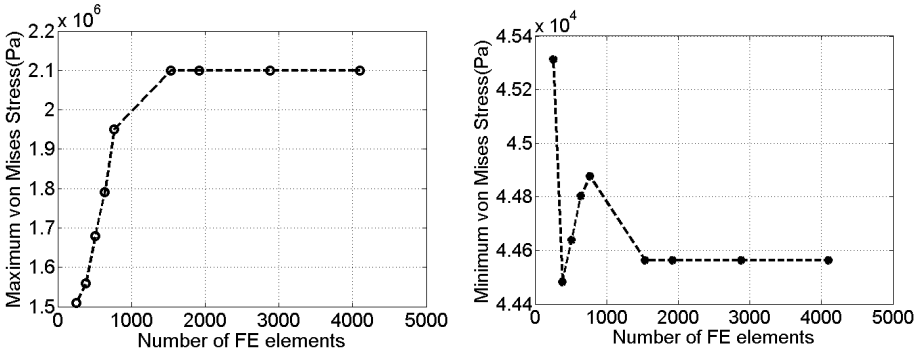

(a) Maximum von Misses Stress Variation Tendency with the Change of Element Number.

(b) Minimum von Misses Stress Variation Tendency with the Change of Element Number.

Figure 2.3: Stress Variation Tendency.

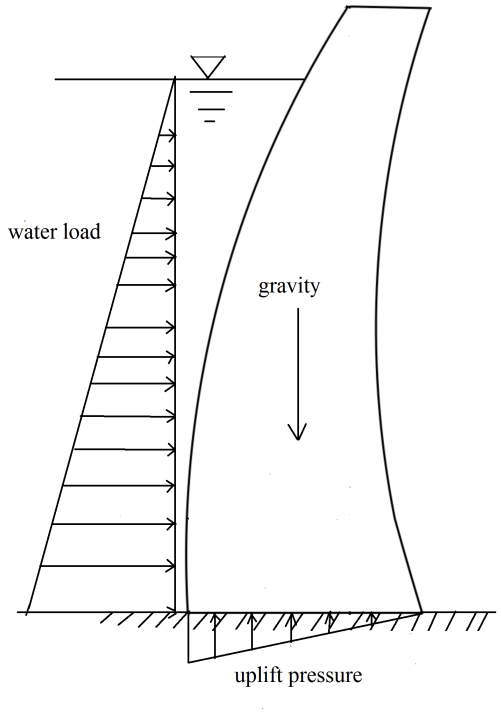

Figure 2.4: Dead Loads Acting on Dams.

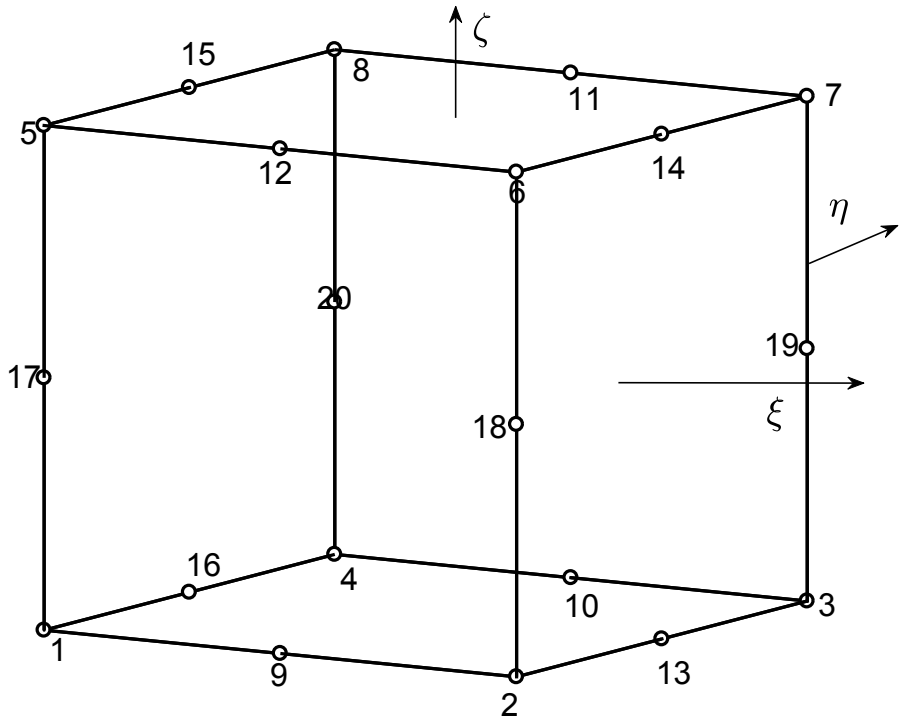

Figure 2.5: 20-node Isoparametric Solid Element.

stresses are generated creating the potential for significant cracking in the dam body. The concerns of cracking are that it affects the durability, stresses state, and the structural safety of the arch dam.

2.2.4.2 Static Stress Analysis with the FE method

To achieve a high degree of accuracy on the calculation of mechanical stress and strain in the three-dimensional arch dam structure by means of a finite element method, the 20-node isoparametric solid element (Fig.2.5) is used for the calculation process. The term 'isoparametric' means that the geometry and displacement fields are specified in parametric form and interpolated with the same functions. The isoparametric formulation allows elements to be created that are nonrectangular and have curved sides.

The arch dam structure is divided into isoparametric elements with Ne nodes for each element, and determined by the coordinates (x, y, z) of the nodes. Unlike the structure body, the isoparametric element is described by non-dimensional local coordinates

$\xi_l, \eta_l, \zeta_l (-1 \leq \xi_l, \eta_l, \zeta_l \leq 1)$. Both coordinates and displacements are interpolated with the same shape functions:

$$\begin{aligned} x &= \sum_{i=1}^{N_e} N_i x_i = N_1 x_1 + N_2 x_2 + \cdots + N_{Ne} x_{N_e}, \\ y &= \sum_{i=1}^{N_e} N_i y_i = N_1 y_1 + N_2 y_2 + \cdots + N_{Ne} y_{N_e}, \\ z &= \sum_{i=1}^{N_e} N_i z_i = N_1 z_1 + N_2 z_2 + \cdots + N_{Ne} z_{N_e}. \end{aligned} \tag{2.15}$$

(2.16)

$$\begin{aligned} u &= \sum_{i=1}^{N_e} N_i u_i = N_1 u_1 + N_2 u_2 + \cdots + N_{Ne} u_{N_e}, \\ v &= \sum_{i=1}^{N_e} N_i v_i = N_1 v_1 + N_2 v_2 + \cdots + N_{Ne} v_{N_e}, \\ w &= \sum_{i=1}^{N_e} N_i w_i = N_1 w_1 + N_2 w_2 + \cdots + N_{Ne} w_{N_e}. \end{aligned} \tag{2.17}$$

Here x, y, z are point coordinates, x_i, y_i, z_i are node coordinates, u, v, w are displacements at the point with local coordinates ξ_l, η_l, ζ_l; and u_i, v_i, w_i are displacements at the nodes. According to the arrangement of the nodes as shown in Fig.2.5, the shape functions are:

$$\begin{aligned} N_i &= \tfrac{1}{8}(1+\xi_l\xi_{li})(1+\eta_l\eta_{li})(1+\zeta_l\zeta_{li}), \\ &\quad i = 1,2,3,\cdots,8 \\ N_i &= \tfrac{1}{4}(1-\xi_l^2)(1+\eta_l\eta_{li})(1+\zeta_l\zeta_{li}), \\ &\quad i = 9,10,11,12 \\ N_i &= \tfrac{1}{4}(1-\eta_l^2)(1+\xi_l\xi_{li})(1+\zeta_l\zeta_{li}), \\ &\quad i = 13,14,15,16 \\ N_i &= \tfrac{1}{4}(1-\zeta_l^2)(1+\xi_l\xi_{li})(1+\eta_l\eta_{li}), \\ &\quad i = 17,18,19,20 \end{aligned} \tag{2.18}$$

(2.19)

In the above relations $\xi_{li}, \eta_{li}, \zeta_{li}$ are the values of local coordinates at nodes.

The strain vector $\{\varepsilon\}$is given as:

$$\{\varepsilon\} = \begin{Bmatrix} \varepsilon_x \\ \varepsilon_y \\ \varepsilon_z \\ \gamma_{xy} \\ \gamma_{yz} \\ \gamma_{zx} \end{Bmatrix} = \{\varepsilon\} = \begin{Bmatrix} \frac{\partial u}{\partial x} \\ \frac{\partial v}{\partial y} \\ \frac{\partial w}{\partial z} \\ \frac{\partial u}{\partial y} + \frac{\partial v}{\partial x} \\ \frac{\partial v}{\partial z} + \frac{\partial w}{\partial y} \\ \frac{\partial w}{\partial x} + \frac{\partial u}{\partial z} \end{Bmatrix}. \tag{2.20}$$

According to Eq.2.17-2.20, the strain can be acquired in terms of nodal displacements:

$$\begin{aligned} \{\varepsilon\} &= [B]\{\delta\}^e, \\ [B_i] &= \begin{pmatrix} \frac{\partial N_i}{\partial x} & 0 & 0 \\ 0 & \frac{\partial N_i}{\partial y} & 0 \\ 0 & 0 & \frac{\partial N_i}{\partial z} \\ \frac{\partial N_i}{\partial y} & \frac{\partial N_i}{\partial x} & 0 \\ 0 & \frac{\partial N_i}{\partial z} & \frac{\partial N_i}{\partial y} \\ \frac{\partial N_i}{\partial z} & 0 & \frac{\partial N_i}{\partial x} \end{pmatrix}, \\ \begin{Bmatrix} \partial N_i/\partial \xi_l \\ \partial N_i/\partial \eta_l \\ \partial N_i/\partial \zeta_l \end{Bmatrix} &= [J] \begin{Bmatrix} \partial N_i/\partial x \\ \partial N_i/\partial y \\ \partial N_i/\partial z \end{Bmatrix}. \end{aligned} \tag{2.21}$$

The transformation of integrals from the global coordinate system to the local coordinate system is performed with the use of the Jacobian matrix:

$$dv = dxdydz = |J|d\xi_l d\eta_l d\zeta_l, \tag{2.22}$$

with equations as mentioned earlier, the finite element equilibrium equation can be written as:

$$[k_g]\{\delta\}^e = \{P_g\}^e. \tag{2.23}$$

The $[k_g]$ is the elemental stiffness, $\{P_g\}^e$ is the elemental nodal force, which is composed by equivalent body force $\{P_g\}^e_{qv}$, surface force $\{P_g\}^e_{qs}$ element matrices and

vectors are:

$$[k_g] = \int_{-1}^{1}\int_{-1}^{1}\int_{-1}^{1} [B(\xi_l,\eta_l,\zeta_l)]^T [D][B(\xi_l,\eta_l,\zeta_l)]|J|d\xi_l d\eta_l d\zeta_l, \tag{2.24}$$

$$\text{body force: } \{P_a\}^e_{q_v} = \int\int\int [N]^T \{q_v\}\, dv, \tag{2.25}$$

$$\text{surface force: } \{P_a\}^e_{q_s} = \int_S [N]^T \{q_s\}\, dS, \tag{2.26}$$

$$\text{thermal strain: } \{P_a\}^e_T = \int\int\int [B]^T [D]\{\varepsilon_T\}\, dv. \tag{2.27}$$

Here, the matrix $[D]$ is defined as the elastic matrix, $\{q_v\}$ is the body force,$\{q_s\}$ is the surface force working on the boundary S, ε_T is the strain caused by the change of temperature.

The global structural balance equation can be written as:

$$K_g \delta = P_g, \tag{2.28}$$

in which, the $[K_g]$ is the global structural stiffness, $\{\delta\}$ is the vector consisted of all the nodal displacements.

The state of displacements at any point is obtained in terms of nodal displacements.

Then the stresses are calculated using Hook's law:

$$\{\sigma\}^e = [D][B]\{\delta\}^e. \tag{2.29}$$

The maximum and minimum stresses which are also treated as tensile and compressive stresses that may be developed at any point within the dam are usually denoted as σ_1 and σ_3 respectively (as shown in Fig.2.6).
The two principal stresses σ_1 and σ_3 are the roots *w.r.t.* ω of the polynomial:

$$\det(\sigma - \omega I) = 0, \tag{2.30}$$

$$\text{stress tensor: } \sigma = \begin{pmatrix} \varepsilon_x & \gamma_{xy} & \gamma_{xz} \\ \gamma_{yx} & \varepsilon_y & \gamma_{yz} \\ \gamma_{zx} & \gamma_{zy} & \varepsilon_z \end{pmatrix},$$

$$I_3 = \begin{pmatrix} 1 & 0 & 0 \\ 0 & 1 & 0 \\ 0 & 0 & 1 \end{pmatrix}.$$

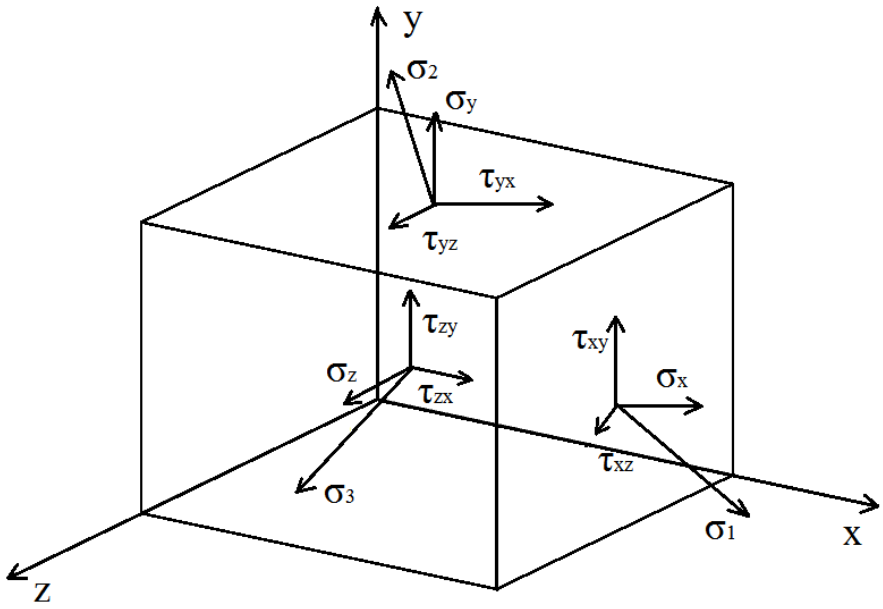

Figure 2.6: Elemental Stress State.

2.2.4.3 Thermal analysis with the FE method

The analysis of the arch dam's thermal behavior is a heat conduction problem. For a cubic elemental volume $dv = dxdydz$, which is part of the structural body, under the influence of temperature distribution inside the body, heat fluxes will occur through the six corresponding surfaces of the cube as shown in Fig.2.7. The heat flow is following the Fourier's law of heat conduction, given by;

$$\begin{aligned} q_x &= -k_{xx}\frac{\partial^2 T}{\partial x^2}, \\ q_y &= -k_{yy}\frac{\partial^2 T}{\partial y^2}, \\ q_z &= -k_{zz}\frac{\partial^2 T}{\partial z^2}. \end{aligned} \tag{2.31}$$

Here T is the temperature, q_x, q_y, q_z are the heat flow through the unit area in three directions, k_{xx}, k_{yy}, k_{zz} are the respective thermal conductivities. In this work, the ma-

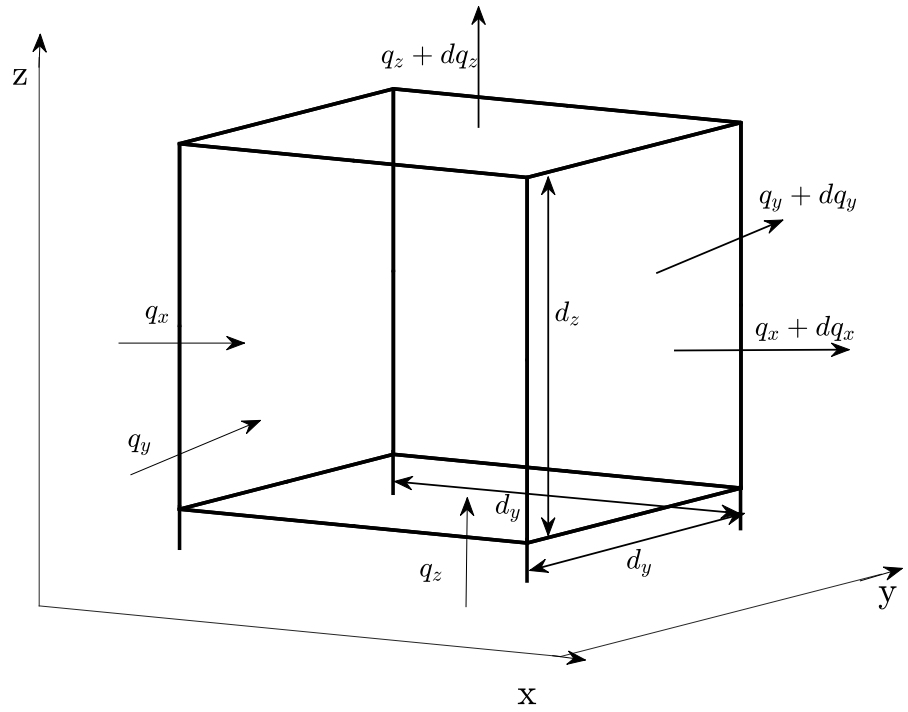

Figure 2.7: Heat Fluxes through a Cubic Solid Element.

terial is assumed to be homogeneous, then $k_{xx} = k_{yy} = k_{zz} = k$.

According to the law of conservation of energy, the fundamental equation of heat transfer has the following formation:

$$k_{xx}\frac{\partial^2 T}{\partial x^2} + k_{yy}\frac{\partial^2 T}{\partial y^2} + k_{zz}\frac{\partial^2 T}{\partial z^2} + Q_{in} = \rho_s c\frac{\partial T}{\partial t} \tag{2.32}$$

Here, ρ_s is the density of the material, c is the specific heat and Q_{in} is the internal heat generation rate per unit volume. In the arch dam analysis, there is no heat source in the dam body, and therefore the Q_{in} is assumed to be zero. In a static situation, the temperature will not change with time, and the heat transfer function can be written as:

$$k_{xx}\frac{\partial^2 T}{\partial x^2} + k_{yy}\frac{\partial^2 T}{\partial y^2} + k_{zz}\frac{\partial^2 T}{\partial z^2} = 0. \tag{2.33}$$

The thermal boundary of an arch dam is separated into two parts (see Fig.2.8) the boundary between water and dam surface (S_1) which is treated as Dirichlet boundary condition (boundary condition of the first type) and the temperature on the boundary

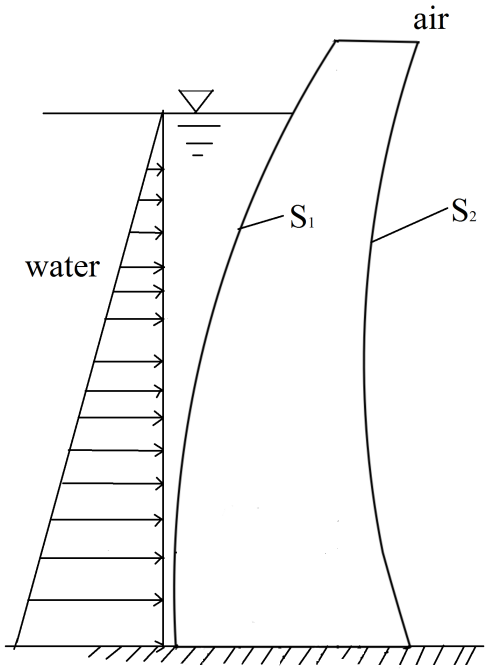

Figure 2.8: The Thermal Boundaries of an Arch Dam.

of the body is prescribed as:

$$T(t,z) = T_w(t,z) \quad \text{on } S_1, \tag{2.34}$$

which means the temperature of the dam's surface is equal to the temperature of the water T_w. The $T_w(t,z)$ is a known temperature function of water changing in terms of height. In this study, the T_w is assumed to be a constant.

The second part is the boundary between the dam surface and air (S_2) which experiences a thermal interaction between the body and the surrounding fluid. The boundary is considered as a control 'volume' with zero thickness for an energy balance, which means the 'volume' cannot store the energy, and the heat entering the surface by conduction has to leave outwards by convection. This boundary is called the Cauchy boundary (boundary condition of the third type):

$$q_x n_x + q_y n_y + q_z n_z = \beta_{T_c}(T - T_c) \quad \text{on } S_2, \tag{2.35}$$

where β_{T_c} is the convection coefficient, T_c is a known air temperature, $n = \{n_x, n_y, n_z\}$ is the outward normal vector of boundary surface.

According to the principle of variation, the thermal problem can be transferred to an extreme functional problem. The functional form of the heat transfer problem is:

$$I(T) = \int\int\int_{\Omega} \frac{a_T}{2}\left[\left(\frac{\partial T}{\partial x}\right)^2 + \left(\frac{\partial T}{\partial y}\right)^2 + \left(\frac{\partial T}{\partial z}\right)^2\right] dxdydz + \int\int_S \frac{\beta_{T_c}}{c\rho_s}\left(\frac{1}{2}T^2 - T_c T\right) ds, \tag{2.36}$$

in which the $a_T = k/c\rho_s$ is the temperature conductivity for isotropic situations. The solution is acquired by solving for the extreme minimum value of the functional equation:

$$\delta I = 0. \tag{2.37}$$

The arch dam structure is divided into n_e finite elements, and the following relations exist according to the divergence theorem;

$$I = \sum_{e=1}^{n_e} I^e, \tag{2.38}$$

$$I^e = \int\int\int_{\triangle\Omega} \left\{\frac{a_T}{2}\left[\left(\frac{\partial T}{\partial x}\right)^2 + \left(\frac{\partial T}{\partial y}\right)^2 + \left(\frac{\partial T}{\partial z}\right)^2\right]\right\} dxdydz + \int\int_{\triangle S} \frac{\beta_{T_c}}{c\rho_s}\left(\frac{1}{2}T^2 - T_c T\right) ds, \tag{2.39}$$

$$\frac{\partial I^e}{\partial T_i} = \int\int\int_{\triangle\Omega} \{a_T\left[\frac{\partial T}{\partial x}\frac{\partial}{\partial T_i}\left(\frac{\partial T}{\partial x}\right) + \frac{\partial T}{\partial y}\frac{\partial}{\partial T_i}\left(\frac{\partial T}{\partial y}\right) + \frac{\partial T}{\partial z}\frac{\partial}{\partial T_i}\left(\frac{\partial T}{\partial z}\right)\right]\} dxdydz + \int\int_{\triangle S} \frac{\beta_{T_c}}{c\rho_s}\left(T\frac{T}{T_i} - T_c\frac{\partial T}{\partial T_i}\right) ds. \tag{2.40}$$

According to the the extreme value condition;

$$\sum \frac{\partial I^e}{\partial T_i} = 0. \tag{2.41}$$

Shape functions N_i are used for interpolation of temperature at any point inside the element regarding the nodal temperature $\{T\}^e$:

$$T(x,y,z) = [N_1(x,y,z), N_2(x,y,z), N_3(x,y,z)\cdots] \begin{Bmatrix} T_1 \\ T_2 \\ T_3 \\ \vdots \end{Bmatrix} = [N]\{T\}^e \tag{2.42}$$

Differentiation of the temperature interpolation equation gives the following interpolation relation for temperature gradients:

$$\begin{Bmatrix} \frac{\partial T}{\partial x} \\ \frac{\partial T}{\partial y} \\ \frac{\partial T}{\partial z} \end{Bmatrix} = \begin{bmatrix} \frac{\partial N_1}{\partial x} & \frac{\partial N_2}{\partial x} & \cdots \\ \frac{\partial N_1}{\partial y} & \frac{\partial N_2}{\partial y} & \cdots \\ \frac{\partial N_1}{\partial z} & \frac{\partial N_2}{\partial z} & \cdots \end{bmatrix} \{T\}^e = [B]\{T\}^e . \tag{2.43}$$

Applying Eq.2.43 to Eq.2.41, we derive the following relations:

$$\begin{aligned} \frac{\partial I^e}{\partial T_i} &= \sum h_{ij}^e T_i + \sum q_{ij}^e T_i - g_i^e T_c = 0, \\ \text{in which} \quad h_{ij}^e &= \int\int\int_{\triangle v} a_T \left([B_i]^T [B_j] \right) dxdydz \\ q_{ij}^e &= \int\int_{\triangle S} \frac{\beta_{T_c}}{c\rho_s} N_i N_j dS \\ g_i^e &= \int\int_{\triangle S} \frac{\beta_{T_c}}{c\rho_s} N_i dS \end{aligned} \tag{2.44}$$

For the whole structure, the assembled finite element equations for heat transfer problem in this study is:

$$([H]+[Q])\{T\} - \{g\}T_c = 0. \tag{2.45}$$

2.2.4.4 Thermal-Mechanical Coupling

The numerical simulation of a thermal-mechanical coupling process is based on a combination of these two systems. The material is assumed to be a homogeneous material with linear thermal expansion. When the temperature changes from T_0 to T, the thermal strain is:

$$\varepsilon_T = \alpha_T (T - T_0), \tag{2.46}$$

in which the α_T is the thermal expansion parameter. Then, the total strain in the coupling system is obtained by integrating the thermal strain ε_T and the strain in the stress field ε_s. Finally, the total strain becomes;

$$\varepsilon = \varepsilon_s + \varepsilon_T . \tag{2.47}$$

2.2.5 General Optimization Procedure

Methods of shape optimization have been applied with success in many practical arch dams. However, the optimization procedure of an arch dam is a computationally expensive procedure. The majority of computing time is used in the stress reanalysis of the dam during the process of optimization. Hence it can be worthwhile to develop a highly efficient method to solve this problem.

Some techniques have been proposed and applied to reduce the cost of the stress analysis. Schmit and Farshi ([63]) used the first-order Taylor's series expansion method to replace the traditional stress analysis procedure, and later, Bofang ([30]) continually developed a method called internal force expansion method to approximately approach the structural stress analysis. These techniques exponentially created leaps in the direction of reducing the calculation consumption. In this study, the Kriging Metamodel is introduced to be an approximation model and an optimization ranking strategy is introduced to improve the efficiency of the optimization process. For the deterministic optimization of the arch dam, the procedure is sketched in Fig.2.9.

2.2.5.1 Kriging Metamodel

A suitable strategy for improving the efficiency of expensive computational optimization problems of arch dam design is to utilize approximation models which are often referred as metamodels to replace the expensive calculation model.

The research mentioned in ([59]), a study conducted on the accuracy of various metamodeling techniques under uncertainty, concludes that the Kriging metamodeling performs well as an approximation model.

Kriging is an interpolation method with the ability to provide the best estimate value of a random field ([64,65]). Its form can be written as:

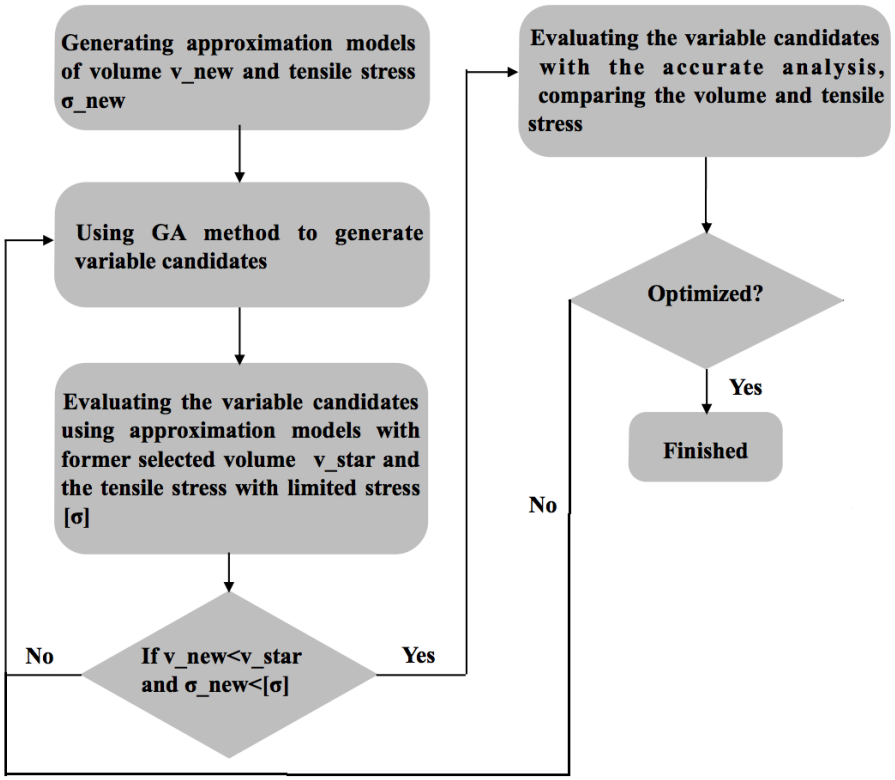

Figure 2.9: The Optimization Flow Chart for the Arch Dam.

$$\hat{y} = \sum_{j=1}^{k} \gamma_j f_j(x) + Z(\mu(x), R(x, x^{'}, \theta)), \tag{2.48}$$

where γ_j is an unknown coefficient, $f_j(x)$ is the basic function of the mean value of a stochastic process, and $Z(\mu(x), R(x, x^{'}, \theta))$ is assumed to be a stochastic process with zero mean. In this work, $Z(\mu(x), R(x, x^{'}, \theta))$ is expressed as a stochastic Gaussian process with zero mean and unit variance. The probability space of the Gaussian process is defined based on the correlation function R and correlation length θ.

The correlation function is a crucial ingredient for a Kriging predictor since it describes the similarities between the observations and the new points. It means that close input points are expected to have similar outputs. It is characterized by the form of $R(x, x^{'}, \theta)$, where x is the prediction point, $x^{'}$ is the observation, and θ is a vector containing a set of parameters. In the current stage, it is assumed that one element of θ is used per dimension for notational clarity.

1. Analytic model of correlation function

   - Triangular correlation function

     Triangular correlation function - is one of the simplest correlation functions as shown in Fig.2.10(a).

     $$R(\tau, \theta) = \begin{cases} 1 - |\tau|/\theta & \text{if} \quad |\tau| \leq \theta \\ 0 & \text{if} \quad |\tau| \, \theta \end{cases} . \tag{2.49}$$

     Here τ is the distance between any two points in the domain.

   - Exponential correlation function associated with a first-order auto-regressive process:

     Exponential correlation function is also widely known as Markov Correlation function (shown in Fig.2.10(b)). It is very commonly used because of its simplicity, and its simplicity since it renders a process where the 'future' depends only on the 'present' and not on the past. The Markov correlation function has the following form:

     $$R(\tau, \theta) = \exp\left\{ -\frac{2|\tau|}{\theta} \right\}. \tag{2.50}$$

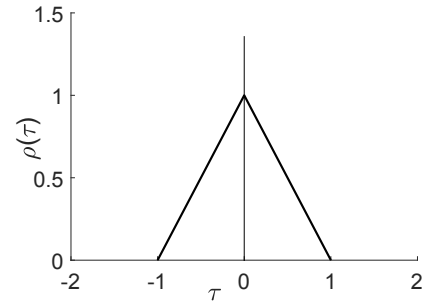

(a) Triangular Correlation Function.

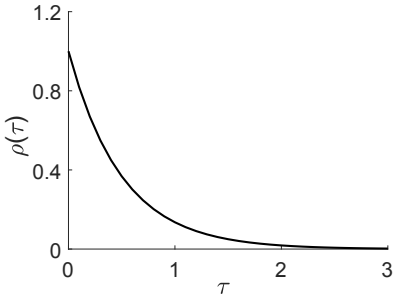

(b) Markov Correlation Function.

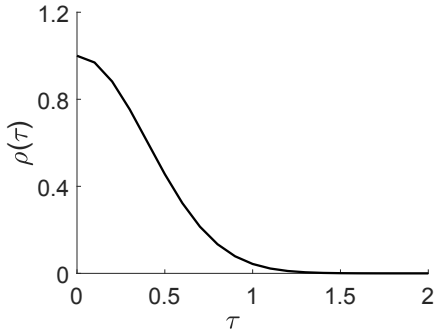

(c) Gaussian Correlation Function.

Figure 2.10: Comparison of Three Types of Correlation Functions for $\theta = 1.0$.

- Gaussian correlation function

  The Gaussian correlation function (shown in Fig.2.10(c)) is a mean square differential, which means its derivative has finite variance and so level excursion statistics are more easily computed. The Gaussian correlation function has the following form:

$$R(\tau,\theta) = \exp\left\{-\pi\left(\frac{\tau}{\theta}\right)^2\right\}. \tag{2.51}$$

2. Correlation length

For simplicity, the correlation length θ is assumed to be isotropic in this work. The correlation length θ is the distance within which points are significantly correlated. Mathematically, θ is calculated from following integration formula ([66]):

$$\theta = \int_{-\infty}^{\infty} R(\tau)d(\tau) = 2\int_{0}^{\infty} R(\tau)d(\tau). \tag{2.52}$$

However, this formula is not convenient to be utilized in the real calculation process. Generally, the correlation length θ is approximately acquired through some simulation models.

(a) Cross-validation

Cross-validation is a method to estimate the expected level of how well a model fits a data set that is independent of the data used to train the mode. It combines the methods that fit to derive a more accurate estimate of model prediction performance. With this estimation model, the correlation length θ can be expressed as the following optimization process:

$$\theta = \arg\min \sum_{i=1}^{N} (\hat{y}_i - \mu_i), \tag{2.53}$$

where $\hat{y}_i$ is the prediction value of x_i, and μ_i is the mean Kriging predictor.

(b) Maximum-Likelihood estimators

The Maximum-Likelihood (ML) estimators have some desirable statistical properties by finding the parameters which yield the highest likelihood of actual observed data. The correlation length θ is acquired by solving the following optimization problem based on the likelihood function:

$$\theta = \arg\min \left(\frac{1}{2}\log(\det(\mathbf{R})) + \frac{N}{2}\log(2\pi\theta^2 + \frac{N}{2}\right)). \tag{2.54}$$

In this study, the random process is based on a Gaussian process, the Gaussian correlation function is selected as the analytic model, and the correlation length θ is estimated by the Maximum-Likelihood method where the results show well enough for the preliminary analysis in the optimization. Here, we used programming UQLab ([67]) to acquire the approximation model. Fig.2.11 and Table 2.1 give the comparison results

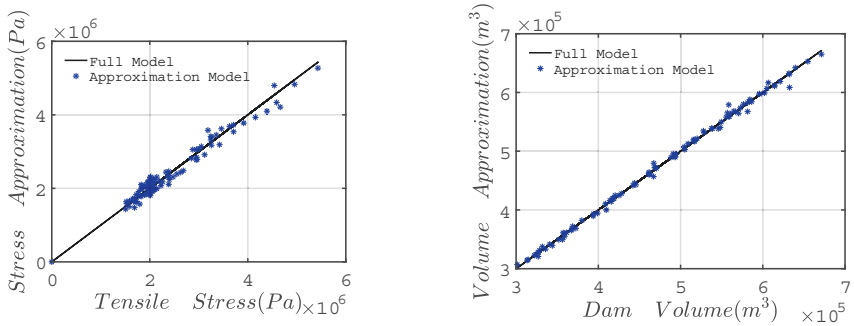

(a) The Approximation of Tensile Stress with Kriging Metamodel.

(b) The Approximation of Dam Volume with Kriging Metamodel.

Figure 2.11: Approximation with Kriging Metamodel.

Table 2.1: Approximation Model of Tensile Stress and Dam Volume

	Samplings	out − error
Tensile Stress Approximation	$LHS : 800$	$9.0534e^{-2}$
Volume Approximation	$LHS : 800$	$4.8018e^{-2}$

of tensile stress and dam volume approximation models.

2.2.5.2 Optimization method

For solving the optimization problems, there are two main concepts: One is local method mostly based on gradients of objective functions, the other one is the global optimization method. The following sections will discuss these two kinds of concepts on optimization methods. The local optimum method mentioned here is the Newton's Method, and the global optimization method used to compare is the genetic algorithm (GA) method.

1. **Local Optimization Method**

   The local optimization algorithms are methods that make optimal decisions at each step without attempting to acquire the best overall decisions. They are gradient-based methods using the derivative information to guide the search process. The direction of the negative gradient along with the objective function decreasing the fastest is the most natural choice. The principle of the gradient

descent algorithm can be obtained by setting the searching direction and finding an optimal step size. By using the gradient descent technique, it is guaranteed to converge to a local minimum from any start point.

In the case of Newton's method, the objective function $f(x)$ is assumed to be a twice differentiable function, and then the method utilizes both the first and second partial derivatives of the objective function to find its minimum. The search direction is $-H(x)^{-1} \bigtriangledown f(x)$, the new point x_{k+1} is acquired by :

$$x_{k+1} = x_k - H(x)^{-1} \bigtriangledown f(x), \tag{2.55}$$

where the $H(x)$ is the Hessian matrix of $f(x)$. The Fig.2.12 is the flow chart of Newton's method, and the Fig.2.13 shows how this method works for the optimization.

2. **Global Optimization Method**

Global optimization is distinguished from local optimization by its focus on finding the maximum or minimum overall input values. The global optimization method GA (genetic algorithm) is adopted in this work. The idea behind GA is to find the global optimal solution searching region, mimicking the procedure of the gene genetics ([68,69]). Therefore, the variable $x = (x_1, x_2, \ldots, x_n)^T$ should be encoded to chromosomes, such as binary encoding, which only contain $0s$ and $1s$.

In practice, the GA optimization procedure is s governed by the following steps:

(1) Generate random population of chromosomes;

(2) Evaluate how well each chromosome in the population fits the model;

(3) Create a new population by selecting two parent chromosomes, crossing over the parents to form new offspring, then mutating the new offspring at each locus, and placing the new offspring in the new population;

(4) If the new population satisfies the final conditions, this one would be the optimization selection, otherwise go back to step(2) until arriving at the best population;

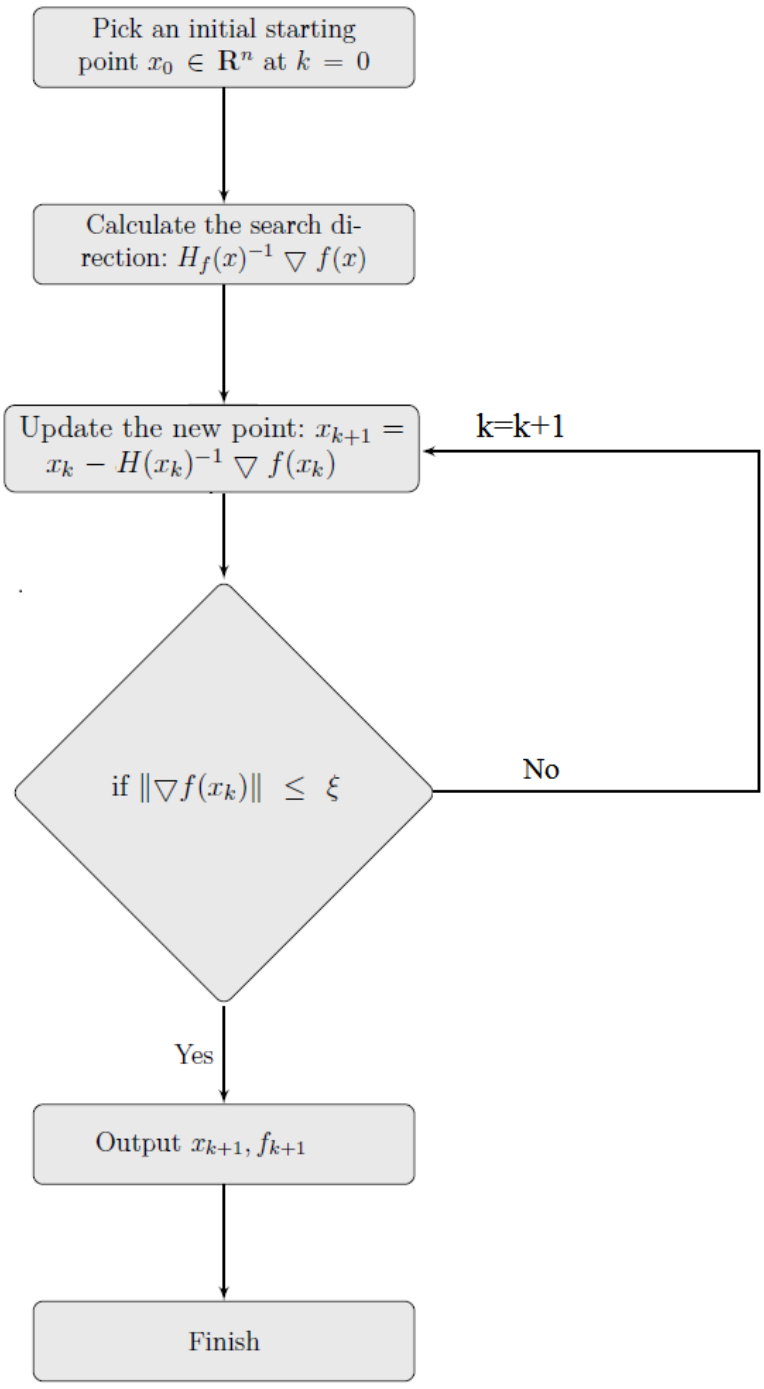

Figure 2.12: Newton's Method Procedure.

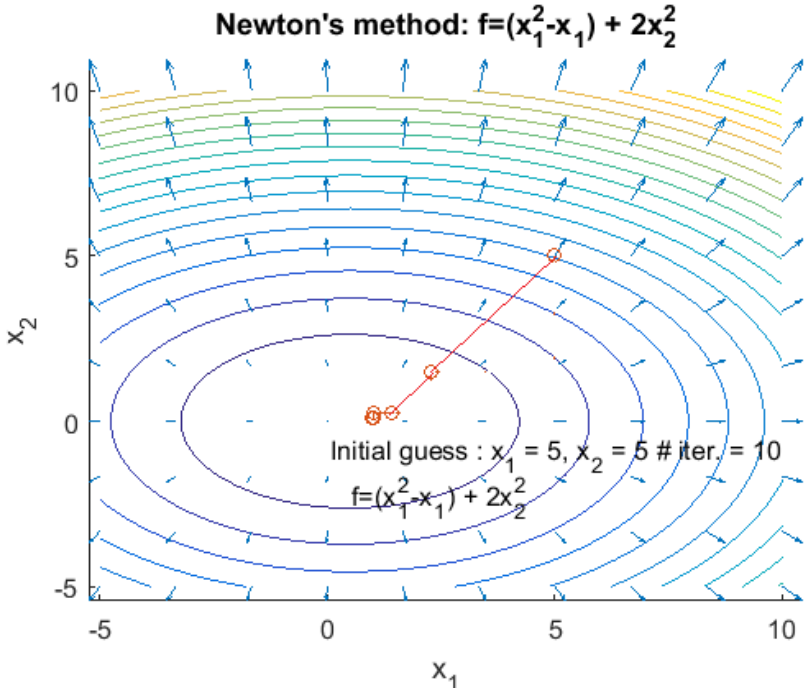

Figure 2.13: Geometric Interpretation for Newton's Method.

In many nonlinear optimization problems, the objective function f has a large number of local minimum or maximum values, which will lead the local methods to poor performance when compared with global methods. In order to test this theory, we apply the following minimum optimization problem with the objective function $f(x) = x\sin(x) + 2x\cos(2x)$. Fig.2.14 gives the optimum results with different initial points for local optimization method, and Fig.2.15 gives the optimum results for the global optimization method.

From Fig.2.14 and Fig.2.15, it can be seen that the local optimization is a point which has the best objective value of any possible point in its neighborhood. With different initial points, the local optimization would lead to different local optimum points. However, the global optimization method only focuses on finding the best objective value over the entire design space.

The object model for engineering problems may have lots of local extreme values, however, for engineering purposes, the best design in the design space is always expected. Besides, the gradient-based local optimization methods are less effective in

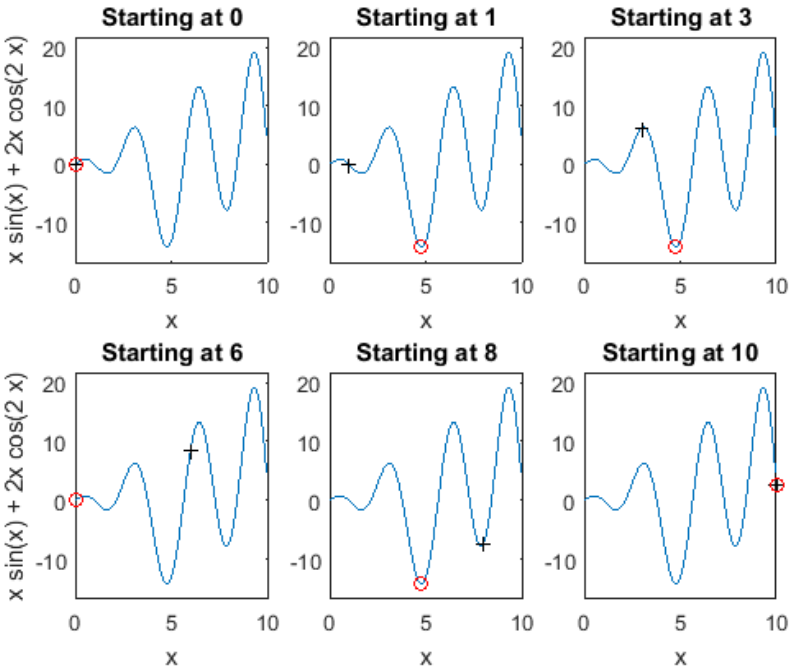

Figure 2.14: Newton's Method (local optimization method) with Different Initial Points for the Objective Function $f(x) = x\sin(x) + 2x\cos(2x)$.

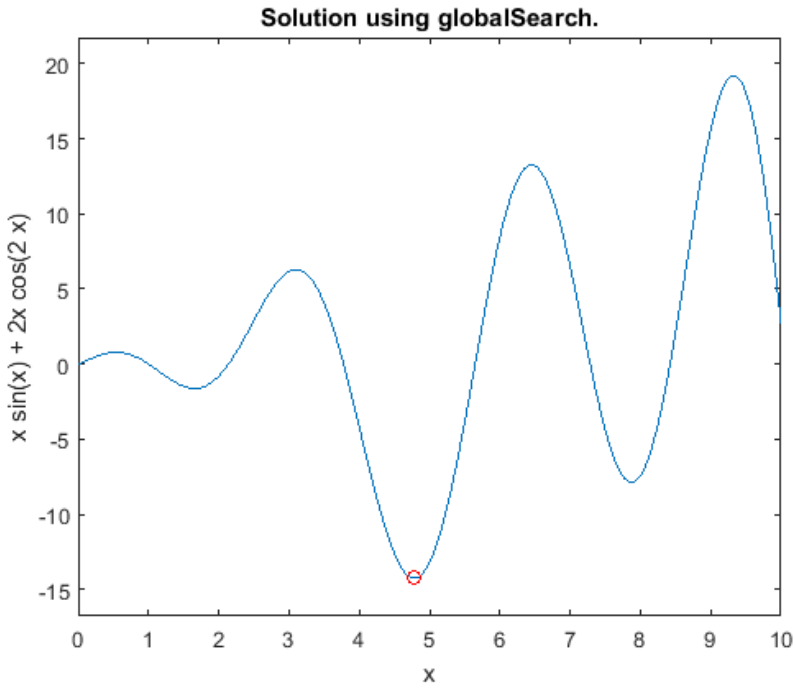

Figure 2.15: GA method (global optimization method) for the Objective Function $f(x) = x\sin(x) + 2x\cos(2x)$.

comparison to engineering optimization for discrete-valued, nondifferentiable objective and constraints, analysis programs which crash for some designs, *etc*. ([70]). Hence, the global optimization is much more suitable for the optimization problem of arch dams, and the GA method is selected as the optimization method in this work.

2.3 Shape Optimization of Arch Dams with Deterministic Optimization Method

2.3.1 Description of Numerical Model

According to Section 2.2, the shape optimization of an arch dam with DO method is described as:

$$\begin{aligned} \text{find} \quad & \mathbf{x} = [\alpha, \beta_1, \beta_2, t_1, t_2, t_3, \phi_1, \phi_2, \phi_3, a_1, a_2, a_3]^T, \\ \text{minimize}: \quad & f(\mathbf{x}) = \text{Vol}(\mathbf{x}) = \int\int |y_u(x,z) - y_d(x,z)|\, dxdz, \\ \text{subject to}: \quad & g_1 = \frac{\sigma_1}{[\sigma_1]} \leq 1, \\ & g_2 = \frac{\sigma_3}{[\sigma_3]} \leq 1, \\ & g_3 = \frac{s}{[s]} \leq 1, \\ & g_4 = \frac{[K_i]}{K_i} \leq 1, \\ & \mathbf{lb} \preceq \mathbf{x} \preceq \mathbf{ub}. \end{aligned} \tag{2.56}$$

The presented methodology shall be applied to the design of a new arch dam with the following data provided:

- The height of the dam is $140m$,
- 'V' shape valley;
- the basements on both sides of the valley are assumed to be rigid foundations;
- the average range of temperature change is assumed to be $5.4°C$, the temperature change of the reservoir water is relatively small and asumed to be $4.1°C$, and the water level is $135m$;
- the lower and upper boundary of design variables selected for the optimization are assumed according to empirical experiences ([29,35,36]) and are shown in Table 2.2.

Table 2.2: The Upper and Lower Boundaries of Shape Design Variables

$0.5 \leq \alpha \leq 0.9$	$0.3 \leq \beta_1 \leq 0.7$	$0.3 \leq \beta_2 \leq 0.7$
$3 \leq t_1 \leq 10$	$10 \leq t_2 \leq 30$	$15 \leq t_3 \leq 35$
$25 \leq \phi_1 \leq 70$	$25 \leq \phi_2 \leq 70$	$15 \leq \phi_3 \leq 40$
$-2 \leq a_1 \leq 2$	$-2 \leq a_2 \leq 2$	$-2 \leq a_3 \leq 2$

Table 2.3: Geometrical Parameters of the Initial Arch Dam Model

Height	Thickness(m)	Central Angle$'2\phi'(^\circ)$	Coefficient$'a'$
140	5	75.64	-1
120	9.43	86.55	-1
105	12.47	91.53	-1
90	16.15	93.88	-1
75	19.40	91.53	-1
55	21.55	86.23	-1
35	23.47	78.37	-1
20	25.14	67.75	-1
0	27	49.32	-1

The load combinations considered in the optimization procedure is listed as follows :

- self-weight ,
- hydrostatic pressure,
- uplift pressure,
- temperature load.

The initial model for the optimization is supposed to be a poorly designed arch type dam under the existing situation discussed above. The geometrical parameters to build the initial model are listed in the Table 2.3:

2.3.2 Comparison of the Optimal and Initial Models

The arch type dam can be designed through the shape design variables as described in Section2.1, the optimal arch dam using the general optimization procedure (DO model) is acquired, and the geometric parameters are listed in the Table 2.4:

The comparison of the principal stress results and sum displacements between initial and optimal models under the same load conditions are shown in Fig.2.16 -Fig.2.20.

Table 2.4: Geometrical Parameters of the Optimal Arch Dam Model

Height	Thickness(m)	Central Angle$'2\phi'(^\circ)$	Coefficient$'a'$
140	3.02	91.09	0.75
120	5.41	91.75	0.64
105	7.07	90.81	0.58
90	8.59	88.62	0.53
75	9.99	85.19	0.50
55	11.64	78.69	0.47
35	13.07	69.98	0.47
20	13.99	62.01	0.49
0	15.02	49.44	0.53

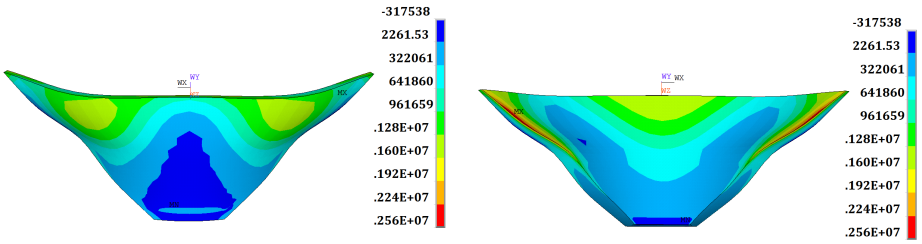

(a) Dam Upstream. (b) Dam Downstream.

Figure 2.16: First Principle Stress of Initial Dam Model (*Pa*).

From these comparisons, we can see that after optimization, the volume is largely reduced with little change in the stress state.

The Table 2.5 illustrates the comparison between the initial arch type dam and the optimal arch type dam. The comparison demonstrates that the optimization can take a poorly designed model and efficiently improve it to a qualified design with increased economic benefits.

Table 2.5: The Comparison of Initial Model and Optimal Model

	Volume (m^3)	Sum Displacement (m)	Tensile Stress (MPa)	Compressive Stress (MPa)
Initial Model	$5.22e5$	$2.25e-2$	2.56	5.75
Optimal Model	$2.841e5$	$1.65e-2$	1.49	2.95

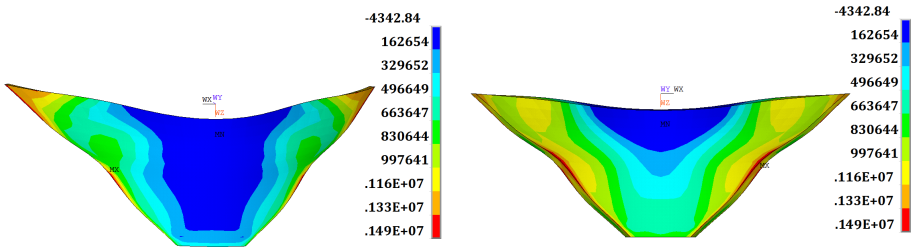

(a) Dam Upstream. (b) Dam Downstream.

Figure 2.17: First Principle Stress of Optimal Dam Model (*Pa*).

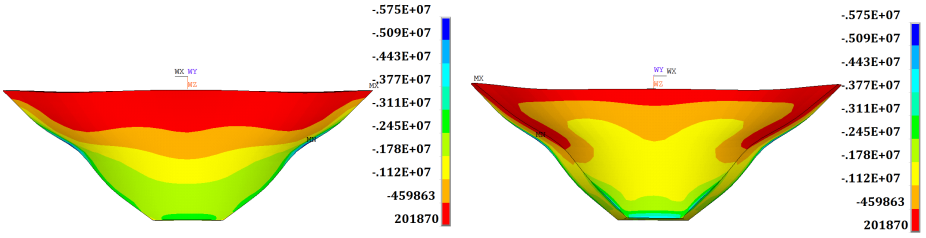

(a) Dam Upstream. (b) Dam Downstream.

Figure 2.18: Third Principle Stress of Initial Dam Model (*Pa*).

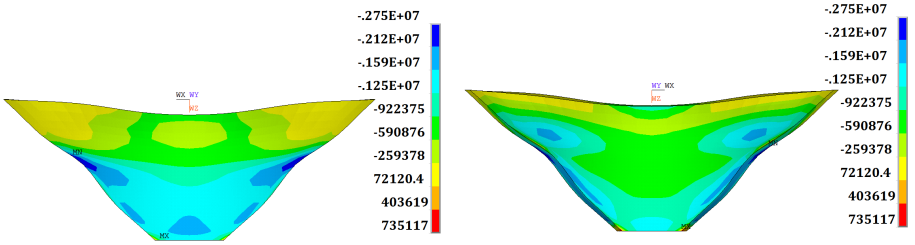

(a) Dam Upstream. (b) Dam Downstream.

Figure 2.19: Third Principle Stress of Optimal Dam Model (*Pa*).

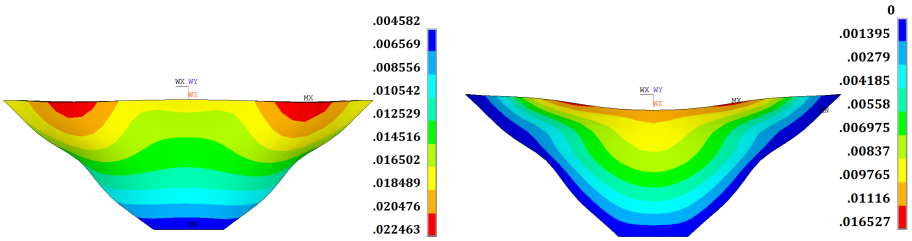

(a) Initial Dam Model. (b) Optimial Dam Model.

Figure 2.20: Sum of Displacement (m).

2.4 Conclusion

From comparing with existing design methodologies for the arch dam, the shape optimization approach can effectively reduce construction cost and leverage the properties of construction materials. In the shape optimization procedure, it is crucial to choose suitable variables to formulate the objective function, i.e., to minimize the volume of the arch dam. Additionally, a series of constraints are derived to form a reasonable and safe design. For the optimization method, a Genetic Algorithm is used to perform a global search avoiding to converge to the local minimum.

The use of metamodeling techniques has shown to be promising for global optimization with time-consuming stress analysis. From the comparison of the Kriging Metamodel and real model with 100 random testing samples (Fig.2.11), the Kriging Metamodel provides a well-performed approximation model to reduce the computational cost during the optimization process and save extra efforts in the stress analysis.

However, the optimization procedure discussed in this section is based on the deterministic optimization (DO) model. The uncertainty existing in the structural analysis system, such as loads uncertainties, material properties variation, *etc*. is not considered in the DO model. In the following sections, the method to solve the optimization problem under uncertainty will be discussed.

Chapter 3

Optimization of Arch-type Dams under Uncertainties with Probabilistic Model

3.1 Introduction

In this chapter, the two different approaches based on the probabilistic model developed to account for the uncertainties will be described. For the probabilistic model, the uncertainty data is assumed to obey a previously known probability distribution. One of the analysis disciplines concerns the minimum value of the objective function under the probabilistic constraints evaluated by the reliability index ([7,43,44]), and characterized to be named as reliability-based design optimization (RBDO). Another method based on the probabilistic model is called robust design optimization (RDO), which aims at minimizing the mean value of the objective function and the variance of the structural response. Earlier, researchers added an estimate of the model's response variance to the objective function, so that they could select the optimal solutions where variance in the input data lead to smaller variations in the output ([9,10,71]).

No matter the RBDO method or the RDO method, these probabilistic approaches are both computational-intensive tasks involving structural and reliability analysis. In order to reduce this computational burden, it is necessary to develop an accurate analytical model providing assessments of the failure probability and structural responses, given the uncertainties in the material, environmental, and loading conditions.

Firstly, an introduction of basic concepts is described in Section 3.2. The uncertainties are expressed using probability distributions, and this description is applied in both the reliability-based optimization and robust design optimization. The reliability analysis

method mentioned in Section 3.3 will be adopted, and it will be used for the RBDO method as an expression of a constraint. After that, in Section 3.3, the formulation of the RBDO is discussed, and a truss structure is used to demonstrate this approach. Section 3.4 describes the RDO approach, and Section 3.5 concludes these two approaches.

3.2 Description of Uncertainties Using Probability Distributions

When we start a probabilistic approach under uncertainties, it is crucial to identify and model the sources of the uncertainties. In the probabilistic definitions, the uncertainties are characterized as random variables $X = [x_1, x_2, x_3, \ldots]$ described by the cumulative distribution function (CDF) $F_X(x)$ and probability density function (PDF) $f_X(x)$ in the sample space S_u.

The probability density function $f_X(x)$ for the random variable X is defined as:

$$\begin{aligned} 0 \leq f_X(x) \leq \infty, \\ \int_{-\infty}^{\infty} f_X(x)dx = 1, \\ P[a < X < b] = \int_a^b f_X(x)dx. \end{aligned} \tag{3.1}$$

Here, $P[a < X < b]$ is the probability of X falling in the range of $[a, b]$.

The cumulative distribution function $F_X(x)$ is defined with the PDF by:

$$F_X(t) = P[X < t] = \int_{-\infty}^{t} f_X(x)dx. \tag{3.2}$$

Here, the Fig.3.1 offers an example of the CDF and PDF for a normal distribution (Gaussian distribution) with mean $\mu_X = 0$ and standard deviation $\sigma_X = 1$.

In engineering practices, the variability of a random quantity is characterized by central tendency and variability. The mean (expected value) tells us about its central tendency and is defined mathematically as:

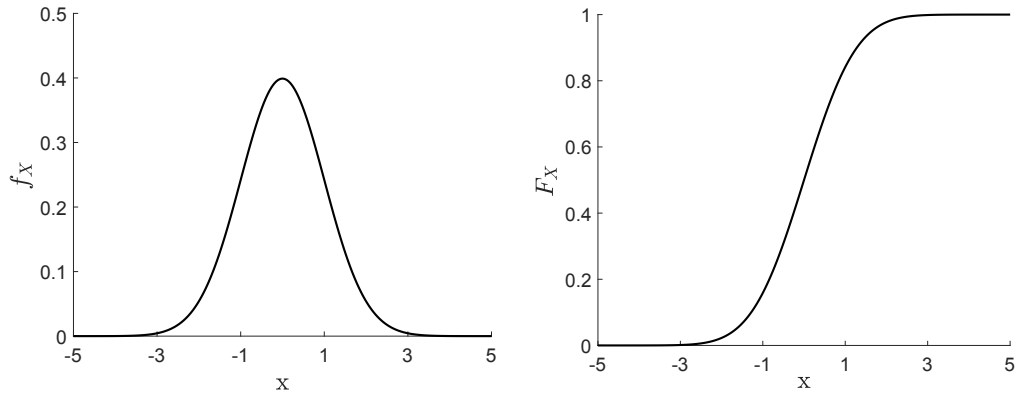

(a) Probability Density Function of Gaussian Distribution for $\mu_X = 0$ and $\sigma_X = 1$.

(b) Cumulative Distribution Function of Gaussian Distribution for $\mu_X = 0$ and $\sigma_X = 1$.

Figure 3.1: Gaussian Distribution.

$$\mu_X = \begin{cases} \sum_x x f_X(x) & \text{(discrete case)} \\ \int_{-\infty}^{\infty} x f_X(x) dx & \text{(continuous case)} \end{cases} . \tag{3.3}$$

The characteristics of the random variables which decides the distribution shape, "wide" or "narrow"(Fig.3.2), is called the variance of X and expressed as:

$$\begin{aligned} \sigma_X^2 &= var[X] = E[(X-\mu_X)^2] \\ &= \begin{cases} \sum_x (x-\mu_X)^2 f_X(x) & \text{(discrete case)} \\ \int_{-\infty}^{\infty} (x-\mu_X)^2 f_X(x) dx & \text{(continuous case)} \end{cases} . \end{aligned} \tag{3.4}$$

More than one random variables are representing the uncertainties considered in the optimization. For each random variable, there may exist some connection to other random variables, and this connection is characterized as a correlation coefficient among random variables.

The correlation coefficient between random variables X and Y is:

$$\rho_{XY} = \frac{Cov[X,Y]}{\sigma_X \sigma_Y}. \tag{3.5}$$

In which, $Cov[X,Y]$ is the co-variance of random variables X and Y, and expressed as:

$$Cov[X,Y] = E[XY] - E[X][Y] - E[X]E[Y] = E[XY] - \mu_X \mu_Y. \tag{3.6}$$

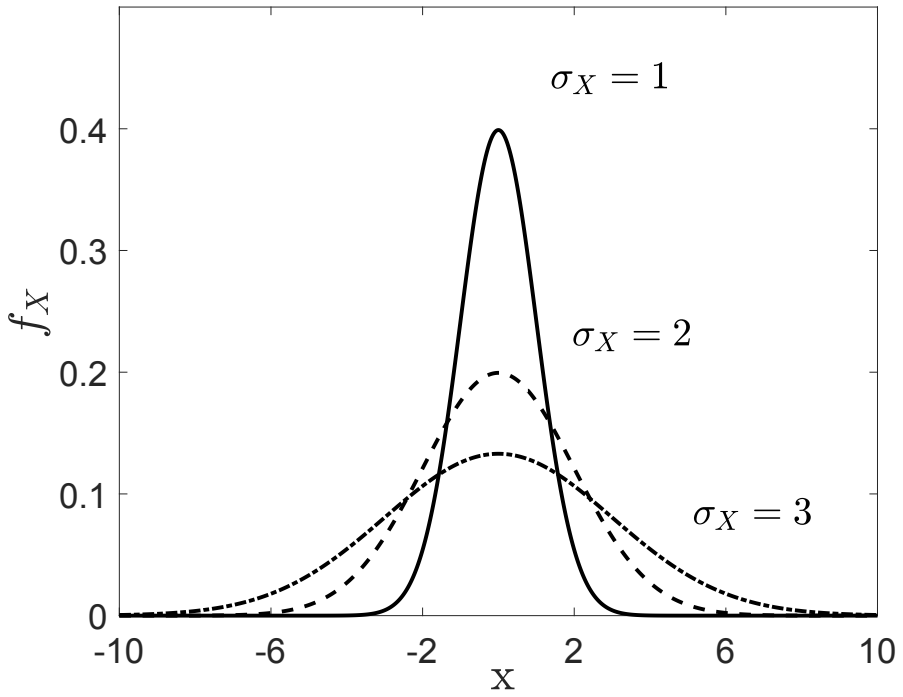

Figure 3.2: Probability Density of Gaussian Distribution with Different Standard Deviations σ_X.

The correlation coefficient, which is always $-1 \leq \rho_{XY} \leq 1$, expresses how profoundly one random variable influences the other variables: when $\rho_{XY} = 0$, it means that the variables X and Y are entirely independent of each other, when $\rho_{XY} = \pm 1$, that means X and Y are perfectly correlated.

3.3 Reliability-Based Optimization Design (RBDO) Method

3.3.1 Safety Concept

The method to define structural safety for classic reliability problems is through the loading action S and the resistance R. The resistance R, also known as loads, is the structural capacity to resist the stress system. The structural system is treated as a failure when the stress S and the resistance R fulfill the following requirements:

$$S \leq R. \tag{3.7}$$

In a statistical model, this problem is transformed to compute the probability of the stress being more significant than the resistance:

$$P_f = P[S > R]. \tag{3.8}$$

In structural reliability analysis, verification that the structure does not exceed a specified limit state is performed. The limit state is what divides the design or variable space into fail and safe regions. It is expressed as the limit state function and is of the form:

$$g_X = R - S. \tag{3.9}$$

The probability of failure refers to the probability that an undesired performance occurs (see Fig.3.3).

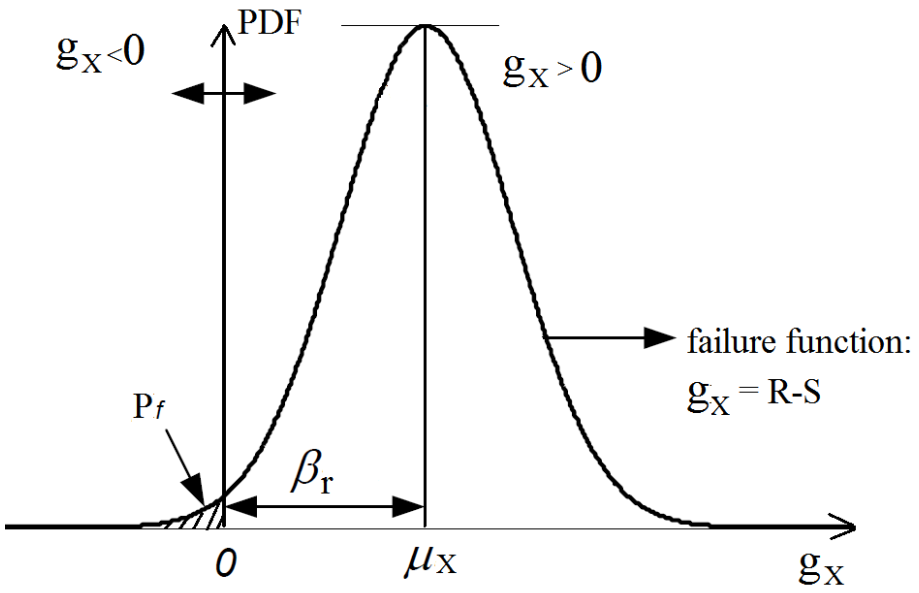

Figure 3.3: Distribution of failure function $g_X = R - S$.

3.3.2 The Selected Limit State Function

The limit state determines the safe and failure regions. It requires an analytical model describing the limit state, and the model must include all the relevant primary variables (loads), material parameters, and geometrical parameters. The structural reliability analysis in this thesis only concerns the failure of the material. Then, the material yield criteria theories under combined stresses are considered as the limit state function.

In this work, the studied structure is the arch dam, and assume the material for the arch dam is isotropic, then the yield criteria for isotropic materials can be expressed as a function of three independent stress invariant or principle shear stresses. The generalized criteria may be expressed as:

$$\begin{aligned} F(\sigma_i) &= F(I_1, J_2, J_3), \\ F(\sigma_i) &= F(\tau_{12}, \tau_{23}, \tau_{31}, \sigma_{12}, \sigma_{23}, \sigma_{31}), \end{aligned} \tag{3.10}$$

where I_1 is the first invariant of stress tensor, J_1, J_2 are the second and third invariant of stress deviator tensor, $\tau_{12}, \tau_{23}, \tau_{31}$ are the principle shear stresses, and $\sigma_{12}, \sigma_{23}, \sigma_{31}$ are the normal stresses acting on the sections where the principle shear stresses act

respectively.

Evaluating the dam's reliability is to check the possibility that the stresses exceed the capacity of the structural resistance of the system. The failure mode or limit state could be chosen to be the evaluation boundary of the reliability analysis. For the arch dam structure, there are several kinds of failure modes, and in this work, the Twin Shear Stress Yield Criterion ([72]), which is proposed by Yu(1961) ([72]), is introduced as an additional condition to judge the failure mode. This criterion assumes that the yielding is determined by two larger principle shear stress. This criterion can be expressed in the following two equations:

$$f = \begin{cases} \frac{f_t - \left(\sigma_1 - \left(\frac{\alpha_f}{2}\right)(\sigma_2+\sigma_3)\right)}{f_t} = 0, & \sigma_2 \leq \frac{\sigma_1+\alpha_f\sigma_3}{1+\alpha_f}, \\ \frac{f_t - \left(\left(\frac{\alpha_f}{2}\right)(\sigma_1+\sigma_2) - \alpha_f\sigma_3\right)}{f_t} = 0, & \sigma_2 > \frac{\sigma_1+\alpha_f\sigma_3}{1+\alpha_f}, \end{cases} \tag{3.11}$$

where f_t is the tensile allowance of material, α_f is the ratio of tension and compression allowances of material, which is $\alpha_f = f_t/f_c$.

The Twin Shear Stress Yield Criterion is involved as the limit state function considers the possibility that the material can yield both in the tensile and compressive stresses. The choice of the exact expression of the twin shear criterion depends on which stress type behaves as the dominant failure reason.

The limiting surface of the generalized Twin Shear Stress Yield Criterion in three-dimensional principle stress space and its cutting section with π-plane are shown in Fig.3.4. The limiting surface is usually a semi-infinite hexagonal cone with unequal sides. The shape and size of the surface are determined by the allowable strength in tension and compression.

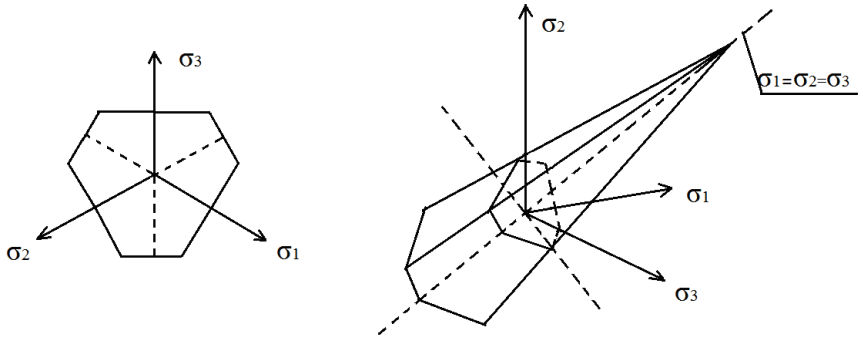

Figure 3.4: Generalized Twin Shear Stress Yield Surface.

3.3.3 General Description of the RBDO Method

From the engineering point of view, the RBDO method enhanced the optimization with stochastic restrictions such as a predefined small failure probability to ensure sufficient structural safety and serviceability (See Fig.3.5).

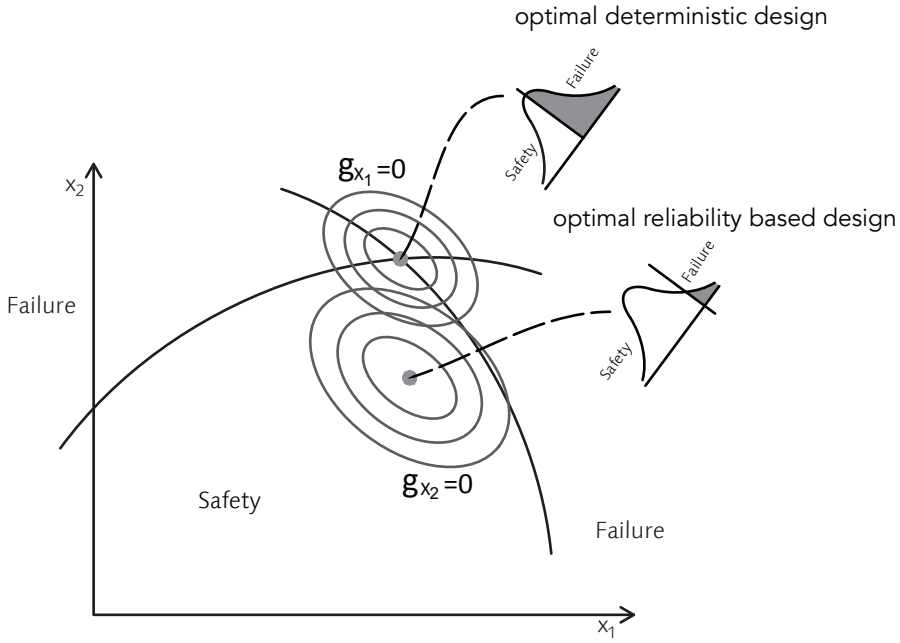

Figure 3.5: Reliability-based Design Optimization and Deterministic Optimization.

The reliability index is involved as a measure to decide if the optimal result is applicable under specific reliability requirements. The constraint expression is characterized as:

$$g_5 = \frac{[\beta_r]}{\beta_r} \leq 1, \tag{3.12}$$

in which, $[\beta_r]$ is the required allowable reliability index, and the β_r is the minimum reliability index for the whole structure. In this work, the minimum reliability index is taken as 3.7.

The reliability index is acquired according to the failure probability with the following relation:

$$P_f = \Phi(-\beta_r) \Longleftrightarrow \beta_r = \Phi^{-1}(P_f). \tag{3.13}$$

Here, $\Phi(\cdot)$ and $\Phi^{-1}(\cdot)$ are the standard normal cumulative distribution function and inverse respectively. The failure probability p_f is calculated through the Eq.3.2:

$$P_f = \int\limits_{\substack{g_X(x)\leq 0 \\ lb\leq x\leq ub}} f_X(x)dx. \tag{3.14}$$

Evaluating the dam reliability involves checking the possibility that the stresses exceed the capacity of the structural resistance of the system. The failure mode or limit state could be chosen to be the evaluation boundary of the reliability analysis. For the arch dam structure, there are several kinds of failure modes, and in this work, the Twin Shear Stress Yield Criterion, expressed as Eq.3.11 mentioned in Section 3.3.2, is considered as the evaluation criteria.

If reliability design is followed in the optimization procedure, higher demands for the computational costs are expected. Moreover, an approximation analysis mentioned in Section 2.2.5.1 can obviously increase the calculation speed, but the accuracy of the result is not satisfied to meet research demands.

In this situation, the proposed approach for the optimization can be ranked into three stages: An initially built preliminary judgment of the geometric constraints, an adaptive exclusion of unsatisfied design samples and finally an accuracy analysis to evaluate the final selections. The detailed procedure of the RBDO method in the frame of the GA optimization method is given as in Fig.3.6.

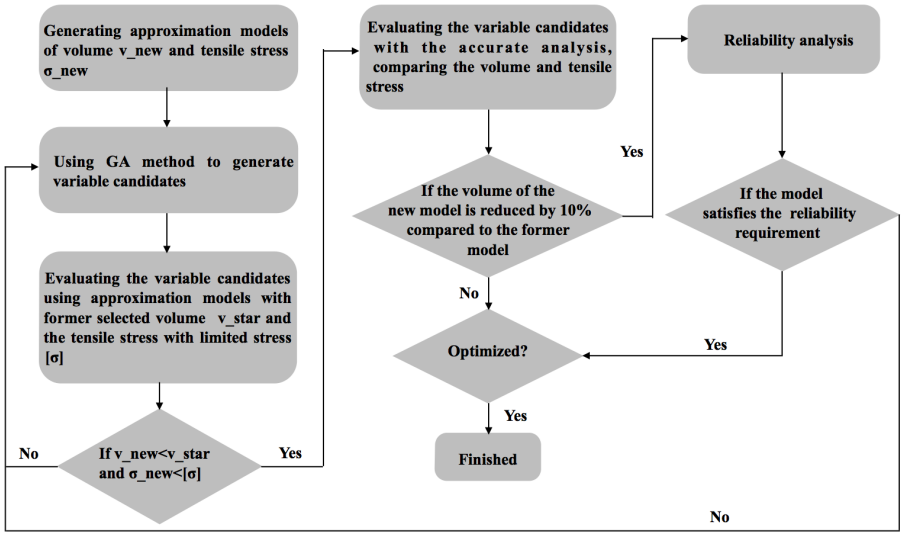

Figure 3.6: The Optimization Procedure of the RBDO Method in This Work.

3.3.4 Numerical Techniques for the Evaluation of the Reliability

Numerical techniques for evaluation of reliability have been proposed and generally classified into two groups: random sampling methods and analytical methods. The random sampling methods are traditional Monte Carlo method and its variants, such as importance sampling ([1]). The analytical methods define a surface, separating the failure and safe regions, based on the limit functions, such as first- and second-order reliability methods, response surface methods, *etc*.

3.3.4.1 First and Second Order Reliability Methods (FORM and SORM)

The basic idea of FORM and SORM is to ease the computation of structural reliability analysis by approximating the limit function. The reliability index is defined to be the minimum distance from the origin to the limit surface. The name of FORM comes from the fact that the limit function $g_X(x)$ is approximated by the first-order Taylor expansion (linearization). SORM is an improved approximation based on FORM by using the second-order surface to approach the limit surface.

1. **First-Oder Reliability Method**

Three steps are involved in acquiring the reliability index in the approximation. Firstly, to make the probability integration easy to be computed, the vector of random variables $X \sim f_X(x)$ are transferred to a standard normal vector $U \sim N(\mu_x, \sigma_x)$. The transferred standard variables are given as:

$$U = \Phi^{-1}[F_X(x)] = \Phi^{-1}\left[\Phi\left(\frac{X-\mu_x}{\sigma_x}\right)\right] = \frac{X-\mu_x}{\sigma_x}. \tag{3.15}$$

Then the limit function is written as:

$$g_X(x) = g_U(u). \tag{3.16}$$

The failure probability function in Eq.3.14 is transformed to given as:

$$P_f = \int f_X(x)dx = \int\limits_{g_U(u)\leq 0} f_U(u)du, \tag{3.17}$$

where $f_U(u)$ is the joint PDF of U:

$$f_U(u) = \prod_{i=1}^{n} \frac{\sigma_x\sqrt{2\pi}}{1} \exp\left(-\frac{1}{2}u_i^2\right), \tag{3.18}$$

and the probability integration can be written as:

$$P_f = \int\limits_{g_U(u_1,u_2,\cdots,u_n)\leq 0} \cdots \int \prod_{i=1}^{n} \frac{\sigma_x\sqrt{2\pi}}{1} \exp\left(-\frac{1}{2}u_i^2\right) du_1 du_2 \cdots du_n. \tag{3.19}$$

After the transformation step, the limit function $g_U(u)$ is approximated with the first order Taylor expansion around the expansion point U^*:

$$g_U(u) \approx g_U(U^*) + \bigtriangledown g_U(U^*)(U-U^*)^T, \tag{3.20}$$

$$\bigtriangledown g(U^*) = \left(\frac{\partial g_U(u)}{u_1}, \frac{\partial g_U(u)}{u_2}, \cdots, \frac{\partial g_U(u)}{u_n}\right)|_{U^*}. \tag{3.21}$$

The point which is closest to the origin, in the domain of failure is called the most probable point (MPP) (shown in Fig.3.7). Maximizing the joint PDF $f_U(u)$

at $g_U(u)$ gives the location of the MPP. Since the joint PDF $f_U(u)$ only depends on the $\| U^* \|^2$, then we obtain the MPP U^* which can be expressed as a minimum value search process, and it is:

$$\begin{aligned} \text{find} \quad & U^*, \\ \text{minimize :} \quad & \| U^* \|, \\ \text{subjected to:} \quad & g_U(u) = 0. \end{aligned} \tag{3.22}$$

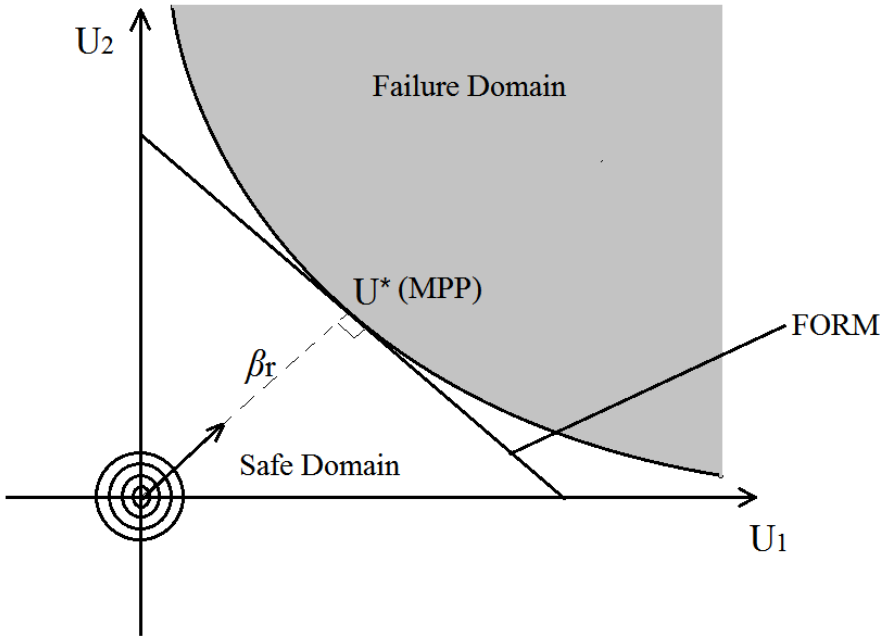

Figure 3.7: First-Order Reliability Method ([1]).

Finally, the reliability index is acquired according to its definition that is the distance from MPP to origin 0. Hence, the reliability index β_r is:

$$\beta_r = \| U^* \| . \tag{3.23}$$

2. **Second-Order Reliability Methods**

The analysis procedure of SORM is almost same with the FORM. The only difference is that the expansion in SORM is a second order Taylor expansion around U^* (see Fig.3.8), which is :

$$g_U(u) \approx g_U(U^* + \bigtriangledown(U^*)(U-U^*)^T) + \frac{1}{2}(U-U^*)H(U^*)(U-U^*)^T, \quad (3.24)$$

where $H(U^*)$ is the Hessian matrix at the MPP:

$$H(U^*) = \begin{bmatrix} \frac{\partial^2 g_U}{\partial u_1^2} & \frac{\partial^2 g_U}{\partial u_1 u_2} & \cdots & \frac{\partial^2 g_U}{\partial u_1 u_n} \\ \frac{\partial^2 g_U}{\partial u_2 u_1} & \frac{\partial^2 g_U}{\partial u_2^2} & \cdots & \frac{\partial^2 g_U}{\partial u_2 u_1} \\ \cdots & \cdots & \cdots & \cdots \\ \frac{\partial^2 g_U}{\partial u_n u_1} & \frac{\partial^2 g_U}{\partial u_n u_2} & \cdots & \frac{\partial^2 g_U}{\partial u_n^2} \end{bmatrix}. \quad (3.25)$$

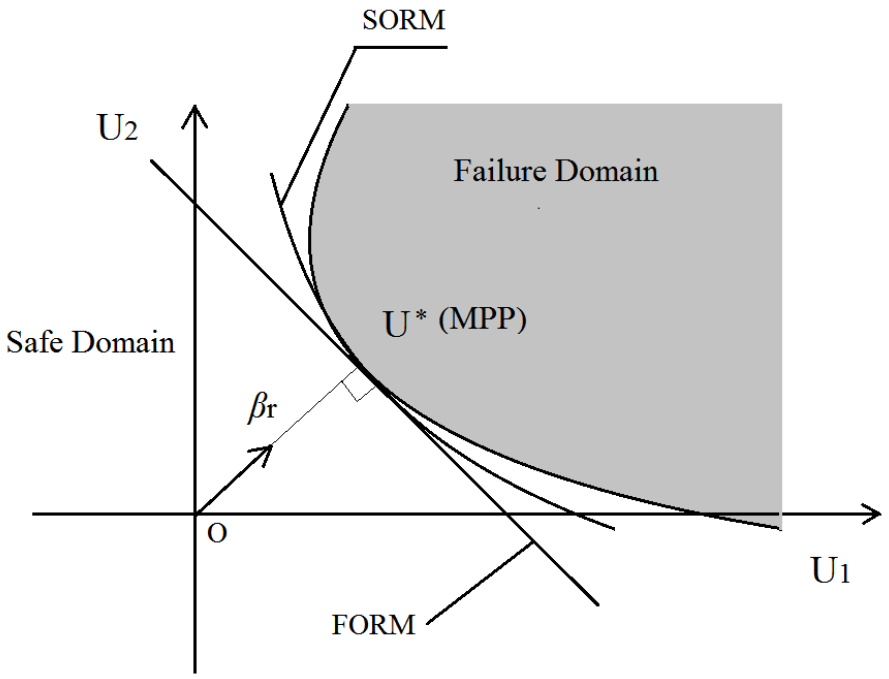

Figure 3.8: Second-Order Reliability Method ([1]).

3.3.4.2 Response Surface Method (RSM)

The idea of the response surface method (see Fig.3.9) is using a sequence of design experiments to build an approximation response model. The application of the Response

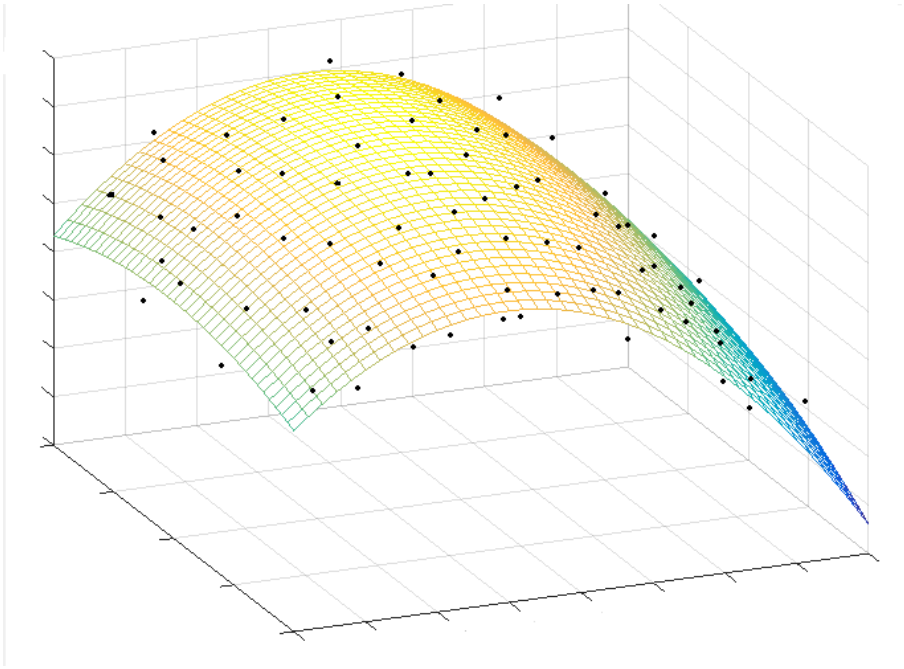

Figure 3.9: Response Surface Method (RSM) ([1]).

Surface Method is to reduce the cost of expensive analyses.

The critical step for RSM is to search for a suitable approximation relation between the response and the independent variables. Generally, this relationship is formed with a low-order polynomial, such as:

$$g_X(x) = Bf^{'}(x) + a, \tag{3.26}$$

where $f^{'}(x)$ is a vector function consisting of elements and cross-products of elements of the vector x up to a certain degree, B is a vector of constant coefficients, and a is a random experimental error assumed to have zero mean.

The obtaining of the approximation response surface is an iteratively building process, and the parameters can be acquired through an optimization procedure which is aimed at finding the best possible quality of the approximation structure. With the response surface of the limit function, the failure probability or the reliability index can be easily acquired by first finding the MPP as mentioned in Section 3.3.4.1.

3.3.4.3 Monte Carlo Simulation (MCS)

The Monte Carlo simulation is an estimation technique fitting for solving those problems which cannot be adequately represented by the mathematical models, or where the solution is not possible through analytical methods. The basic concept of the Monte Carlo simulation is shown in Fig.3.10. The sampling selects the value of uncertain variables according to their probability distribution functions randomly. The failure probability integral can be written as:

$$P_f = \int\limits_{g_X(x)\leq 0} f_X(x)dx = \int I_g(x) f_X(x)dx, \tag{3.27}$$

where $I_g(x) = I[g_X(x) \leq 0]$ is an indicator function equal to 1 if $g_X(x) \leq 0$ and otherwise equal to zero.

The basis for the Monte Carlo simulation is the assumption that for the number of sampling N approaches infinity then the failure probability is close to the ratio of the number of samples (n_f) violating the constraints to the limit function $g_X(x)$. Then, the estimation of MCS is given by:

$$P_f = \frac{1}{N}\sum_{j=1}^{N} I_g(X) = \frac{n_f}{N}. \tag{3.28}$$

The coefficient of variation Cov is estimated by:

$$Cov = \sqrt{\frac{1-P_f}{NP_f}}. \tag{3.29}$$

From the Eq.3.29, the accuracy of MCS depends heavily on the number of samples, which can lead to an expensive simulation procedure. Some sampling techniques are referred to as variance reduction methods.

3.3.4.4 Importance Sampling

The basic idea of importance sampling is to concentrate the distribution of sampled candidates in the region of most importance or the area which mainly contributes to the failure probability, instead of spreading them out evenly among the whole range of possible values (see Fig.3.11).

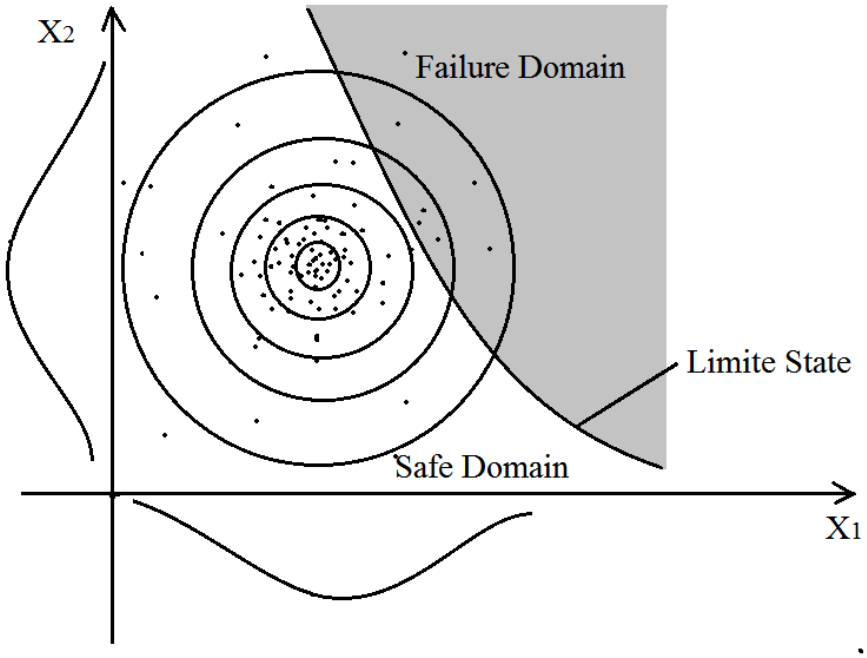

Figure 3.10: Monte Carlo Simulation (MCS)([1]).

The basic idea is to introduce a positive weighting function $h_y(x)$, which can be interpreted as the density function of a random vector Y, and samples are taken according to $h_y(x)$. Then the Eq.3.28 can be rewritten as:

$$P_f = \frac{1}{N}\sum_{j=1}^{N}\frac{f_X(x)}{h_y(x)}I_g(x) = E\left[\frac{f_X(x)}{h_y(x)}I_g(x)\right]. \tag{3.30}$$

The variance of the p_f is:

$$\sigma^2_{P_f} = \frac{1}{N}E\left[\frac{f_X(x)^2}{h_y(x)^2}I_g(x)\right]. \tag{3.31}$$

The selection of $h_y(x)$ is based on obtaining the minimum variance $\sigma^2_{P_f}$.

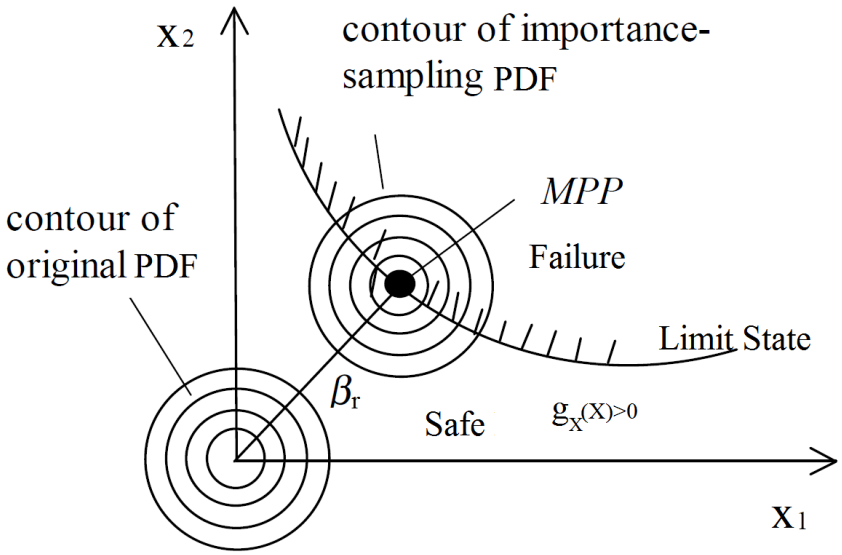

Figure 3.11: Importance Sampling ([1]).

3.3.4.5 Adaptive Kriging Monte Carlo Simulation (AK-MCS)

In the work of ([62]), a method called Adaptive Kriging Monte Carlo Simulation (AK-MCS) is described to evaluate the failure probability. The method combines Monte Carlo simulation with adaptively built Kriging metamodels by generating a corresponding limit-state function response with the Kriging metamodel (details mentioned in Section 2.2.5.1) and then evaluating the failure probability through Monte Carlo simulation with the final limit state function responses.

In the work of AK-MCS, an adaptive experimental design algorithm is introduced to increase the accuracy of the surrogate model, and the procedure summarized as follows:

1. Generate the initial experimental design $X = (x_1, x_2, \ldots, x_N)^T$ and evaluate the corresponding limit function responses $G = [g_X(x_1), g_X(x_2), \ldots, g_X(x_N)]^T$.

2. Train a Kriging metamodel $\widehat{G}$ based on experimental design $\{X, G\}$.

3. Generate large numbers of samples and predict the corresponding $\widehat{G}$.

4. Choose the best next sample to be added to the experimental design X.

5. Check whether the surrogate model meet the convergence criterion. If it is, skip to step(7), otherwise, continue the procedure to step (6).

6. Add the best next sample and the corresponding limit function response to the experimental design of the metamodel.

7. Estimate the failure probability through Monte Carlo simulation with the final limit function surrogate.

3.3.5 Studies on the Evaluation Methods of Structural Reliability

In order to select an effective method for the structural analysis of an arch dam, several examples are tested to compare the properties of these Evaluation Methods of Structural Reliability.

1. **Example of a simple abstract structural expression for the sampling difference**
   Here is a simple abstract expression for the reliability analysis which only contains the resistance R and the stress S. The structural limit state function is expressed as:

$$g_X = R - S. \tag{3.32}$$

   The structural system fails when the resistance is less than the stress. The input data are assumed to follow the distributions: $R \sim \mathcal{N}(5, 0.8)$, $S \sim \mathcal{N}(2, 0.6)$. The following Fig.3.12-Fig.3.13 give the analysis results with different evaluation methods.

2. **Example for a two-bar truss structure**
   The two-bar structure shown in Fig.3.14 is defined such that the mass density and Young's Modulus are supposed to be 1, the resistance of the structural system is influenced by the cross-sectional areas of the bars(a_1, a_2), and the values of the sectional areas obey the distribution that $a_1 \sim \mathcal{N}(1, 0.1), a_2 \sim \mathcal{N}(1, 0.1)$. The stress applied to the system acts at the node 3 and follows the distribution $f \sim \mathcal{N}(1, 0.3)$. The limit state is expressed as the nodal displacement at node 3

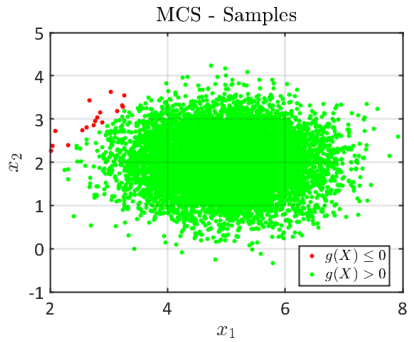

(a) Monte Carlo Sampling.

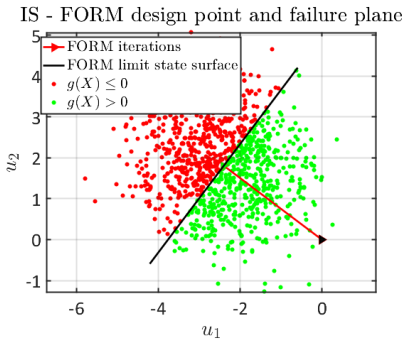

(b) Importance Sampling.

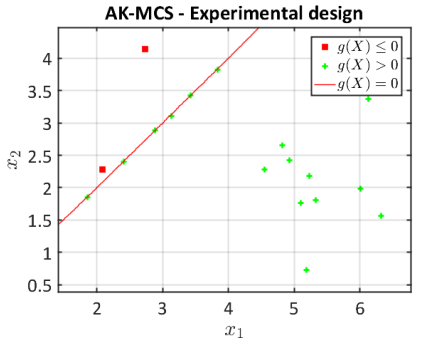

(c) AK-MCS Experimental Design.

Figure 3.12: The Experimental Sampling Design for $g_X = R - S$.

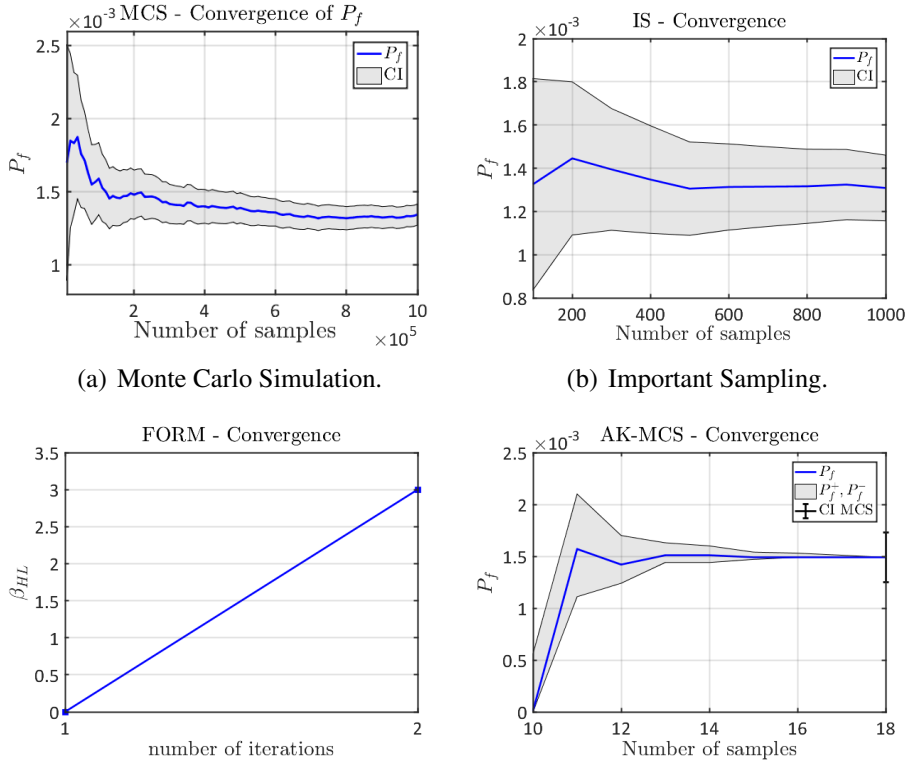

(a) Monte Carlo Simulation.

(b) Important Sampling.

(c) FORM Simulation.

(d) AK-MCS Simulation.

Figure 3.13: The Convergence Comparison for $g_X = R - S$.

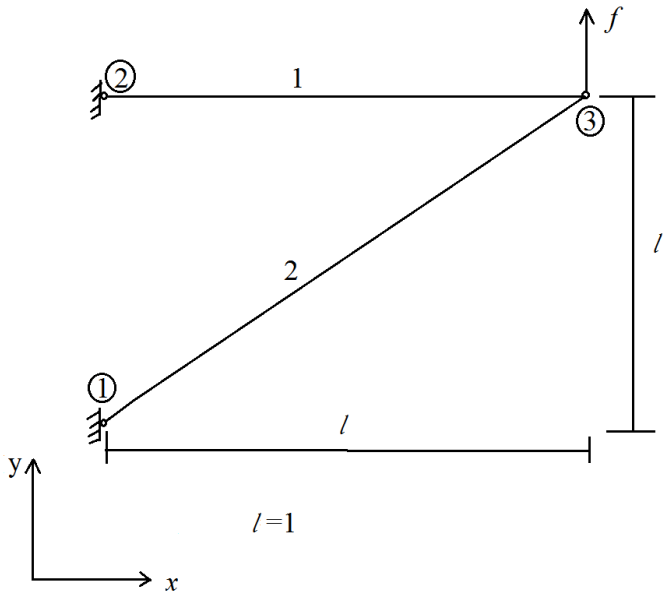

Figure 3.14: Two-bar Truss Structure.

which is required to be less than 5. The acquired reliability results of the two-bar structure with different analysis methods are shown in Fig.3.15(a), and Table 3.1.

Table 3.1: Reliability Analysis Results of Two-bar Truss Structure with Different Evaluation Methods

Evaluation Methods	Failure Probability	Reliability Index	Numbers of Experimental Designs	Failure Probability Confidence Interval
MCS	$4.92e-4$	3.30	$10e5$	$[4.49e-4, 5.35e-4]$
FORM	$4.34e-4$	3.33	40	–
IS	$5.04e-4$	3.29	60040	$[4.95e-4, 5.13e-4]$
AKMCS	$4.80-4$	3.30	25	$[3.44e-4, 6.16e-4]$

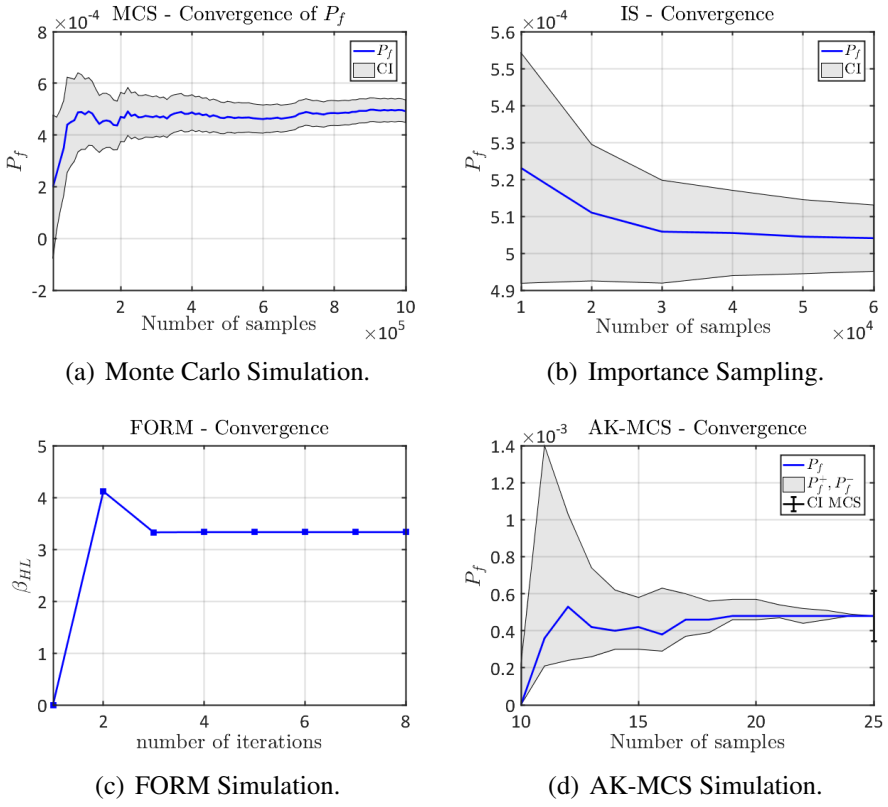

(a) Monte Carlo Simulation.

(b) Importance Sampling.

(c) FORM Simulation.

(d) AK-MCS Simulation.

Figure 3.15: The Convergence of the Failure Probability for the Two-bar Truss Structure.

3.3.6 Comparison of the Simulation Techniques

(a) FORM and SORM

For using FORM or SORM methods, some special requirements need to be satisfied. Firstly, all the random variables must be in the form of standard normal distribution, and then all the random variables must be independent of each other. Finally, the limit state function must be suitable enough to be represented with lucid expression and differential.

However, some nonlinear limit state functions apparently do not satisfy the requirements for the FORM or SORM. Sometimes the limit state cannot always be expressed with a function in real life, and this makes the use of FORM and SORM impossible in these cases. Besides, FORM and SORM may lead to non-convergence due to the presence of numerical noise.

(b) Monte Carlo Simulation

Monte Carlo simulation uses randomness to solve problems that might be deterministic. The problems could be difficult or impossible to use other approaches. The accuracy of the Monte Carlo simulation relies on the number of samples. Thus, a high number of evaluations of the objective function or limit state function are required.

The Monte Carlo simulation can be used as long as the deterministic solution is analytically available, without any modifications of the existing algorithm for structural analysis. However, a direct Monte Carlo simulation would, therefore, be unpractical in the applications of computationally expensive evaluations. For the analysis of the arch dam structure in this work, it is impossible to evaluate the limit state with the given sample size.

(c) Importance Sampling

Importance sampling is to concentrate the distribution of sampling points in the region of most importance. The area that mainly contributes to the failure probability, instead of spreading them out evenly among the whole range of possible values of the basic variables. (see Fig.3.13(a) and Fig.3.13(b))

With the help of importance sampling, it makes an otherwise infeasible problem amenable to Monte Carlo. It can also yield an estimate with infinite variance when simple Monte Carlo would have infinite variance. However, the importance sampling can only improve the calculation efficiency to a certain degree. It is still a computationally expensive method for complex analysis problems as the structural analysis of the arch dam.

(d) Metamodel-based Approach: RSM and AK-MCS

Metamodel approach is to use a sequence of designed experiments to explore the relationships between objective or limit state and several independent variables. The metamodel types most encountered in literature are response surface model (RSM), Kriging Metamodel, *etc*. The Metamodel is acknowledged as an approximation model, but it is easy to be estimated and applied, even when little is known about the process.

The advantage of the metamodel approach is to save the simulation time by reducing the number of structural FE analyses. However, attention should be paid to the accuracy and the model complexity. Even the best model acquired by the metamodel approach is an approximation in comparison to the reality.

How is a metamodel selected to be an approximation model is another challenge. Some works have approved the Kriging metamodel as a more suitable option compared with RSM since it provides more accurate predictions. Combining the metamodel and Monte Carlo simulation gives an efficient and convenient way to solve the probability problem such as the evaluation of the arch dam.

From the above comparisons and studies on different reliability evaluation methods, it can be seen that for an arch dam structural analysis, the FORM or SORM will not satisfy the requirements namely accuracy and applications in complex structural analyses. The Monte Carlo simulation cannot be applied in the structural analyses of large numbers due to the high expenses of the analysis of the structural dam. Even with the help of the importance sampling method, the required analysis number is obviously reduced, it is still too time-consuming to be applied to the reliability analysis method.

The Adaptive Kriging Monte Carlo method shows its advantage in the reliability analysis of the arch dam. The Kriging metamodel provides an ideal approximation model for the complex structural analysis to make it possible to use Monte Carlo simulation to do the reliability analysis with a sufficient number of samples. Hence, the AK-MCS is selected as the reliability analysis method for the RBDO process of the arch dam.

3.3.7 Examples for the Illustration of RBDO

In this section, the 10-bar truss structure shown in Fig.3.16 is used to illustrate the numerical performance of the proposed RBDO. To display this method in a simple and clear way, the design for a truss structure, which needs the design of the cross-sectional area of bars, $a_1, a_2, \ldots, a_{10}$, under the action of loads on the nodes 4 and 6. The objective is to find the minimum structural weight with the performance constraint, which is considered as the displacement at node 6 in this case.

The Young's Modulus and the mass density of the truss material are supposed to be 1.0. The cross-sectional areas of the bars are random design variables. The loads acting on the fourth and sixth nodes are supposed to follow a normal distribution with mean value $\mu_f = 1$, and standard deviation $\sigma_f = 0.3$.

The constraints considered in this problem include:

(a) reliability constraint, which is expressed as the reliability index $[\beta_r] \leq \beta_r$,

(b) nodal displacement constraint, also as limit state, which requires the nodal displacement for the sixth node, $\|u_6\|^2 = u_{6x}^2 + u_{6y}^2 \leq 5^2$,

(c) bound limits for the design variables: $1.0e-5 \leq a_1 \leq 6.0 \quad (i = 1, 2, \ldots, 10)$.

Then, the formulation of the RBDO for optimization problem of the truss structure can be expressed as:

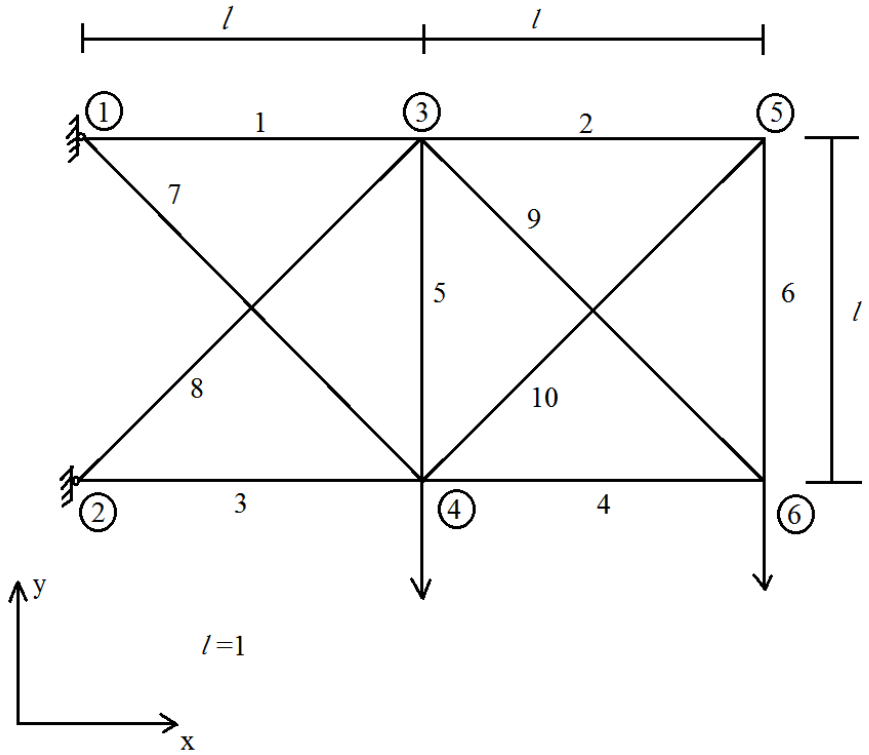

Figure 3.16: 2D Truss Structure.

$$\begin{aligned} \text{find} \quad & (a_1, a_2, \ldots, a_{10}) \\ \text{minimize}: \quad & Weight(a_1, a_2, \ldots, a_{10}) = \sum_{i=1}^{10} \rho_i l_i a_i \\ \text{subject to} \quad & \frac{u_6}{[u]} - 1 \leq 0 \\ & \frac{[\beta_r]}{\beta_r} - 1 \leq 0 \end{aligned} \tag{3.33}$$

In this work, the GA method is selected to discover the global optimum design. The Fig.3.17 shows the optimum results where the GA method has some fluctuations around their mean values, therefore, the mean values of the optimum results are chosen as the optimum design.

The optimization process, using the DO and RBDO methods are shown in Table 3.2, the optimum design with different $[\beta_r]$ are also listed in this table.

From the comparison of the optimum results, the RBDO is much more feasible but conservative than the optimum design from the DO method.

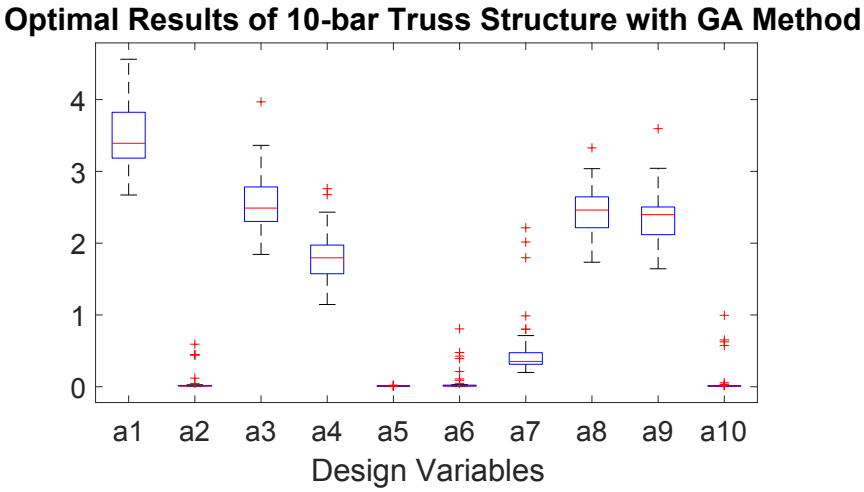

Figure 3.17: Fluctuation of Optimum Results with GA Method.

Table 3.2: Optimum Designs of Truss Structure with RBDO Method for Different Reliability Index Constraints

Design Variables	DO method	$[\beta_r] = 3.5$	$[\beta_r] = 3.7$	$[\beta_r] = 4.0$	$[\beta_r] = 4.2$
a_1	2.924	3.302	3.792	3.242	3.315
a_2	0.010	0.010	0.672	0.409	0.877
a_3	2.160	1.370	2.521	2.481	3.157
a_4	2.016	2.617	1.313	1.343	1.220
a_5	0.010	0.010	0.011	0.010	0.010
a_6	0.010	0.010	0.526	1.066	0.762
a_7	0.316	0.222	1.025	1.015	1.271
a_8	2.545	3.050	1.570	2.198	2.264
a_9	1.869	2.396	1.988	2.721	2.033
a_{10}	0.010	0.010	0.492	0.534	0.739
Weight	13.832	15.348	16.081	17.698	18.260

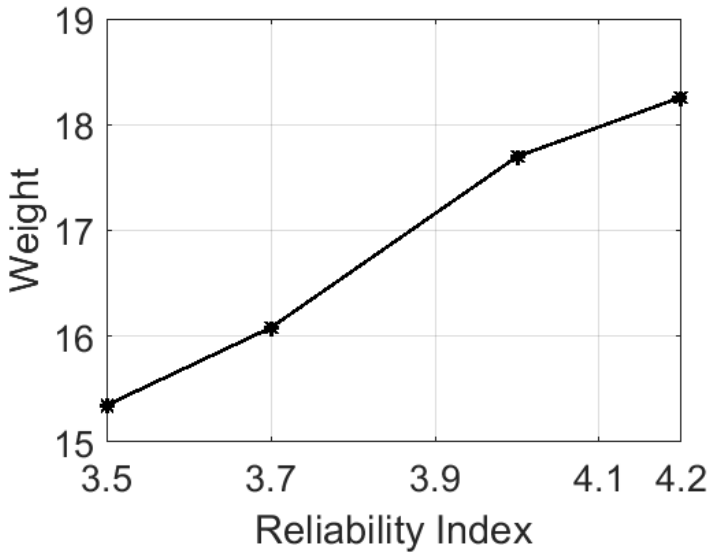

Figure 3.18: Relation between Reliability Index and Structural Weight(10-bar Truss)(AK-MCS Method).

In order to see the influence of the reliability constraints on the optimum design, a series of tests are performed. From Fig.3.18, the weight of the optimum tends to increase to satisfy the higher demands on the reliability constraint.

3.3.8 The Shape Optimization of Arch Dams with RBDO

A reliability constraint is involved in judging on the prediction and evaluating the dam's safety. The success of the reliability analysis relies on the modeling of uncertainties in the parameters, which are treated as random variables while computing the limit state.

The stability of the dam is influenced by various sources of uncertainties existing in the structure and surrounding environment, and these uncertainties can be mainly classified into loads and material properties.

In this study, the main considered load uncertainties are the variation of the temperature and water level on the upstream surface. The properties of constructing material, for which are chosen to reflect the uncertainties in the materials, are the tensile strength, compressive strength, Young's Modulus, and density, as they have been identified as the main parameters in a preliminary sensitivity analysis. The distributions of the statistical random variables are listed in Table 3.3, where the data is assumed according to ([30,35]).

Parameter	Mean	Standard Deviation	Distribution
Temperature Variation (°C)	5.4	1.378	Normal
Water level(m) (m)	135.00	2.835	Normal
Tensile strength (MPa)	3.00	0.3	Normal
Compressive strength (MPa)	30.00	3.00	Normal
Young's Modulus (MPa)	2.1×10^4	2.1×10^3	Normal
Density (kg/m^3)	2400	240	Normal

Table 3.3: Assumptions on Material Parameters

However, for the dam structure, uncertainties are existing in the distribution of the material, i.e., the values of the material properties are not isotropic throughout the structure, and the random field analysis is introduced to evaluate these particular uncertainties. In order to simplify the analysis, the uncertainties are considered only in two directions along the surface of the dam, and the material properties are kept constant in the direction of thickness.

Assuming two positions τ_1 and τ_2, which are separated by distance $\tau = \tau_1 - \tau_2$, the random variables $X(\tau_1)$ and $X(\tau_2)$ at these two positions show some dependence on each other. The probability density function, which describes the complete probabilistic behavior of a random process, can be written as follows:

$$f_{X_1,X_2,X_3,\ldots}(x_1,x_2,x_3,\ldots), \tag{3.34}$$

where $X_1, X_2, \ldots$ are different locations in the computational domain and $x_1, x_2, \ldots$ are possible values that the random field may have at these locations. In order to characterize the degree of dependence of the two positions, a correlation function is introduced.

There are many models to express the correlation function, such as the triangular correlation function, the polynomially decaying correlation function, the Markov correlation function or the Gaussian correlation function, e.g., ([64]). In this work, the Markov correlation function is used, and the fields are generated by Karhunen-Loève expansions:

$$\begin{aligned} \rho(\tau_1,\tau_2) &= \frac{C(\tau_1,\tau_2)}{\sigma^2} \\ &= \exp\left\{-\frac{2}{\theta}(|\tau_1|+|\tau_2|)\right\} \\ &= \exp\left\{-\frac{2|\tau_1|}{\theta_1}\right\}+\exp\left\{-\frac{2|\tau_2|}{\theta_2}\right\}, \end{aligned} \tag{3.35}$$

where θ_1, θ_2 are the correlation lengths along two directions. The random fields of each material property are created. Assuming that the correlation length is larger than the length of the dam. Fig.3.19 gives the random fields of each property used in the analysis:

The evaluation of the limit state function $g_X(X_1, X_2, \ldots, X_n)$ is costly using Monte Carlo simulation requiring a large number of samples, especially for a big and complex analysis model. Based on the characteristics of Kriging metamodels which assures comparably accurate prediction value of the limit-state function with a corresponding limit-state function response.

With the application of Adaptive Kriging Monte Carlo Simulation (AK-MCS), a corresponding limit-sate function response with the adaptive Kriging metamodel

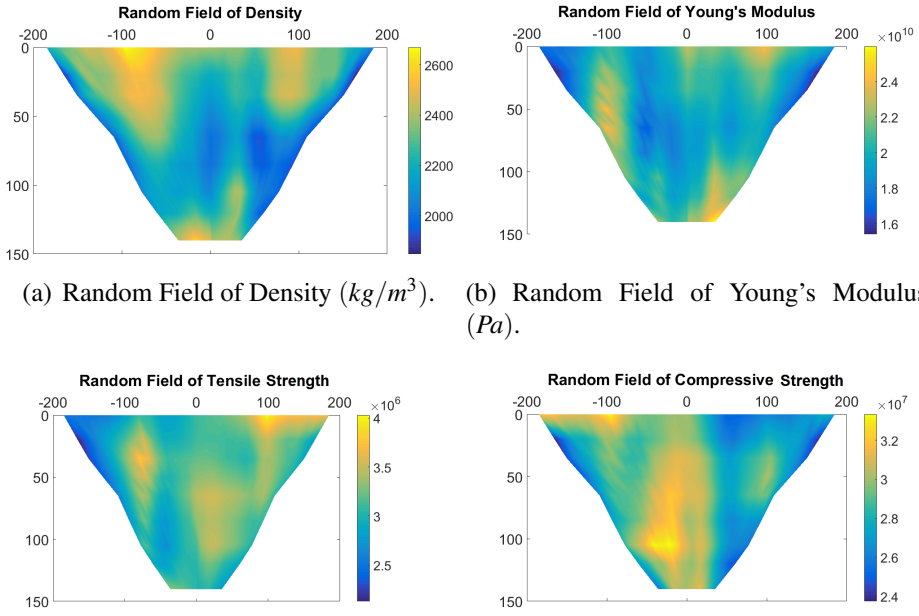

(a) Random Field of Density (kg/m^3). (b) Random Field of Young's Modulus (Pa).

(c) Random Field of Tensile Strength (Pa). (d) Random Field of Compressive Strength (Pa).

Figure 3.19: Random Field of Material's Properties.

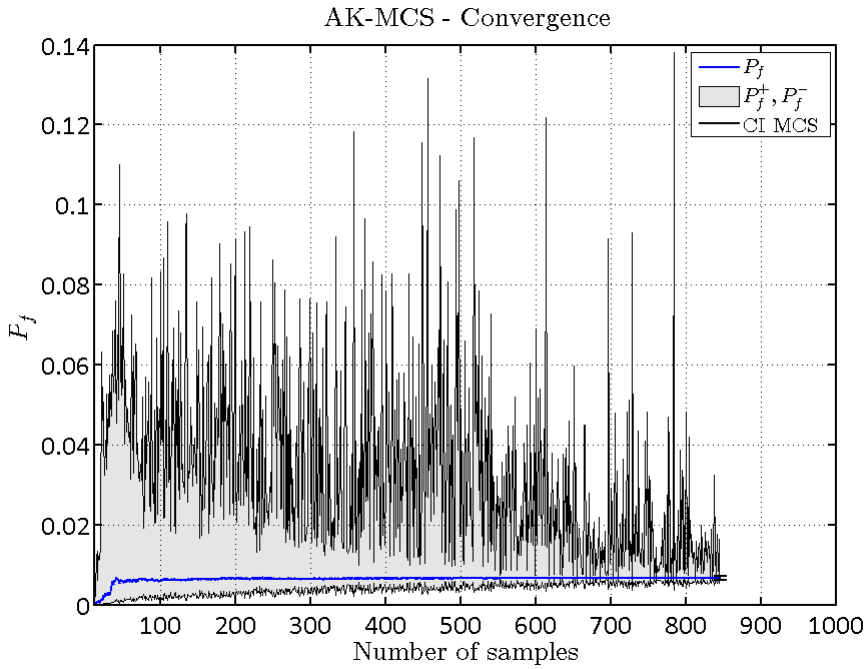

Figure 3.20: AK-MCS Convergence.

is generated, and then the failure probability is evaluated through Monte Carlo simulation with the final limit-state function response. This reliability analysis is realized by the program UQLAB ([67]) developed at the Chair of Risk, Safety an Uncertainty Quantification of ETH Zurich. Fig.3.20 and Table 3.4 show values of the reliability analysis results with AK-MCS method.

Failure Probability	$1.16e-4$
β_r	3.86
Model Evaluations	846

Table 3.4: The Reliability Analysis Results with AK-MCS

The structural state analysis is obtained through ANSYS with a mesh-convergence test checked element size. The dam body is divided into 1536 elements, the detail geometrical description of the arch dam is mentioned in Section 2.2. The optimization procedure is performed by coupling ANSYS with MATLAB where the optimization and reliability analysis are implemented.

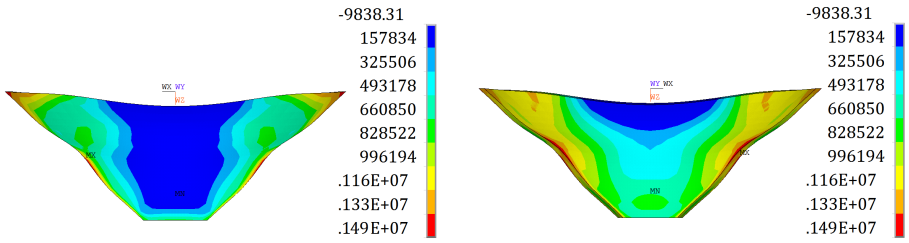

(a) Dam Upstream. (b) Dam Downstream.

Figure 3.21: First Principal Stress of the Optimal Model(Pa).

The loads considered in the optimization procedure are: dead load, hydrostatic pressure on the upstream face and the uplift pressure on the foundational interface. Additionally, a realistic assessment of loading of water flow and temperature are also considered for the coupled response of shape optimization. The load combination is Self-weight, hydrostatic pressure, uplift pressure, and temperature.

Through the above-mentioned procedure, the optimized arch type dam is generated (see Table 3.5). Since the tensile stress shows an important influence on the structure's safety, the comparison between tensile stresses is used to illustrate the advantages of the optimized results. The following Fig.3.21- Fig.3.22 and Table 3.6 illustrate the optimization results of the arch type dam.

Table 3.5: Geometrical Parameters of the Optimal Arch Dam with RBDO Method

Height	Thickness(m)	Central Angle$'2\phi'(^\circ)$	Coefficient$'a'$
140	6.51	130.68	−0.799
120	7.49	116.23	−0.579
105	8.40	105.62	−0.457
90	9.83	91.75	−0.354
75	11.52	78.23	−0.317
55	12.95	68.30	−0.333
35	14.53	58.57	−0.386
20	16.25	49.02	−0.477
0	18.78	36.58	−0.657

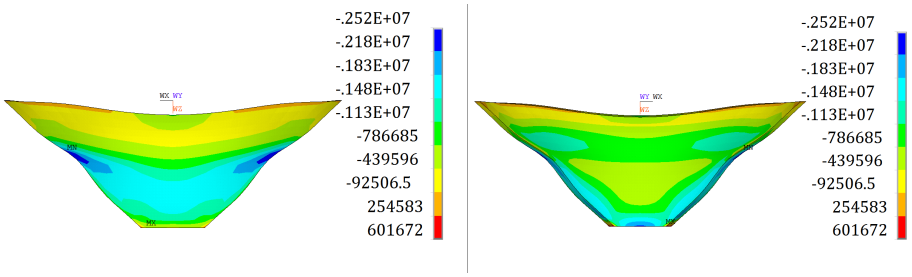

(a) Dam Upstream. (b) Dam Downstream.

Figure 3.22: Third Principal Stress of the Optimal Model(Pa).

	Volume (m^3)	Maximum tensile stress(MPa)	Maximum compressive stress(MPa)	Reliability index
Optimized Model	3.42e5	1.79	4.61	3.863

Table 3.6: The Optimization Results of Arch Dam with RBDO

3.4 Robust Design Optimization (RDO)

3.4.1 General Description of the RDO Method

Robust Design Optimization aims at searching out a design candidate that is less sensitive to changes in the variable parameters and was first introduced by Taguchi ([12,53]). It has and continues to gain recognition in recent years, as an effective design method to improve the quality of the design for engineering products. The RDO is involved in the concepts of minimum tolerance design.

For general optimal designs, the structure is subjected to large scatter at different stages of service lifecycle, which may not only concern the structural quality with deviations from expected performance but also may add to the structural maintenance costs. For an engineering perspective, a well-designed structure minimizes costs by performing in the presence of uncontrollable variations during the whole life-cycle. Another indicator of a poorly designed structure is the variation of the structural performance.

In robust design optimization, the structure must minimize the costs from the deviation of the structural performance. To fulfill the idea, the design in which the structural performance must be less sensitive to the variation of the struc-

tural system. The RDO is mainly focused on the minimum range of variation and only partly on the mean value. The principle behind the RDO is that the quality of structural design is evaluated not only by the mean value but also by the ability to resist the uncertainty factors. The multi-objective optimization is involved in offering an objective function combining both minimum mean value and minimum variation of structural performance.

3.4.2 Mathematical Formulation of the Robust Design Optimization

The idea behind the robust design optimization is to acquire an optimum design and improve the structural quality by minimizing the variation of the structural performance. Hence, the optimization problem is stated as a multi-objective problem expressed by a weighted sum function.

The mean value of the object $E(f(\mathbf{x}))$, as well as the standard deviation of the performance response $\sigma(h(\mathbf{x}))$, is used to define the objective function and constraints in a weighted sum function. Similar with the RBDO approach, uncertainty is introduced using probability distributions. The formulation for a robust design optimization can be formed as:

$$\begin{array}{rc} \text{find} & \mathbf{x}, \\ \text{minimize} & \{E(f(\mathbf{x})), \sigma(h(\mathbf{x}))\}, \\ \text{subject to} & P_f[g(\mathbf{x}) \leq 0] \leq P_0, \\ & \mathbf{lb} \preceq \mathbf{x} \preceq \mathbf{ub}, \end{array} \tag{3.36}$$

where $f(\mathbf{x})$ and $g(\mathbf{x})$ are the objective function and constraints described in the deterministic optimization problem, $h(\mathbf{x})$ is any selected structural response (or a combination of several ones), for which minimal variations are sought-for.

One of the attempts to reduce the computational costs of the above optimization problem is the moment matching method ([73]), which assumes the constraint is normally distributed and is as follows :

$$\mu_g + k\sigma_g \leq 0, \tag{3.37}$$

where μ_g and σ_g are the vectors containing the mean value and the standard deviation of constraints, and $k = \Phi^{-1}$ is the inverse function of the CDF of a standard normal distribution. For example, when $k = 2$ represents for a failure probability of 0.0228 and $k = 3$ represents for a failure probability of 0.0087.

From here, it is shown that the exact failure probability is not the main concern of the robust design optimization problem, although the feasibility may be improved with the increase of the value of the parameter k. Also, it should be aware that the probability distribution of the function value $g(\mathbf{x})$ is still assumed to be normal, and it is reasonable from an engineering point to give such an assumption of the structural performance.

For the calculation purpose, the formulation of Eq.3.37 does not result in an efficient way to solve the problem. In order to improve the calculation process, the linear weighted sum function is involved. The objective function is transformed into a linear combination of the individual objectives with a series of weights. In this way, the trade-offs between the individual objects depend on the relative weights occupied in the combined objective function. Introducing Eq.3.37 into Eq.3.37, the problem of RDO can be written as follows:

$$\begin{array}{ll} \text{find} & \mathbf{x}, \\ \text{minimize} & \alpha_w \frac{\mu_f}{\mu_f^*} + (1-\alpha_w)\frac{\sigma_h}{\sigma_h^*}, \\ \text{subject to} & \mu_g + k\sigma_g \leq 0, \\ & \mathbf{lb} \preceq \mathbf{x} \preceq \mathbf{ub}\ . \end{array} \tag{3.38}$$

Here $0 \leq \alpha_w \leq 1$ is the factor weighting the two objectives, the μ_f^* and σ_h^* are normalization factors.

From Eq.3.39, we can see that when $\alpha_w = 1$, the problem could be transformed to a pure function value optimization problem, and when $\alpha_w = 0$, it is changed to be a pure standard deviation minimization problem.

Different calculation techniques can be used to solve the RDO problem, as described in Section 3.3.4. In this study, the metamodel is introduced to solve this RDO problem. The advantage of using approximation metamodel in combination with the evolution optimization method, referred as the GA method in this work, is that it simplifies the calculation of standard deviation and mean value using an approximation model instead of doing a FE analysis for such a complex

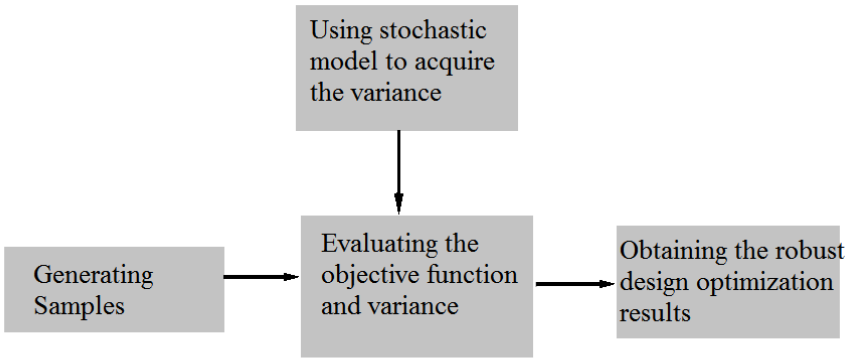

Figure 3.23: The Optimization Procedure of the RDO.

structure and increase the computational efficiency. The procedure of the RDO method can be concluded as in Fig.3.23.

3.4.3 Example for Implementation

For the sake of comparison, the 10-bar truss structure used in Section 3.3.7 is analyzed using the RDO method and the above proposed mathematical model. In this problem, the parameter $k = 3$, the performance constraint condition is the displacement on the node 6, which is $\mid u_6 \mid \leq 5$. The searching target is to find the design candidate for the minimization of the structural weight and nodal displacement. The optimization for the truss structure is represented as:

$$\begin{array}{ll} \text{find} & \mathbf{x} = [a_1, a_2, \ldots, a_{10}]^T, \\ \text{minimize} & \alpha_w \frac{Weight(a_1,a_2,\ldots,a_{10})}{Weight(a_1,a_2,\ldots,a_{10})^*} + (1-\alpha_w)\frac{\sigma_{u_6}}{\sigma^*_{u_6}}, \\ \text{subject to} & \mu_g + k\sigma_g \leq 0, \\ & \mathbf{lb} \preceq \mathbf{x} \preceq \mathbf{ub}. \end{array} \tag{3.39}$$

The $Weight(a_1,a_2,\ldots,a_{10})^*$ is the weight at nominal design, and the $\sigma^*_{u_6}$ is the standard deviation of selected structural performance at the nominal design . The following Fig.3.24 shows a comparison of the variation of nodal displacements

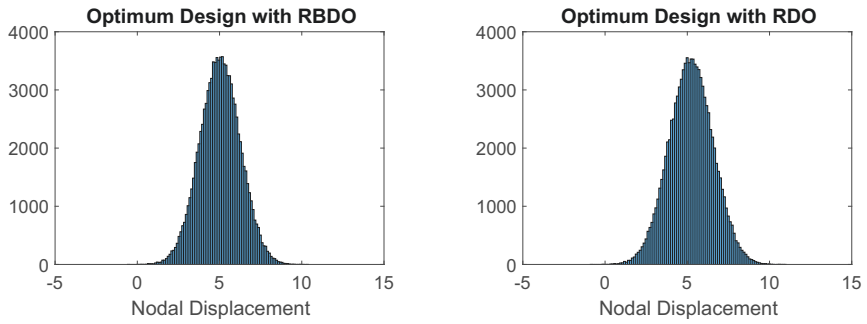

(a) Optimal Design with RBDO for $\beta_r = 3.7$.

(b) Optimal Design with RDO for $\alpha_w = 0.5$.

Figure 3.24: Occurrence Frequency Distribution of Nodal Displacements for the 10-bar Truss Structure.

Table 3.7: Comparison of Optimal Truss Structures Acquired by the RBDO and the RO Method

RBDO	Mean Value	Standard Deviation	RDO	Mean Value	Standard Deviation
$[\beta_r] = 3.5$	5.293	1.352	$\alpha_w = 0.7$	5.522	1.418
$[\beta_r] = 3.7$	5.030	1.338	$\alpha_w = 0.5$	5.280	1.298
$[\beta_r] = 4.0$	5.001	1.286	$\alpha_w = 0.3$	5.161	1.256
$[\beta_r] = 4.2$	4.9463	1.206	$\alpha_w = 0$	1.810	0.428

on node 6 between RBDO ($[\beta_r = 3.7]$) and RDO ($\alpha_w = 0.5$) under the same uncertainty assumption for the load condition.

From the comparison, the mean value of the displacement on the selected node for the two designs are 5.030 for RBDO and 5.280 for RDO respectively, whereas the standard deviation is 1.790 for RBDO and 1.685 for RDO. The detailed comparison is listed in Table 3.7.

As can be seen from the results, the RDO method leads to a higher expected value but a much smaller range of variation of the nodal displacements on the selected node. It implies that the design acquired by RDO method is superior in terms of robustness since the corresponding structural performance is less sensitive to the variation of the system and has a smaller scatter.

Table 3.8: Optimal Truss Structure with Different Weighting Parameters

Design Variables	$\alpha_w = 0$	$\alpha_w = 0.3$	$\alpha_w = 0.5$	$\alpha_w = 0.7$	$\alpha_w = 1$
a_1	6	3.152	3.3020	3.094	2.924
a_2	6	0.697	0.6724	0.010	0.010
a_3	6	3.222	2.6450	2.282	2.160
a_4	6	1.343	1.4215	2.318	2.016
a_5	6	0.010	0.0106	0.010	0.010
a_6	6	0.795	0.6010	0.010	0.010
a_7	6	1.387	0.3025	0.300	0.316
a_8	6	1.668	3.0171	2.312	2.545
a_9	6	1.896	2.3458	1.821	1.869
a_{10}	6	0.974	0.0429	0.010	0.010
Weight	63.9511	17.598	16.076	14.008	13.832

Also, to illustrate the influence of parameter α_w, the optimal design obtained with different weighting factors α_w are summarized in Table 3.8. As can be seen from the results, when the weight ratio for minimum standard deviation increases, the optimal solution results in a larger mean value but a smaller standard deviation of the structural performance.

3.4.4 Optimization of Arch Dams with RDO Method

We apply the above mentioned RDO method to the optimization of the arch dam model which is described in Section 3.3.8. The acquired optimal design is described in the following Table 3.9. Fig.3.25-Fig.3.26 give the stress state of the optimized model using RDO method, and the optimized results are reported in Table 3.10.

Table 3.9: Geometrical Parameters of the Optimal Arch Dam with RDO Method

Height	Thickness(m)	Central Angle$'2\phi'(^\circ)$	Coefficient$'a'$
140	5.23	111.70	−0.31
120	6.57	102.97	−0.18
105	7.59	96.12	−0.100
90	8.61	89.02	−0.03
75	9.65	81.66	0.02
55	11.05	71.45	0.06
35	12.47	60.77	0.09
20	13.55	52.47	0.08
0	15.04	40.99	0.06

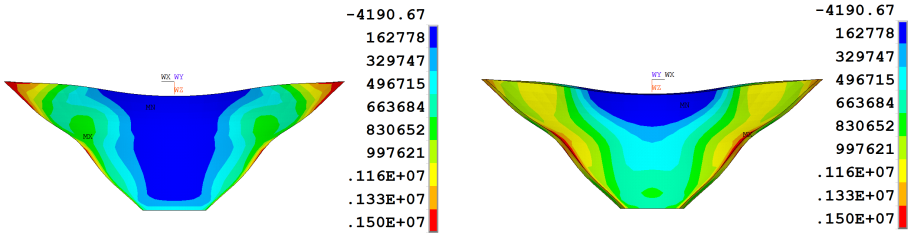

(a) Dam Upstream. (b) Dam Downstream.

Figure 3.25: First Principal Stress of the Optimal Model (Pa).

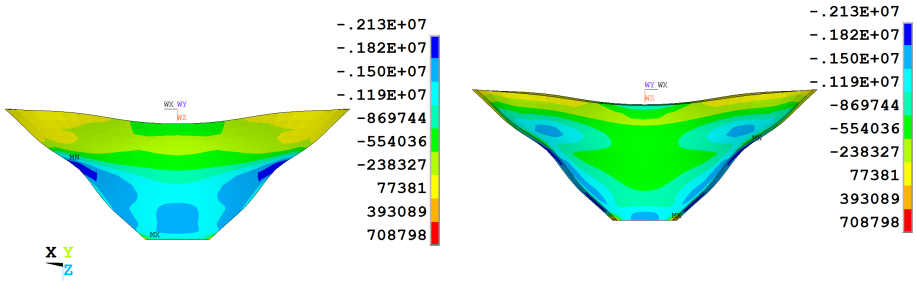

(a) Dam Upstream. (b) Dam Downstream.

Figure 3.26: Third Principal Stress of the Optimal Model (Pa).

Table 3.10: The Optimization Results of the Arch Dam with RDO

	Volume (m^3)	Maximum tensile stress (MPa)	Maximum compressive stress (MPa)
Optimized Model	3.068e5	1.50	2.51

3.4.5 Comparison of the Optimal Designs of the Arch Dams between RBDO and RDO

As a non-deterministic structural optimization formulation for the design of the arch dam, both methods aim at incorporating random performance into the optimization process to acquire a robust and reliable structure. The RBDO is to minimize the structural volume under failure probability constraints in extreme events, and the RDO is to reduce the variability of structural performance as well as minimizes the structural volume. Since the evaluation of failure constraint and structural performance are both the tensile stresses, the comparison of the tensile stresses of these two optimal designs for arch dams under 200 randomly generated samples are shown in Fig.3.27 to see the difference between these two acquired optimal designs.

It can be seen that the tensile stress is highly concentrated around the mean value for the optimal design acquired by the RDO method, the optimal design acquired by RBDO tends to have a smaller mean value but a larger deviation range.

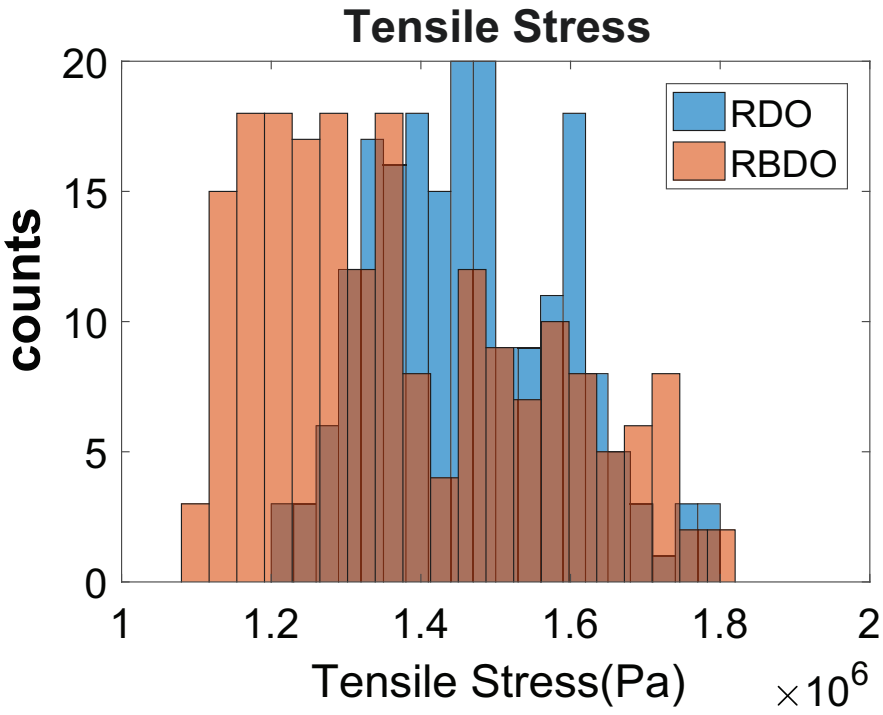

Figure 3.27: Comparison of Occurrence Frequency Distribution of the Maximum Tensile Stress for RDO and RBDO.

3.5 Conclusion

Both RBDO and RDO provide non-deterministic structural optimization formulations. Although both of them incorporate statistical models into the design process, the optimal solutions of these two methods both exhibit increased reliability. However, there still exist differences between these two methods.

- The reliability-based design optimization approach takes the reliability index into account as a constraint condition. Note, that the objective function is expressed in the same way as the deterministic optimization method, which means the RBDO method concerns less the variation of the structural performance under uncertainties. Unlike the RBDO, the robust design optimization approach takes the variation of performance as part of the objective function. Comparing to RBDO, RDO concerns more on finding a design that is relatively insensitive to uncertainties. In another word, the RBDO is to move the mean of the performance, and the RDO is to reduce the performance variability.

- Since the RBDO takes the reliability index as a constraint condition, it evaluates the structural safety or design quality in the extreme events, while in contrast, the RDO evaluates the structural design by the structural performance variation under the fluctuations of the whole structural system. Although, both RBDO and RDO rely on the predefined distributions of inputs, RBDO shows a more profound dependence on the accuracy of the assumption on the probabilistic distributions. However, the RDO method concerns less on the precise description of the statistical model than the RBDO method, for that the RDO method involves only the prediction of basic characteristics of the performance variability.

- The RDO approach is solved by using a multi-criteria optimization problem, where the influence of choosing the weighting factor becomes an essential part of this approach. Currently, there are no defined rules on how to determine the best weighting factors. The decision may be made according to practical design requirements.

Chapter 4

Optimization of Arch-type Dams with non-probabilistic Model under Uncertainties

4.1 Introduction

A probabilistic model relies sometimes rather visibly on the precise information given by the probability distribution of the uncertain variables, and this character makes the results less conservative. It is usually difficult to identify the underlying distribution of the actual data accurately. Even for a small number of parameters that can be further estimated by observations, accurate identification of the probability distributions requires an astronomical number of observations. Hence, the probabilistic approach more often than not is forced to be determined through assumptions of the actual distributions, and it is difficult to evaluate the influence of the uncertainties in the probability distribution.

An alternative approach to deal with the uncertainty is proposed as the robust optimization (RO), which is based on a non-probabilistic model that considers the uncertainty as the a parameter within an uncertainty dataset **U**. In this approach, it aims at finding a solution candidate that is relatively insensible to any realization of uncertainty in the given dataset **U**. With the robust optimization approach, the desire to stay on the safe side can be easily achieved by enlarging the uncertainty data set. For this character, this approach is also named as worst case design and optimization. Based on this frame, much research has been carried out to solve this optimization problem. A so-called convex model has been well analyzed by Ben-Haim ([54]) to describe the uncertainty of a system. Lat-

ter, Ben-Tal ([19]) proposed a unified methodology of a robust counterpart of a broader class of convex programming.

The RO methodology can be applied into every generic optimization problem where one can separate the uncertain data, which is known to belong to a given dataset, for structural optimization problem under uncertainties. In recent years, there is a burst of application of the RO for structural optimization problems, for example, Sun *et al.* ([16]) described a design in sheet metal forming using robust optimization, Kanno ([17]) and Guo ([18]) realized a bar truss structure's optimization under uncertainties with RO methods.

The focus of this chapter will be on the calculation frame and the mathematical techniques of the RO method. In Section 4.2, the robust optimization function is formulated. Some techniques, such as SDP, convex programming, bi-level formulation, *etc*., are introduced and discussed. Section 4.2.4 is devoted to a numerical example to illustrate the calculation procedure of the RO method in a specific way. Through the numerical example, the effectiveness of the RO approach is demonstrated. Finally, the RO method is applied to the optimization of the arch type dam, and some conclusions are given in the final section.

4.2 Description of the Robust Optimization Method

4.2.1 Uncertainty Analysis with Non-probabilistic Models

4.2.1.1 The Worst Case Analysis

The worst case analysis has been applied to various fields, such as environmental engineering, structural design, computer science, *etc*. In the approach of the worst case analysis ([73]), it is attempted to search out a point as far away as possible from the failure constraints. The idea behind this analysis is to minimize the objective function when all fluctuations are simultaneously in the worst possible combination. Uncertain parameters are modeled as deterministic data sets instead of probability density functions. Hence, this approach can simplify the incorporation of the variability into a deterministic problem.

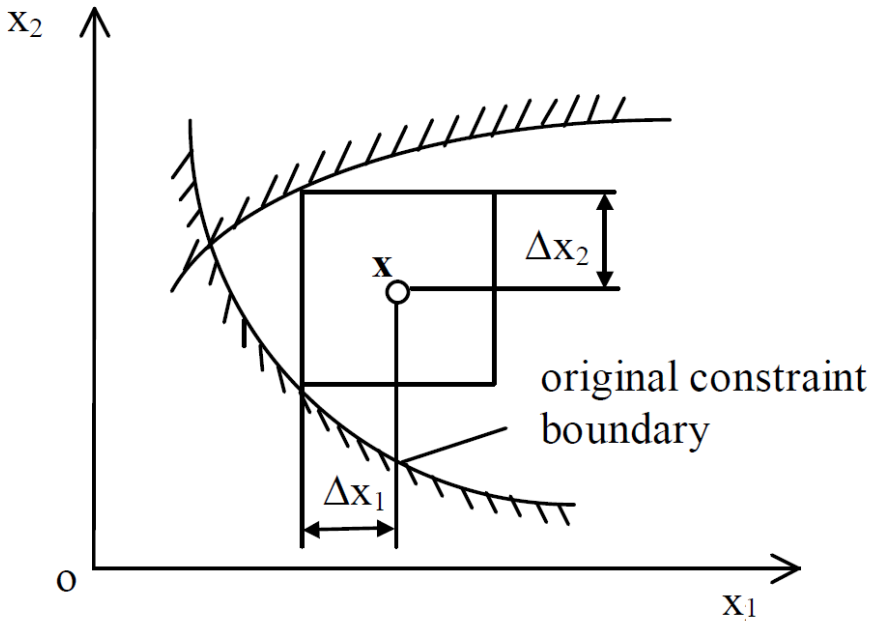

Figure 4.1: The Corner Space Evaluation ([2]).

4.2.1.2 The Corner Space Evaluation

Sundaresan *et al.* ([2]) proposed another estimating method, called the corner space evaluation. Similar with the worst case analysis, it is not required to define a probability distribution of uncertain parameters in advance. However, unlike the worst case analysis, the uncertain parameters are not transmitted into constraint functions in this approach.

Assume the uncertainty parameters have nominal values and tolerances. The tolerance space is defined as a set of points close to the target design point. In order to maintain the design feasibility, the design candidate should be inside the feasible region by maintaining contact between the corner space and original constraints (see Fig.4.1).

4.2.2 Robust Optimization Function

In general, a robust optimization problem with worst-case analysis can be expressed as the minimum value of the objective function at which the performance constraints cannot be violated, and subjected to any situation in confined data space. With a single level semi-infinite program, it can be written as:

$$\begin{aligned} \text{find} \quad & \mathbf{x} = (x_1, x_2, \ldots, x_n)^T \in \mathbf{R}^n, \\ \text{minimize} \quad & f(\mathbf{x}), \\ \text{subjected to:} \quad & g_i(\mathbf{x}, \boldsymbol{\xi}) \leq 0, \quad \forall \boldsymbol{\xi} \in \mathbf{U}, \quad i = 1, \ldots, m, \\ & \mathbf{lb} \preceq \mathbf{x} \preceq \mathbf{ub}, \end{aligned} \tag{4.1}$$

where $\mathbf{x} \in \mathbf{R}^n$ is the vector of design variables and $\boldsymbol{\xi} \in \mathbf{U}$ is the vector of uncertain parameters within the data set $\mathbf{U}$.

Here, semi-infinite means the optimization problem possibly has an infinite number of constraints, and it is worth nothing to solve a numerically intractable optimization problem with infinitely many constraints. In order to avoid this problem, one possible method is to replace Eq.4.1 with the following bi-level format:

$$\begin{aligned} \text{find} \quad & \mathbf{x} = (x_1, x_2, \ldots, x_n)^T \in \mathbf{R}^n, \\ \text{minimize} \quad & f(\mathbf{x}), \\ \text{subject to:} \quad & \max_{\boldsymbol{\xi} \in \mathbf{U}} g_i(\mathbf{x}, \boldsymbol{\xi}) \leq 0, \quad i = 1, \ldots, m, \\ & \mathbf{lb} \preceq \mathbf{x} \preceq \mathbf{ub}. \end{aligned} \tag{4.2}$$

In the bi-level Eq.4.2, the upper level is to find the design which is optimum for the structural objective function, while the lower level aims at finding the worst case structural performance responses, which are used to test the feasibility of the selected design candidate.

For the lower level problem in Eq.4.2, only the global optimum can accurately determine the feasibility of a given design. However, if the lower level problem is a non-convex problem, it is highly possible to get a local minimum if the initial point of optimization is not chosen appropriately. Furthermore, it is always NP-hard (nondeterministic polynomial) to find the optimal global solution for a non-convex optimization problem.

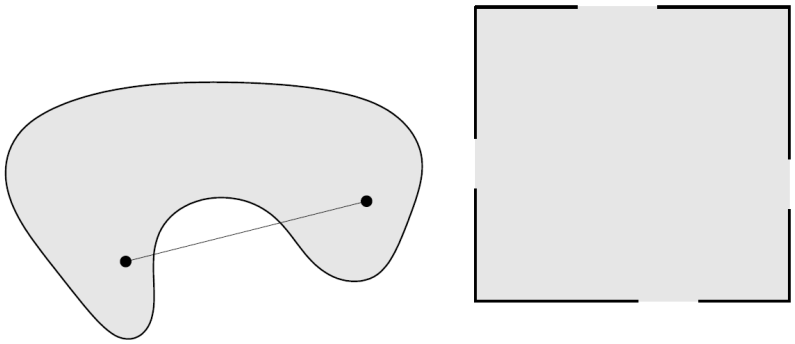

(a) The Kidney Shaped Set.

(b) The Square Contains Some Boundary Points But Not Others.

Figure 4.2: Some Non-convex Sets ([3]).

4.2.2.1 Convex Sets

Considering a set C is a convex set, it means the line segment between any two points x_1, x_2 in C have the following relation:

$$\kappa x_1 + (1-\kappa)x_2 \in C. \tag{4.3}$$

Here, κ is a parameter with $0 \leq \kappa \leq 1$. Following Fig.4.2-Fig.4.3 give some simple examples to illustrate the difference between convex and non-convex sets.

In the most general form, a point of the form $\kappa_1 x_1 + \cdots + \kappa_k x_k$, where $\kappa_1 + \cdots + \kappa_k = 1$ and $\kappa_i \leq 0, i = 1, \ldots, k$,is called a conic combination. When x_i are in a convex cone C, every conic combination of x_i is in C. Herein we discuss some critical examples of convex sets which are mostly used in mathematical techniques ([3]).

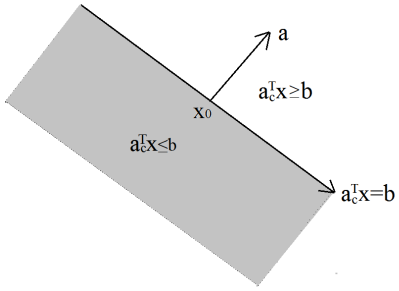

(a) Hyperplanes and Halfspaces.

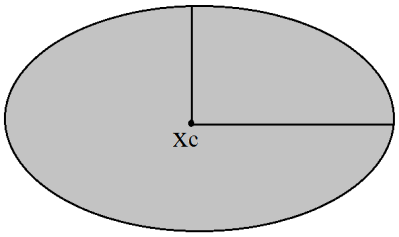

(b) An Ellipsoid in $\mathbf{R}^2$.

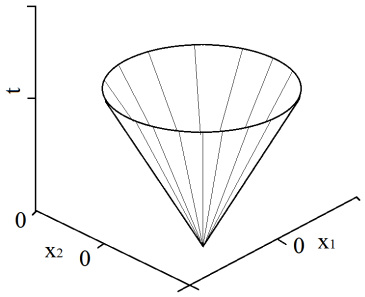

(c) A Norm Cone in $\mathbf{R}^3$.

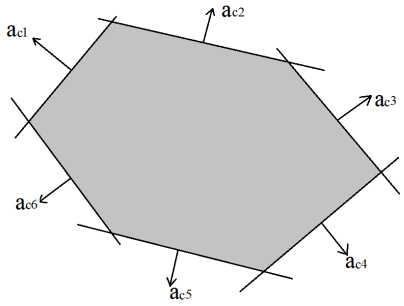

(d) A Polyhedra for the Intersection of Six Halfspaces, with Outward Normal Vectors $a_{c1}, \ldots, a_{c6}$.

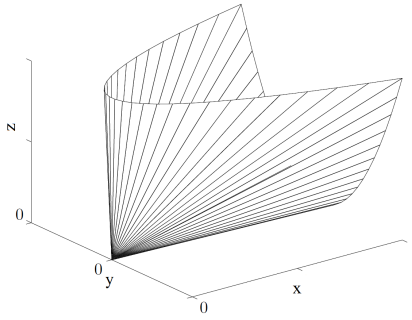

(e) A Semidefinite Cone in S^2.

Figure 4.3: Some Often Used Convex Sets ([3]).

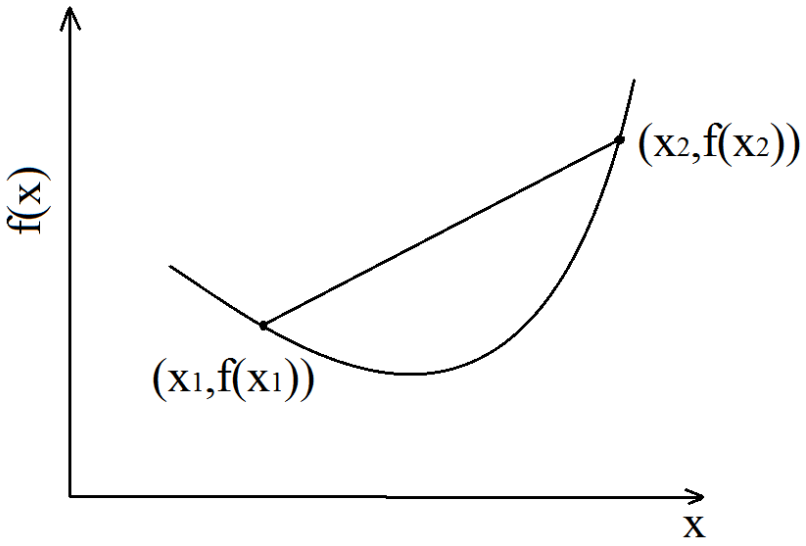

Figure 4.4: A Graph of the Convex Function.

4.2.2.2 Convex Function

A real-valued function is called a convex function only if the line segment between any two points on the graph of the function lies above the graph of the function (see Fig.4.4). In mathematical form, it can be expressed as:

$$f(\kappa x_1 + (1-\kappa)x_2) \leq \kappa f(x_1) + (1-\kappa) f(x_2) \quad (x_1, x_2 \in X), \tag{4.4}$$

where, $X \in \mathbf{R}$ is a convex set in a real vector space, κ is a parameter that is $0 \leq \kappa \leq 1$. If the strict inequality holds in Eq.4.4 whenever $x_1 \neq x_2$ and $0 < \kappa < 1$, the function is said to be strictly convex.

Generally, it is difficult to judge if the function is a convex function from the form of the function. Here are some steps to determine whether or not the function is convex.

(a) First-order Condition

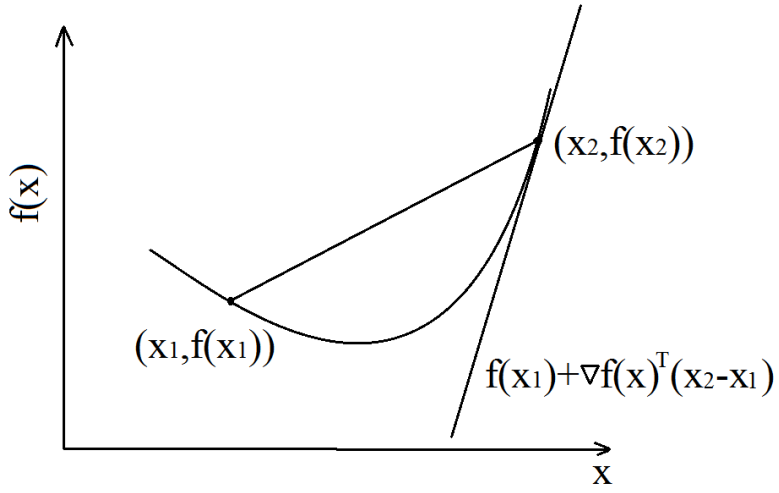

Figure 4.5: First-order Condition for Convex Function.

If f is differentiable, then f is convex only if the function lies above all of its tangents(Fig.2a), and its domain X is a convex set which means:

$$f(x_1) \leq f(x_2) + \nabla f(x_2)^T (x_2 - x_1). \tag{4.5}$$

This function holds for all $x_1, x_2 \in X$.

(b) Second-order Condition

If f is twice differentiable, which means its Hessian matrix exists at each point, then the conditions to judge whether the function f is convex are that the domain X is convex and its Hessian matrix is positive semi-definite, which means for all $x \in X$, there is :

$$\nabla^2 f(x) \succeq 0. \tag{4.6}$$

However, for structural optimization problems, the criteria are difficult to evaluate.

4.2.2.3 Duality

In mathematics, duality refers to the translation of mathematical structures into related structures. Let us consider the standard form of the optimization problem, which is:

$$\begin{array}{lll} \text{minimize:} & f(\mathbf{x}) & \mathbf{x} \in \mathbf{R}^n, \\ \text{subject to:} & g_i(\mathbf{x}) \leq 0, & i = 1, \ldots, m, \\ & h_i(\mathbf{x}) = 0, & i = 1, \ldots, p. \end{array} \tag{4.7}$$

The optimal value of this optimal problem is denoted as f^*, and the problem in Eq.4.7 is not convex. The commonly used duality function is the Lagrange duality function. The idea behind the Lagrange duality is to take the constraints in Eq.4.7 into account by augmenting the objective function with the sum of the weighted constraint function, and the Eq.4.7 can be rewritten as:

$$L(\mathbf{x}, \lambda, \nu) = f(\mathbf{x}) + \sum_{i=1}^{m} \lambda_i g_i(\mathbf{x}) + \sum_{i=1}^{p} \nu_i h_i(\mathbf{x}), \tag{4.8}$$

where λ, ν are the Lagrange multipliers associated with the constraint functions.

Then the Lagrange dual function G is defined as the minimum value of the Lagrange function over $\mathbf{x}$: for $\lambda \in \mathbf{R}^m, \nu \in \mathbf{R}^p$.

$$G(\lambda, \nu) = \inf_{\mathbf{x} \in \mathbf{R}^n} L(\mathbf{x}, \lambda, \nu) = \inf_{\mathbf{x} \in \mathbf{R}^n} \left(f(\mathbf{x}) + \sum_{i=1}^{m} \lambda_i g_i(\mathbf{x}) + \sum_{i=1}^{p} \nu_i h_i(\mathbf{x}) \right). \tag{4.9}$$

We can see that the dual function is the infimum of a family of affine functions of (λ, ν). Therefore, the function g is concave even if the function in Eq.4.7 is not convex. When the optimal value of the Lagrange dual problem is G^*, the important inequality exists:

$$G^* \leq f^*, \tag{4.10}$$

and it holds even if the original optimization problem is not convex. This property is characterized as weak duality. If the gap between the original problem and duality problem is zero, which is:

$$G^* = f^*, \tag{4.11}$$

it is called strong duality. Generally, the strong duality does not hold except if the original problem is convex.

4.2.3 Formation of the RO Method under Load Uncertainty

Generally, the uncertainty factors originate from both the variations of manufacturing material and operational conditions, which can also be treated as uncertainties in the structural stiffness and load. However, for an efficient application of the present approach, the uncertainties from the material's or resistance side are shifted towards the loading side, resulting in an increase in the assumed uncertainties in the loads and keeping the material constants fixed. The calculation processes for the load uncertainty and the stiffness uncertainty are different processes.

Compared to the problem of stiffness uncertainty, the problem under load uncertainty is easier solved, and the influence of material properties on structural response can be treated as a kind of loading response. Another reason is the complex relationship between material properties and structural design variables, and it is difficult to build a clear expression between design variables and structural stiffness for such a complex structure.

4.2.3.1 Problem Statement

Now, the range of the uncertainties of applied load is assumed to be expressed as an ellipsoidal model:

$$\mathbf{U} = \{\xi \in \mathbf{R}^n \mid (\xi - \xi_{\mathbf{0}})^T B_h (\xi - \xi_{\mathbf{0}} \leq 1\}, \tag{4.12}$$

where ξ is the applied load vector, $\xi_{\mathbf{0}}$ is the nominal value of ξ and B_h forms the shape matrix of the ellipsoid.

The goal is to find a robust design of the structure, considering both the minimum objective function and safe structural performance. The basic single-level programming including the uncertain variables does not fit into this problem

anymore; instead, bi-level programming is involved as follows:

$$\begin{aligned} \text{find} \quad & \mathbf{x} = [x_1, x_2, x_3, \ldots, x_n]^T \in \mathbf{R}^n, \\ \text{minimize:} \quad & f(\mathbf{x}) := Vol(\mathbf{x}), \\ \text{subject to:} \quad & \max_{\substack{K_g(\mathbf{x})u=\xi \\ \xi \in \mathbf{U}}} g_i(\mathbf{x};\xi) - g_i^u \leq 0, \, i = 1, \ldots . m, \\ & - \max_{\substack{K_g(\mathbf{x})u=\xi \\ \xi \in \mathbf{U}}} g_i(\mathbf{x};\xi) + g_i^l \leq 0, \, i = 1, \ldots . m, \\ & x_i^l \leq x_i \leq x_i^u, \end{aligned} \tag{4.13}$$

where $g_i(\mathbf{x};\xi)$ are the selected structural performance constraints, g_i^u and g_i^l are upper and lower boundaries respectively.

Solving this problem equals to solving the lower level program with global optimality. In the lower level program, the optimal value of $g_i(\mathbf{x};\xi)$ is acquired under the uncertain load ξ with known resistance leading to a well-defined stiffness matrix $K_g(\mathbf{x})$, which is naturally a function of the current design $\mathbf{x}$.

Let $\zeta = \xi - \xi_{\mathbf{0}}$, and then the ζ runs around the nominal value $\xi_{\mathbf{0}}$ within the boundary of the uncertainty ellipsoid. Thus, for a given design $\mathbf{x}$, we find a combination of the vector ζ to increase the structure's performance. The value of $g_i(\mathbf{x};\xi)$ reflects the resistance ability of the design $\mathbf{x}$ against the uncertainty. By this, the problem can be rewritten as :

$$\begin{aligned} \text{find} \quad & \zeta \in \mathbf{R}^n, \\ \text{minimize:} \quad & -g_j(\mathbf{x};\zeta), \\ \text{subject to:} \quad & \zeta^T B_h \zeta - 1 \leq 0. \end{aligned} \tag{4.14}$$

The selection of different performance constraints would lead to different degrees of difficulty for finding the global optimum. Here the algebraic value of nodal displacement of the node with the maximum displacement of FEM expression of the studied problem is considered as the performance constraints. The expression is:

$$u_x^2 + u_y^2 + u_z^2 = \xi^T (K_g^{-1} d_x d_x^T K_g^{-1} + K_g^{-1} d_y d_y^T K_g^{-1} + K_g^{-1} d_z d_z^T K_g^{-1}) \xi = \xi^T A \xi. \tag{4.15}$$

In Eq.4.15, K_g is the global stiffness matrix, d_i $(i = x,y,z)$ is the vector for which $d_i^T u = u_i$ $(i = x,y,z)$, and u_i are the nodal displacements on the nodes that have the maximum displacement in x,y,z directions. Since $K_g^{-1} d_i d_i^T K_g^{-1} \succeq 0, (i = x,y,z), A \succeq 0$.

Based on the conditions as mentioned above, the robust optimization problem is formed as:

$$\begin{array}{rc} \text{find} & \mathbf{x} = [x_1, x_2, x_3, \ldots, x_n]^T \in \mathbf{R}^n, \\ \text{minimize:} & f(\mathbf{x}), \\ \text{subject to:} & d_l^T K_g^{-1} \xi_{\mathbf{0}} + \sqrt{h(\mathbf{x})} \leq \hat{u}, \\ & x_i^l \leq x_i \leq x_i^u, i = 1,2,...,n. \end{array} \tag{4.16}$$

In the Eq.4.16, $d_l^T K_g^{-1} \xi_{\mathbf{0}}$ is the displacement of the node which owns the maximum displacement under the nominal value of load with design $\mathbf{x}$. The predefined performance in the structure is denoted with $\hat{u}$. The $h(\mathbf{x})$ is the optimal value of the following lower-level program:

$$\begin{array}{rc} \text{find} & \zeta \in \mathbf{R}^n, \\ \text{minimize:} & -(\zeta + \xi_{\mathbf{0}})^T A (\zeta + \xi_{\mathbf{0}}), \\ \text{subject to:} & \zeta^T B_h \zeta - 1 \leq 0. \end{array} \tag{4.17}$$

The Lagrange duality (see section 4.2.2.3) of this lower level problem is:

$$L(\zeta, \lambda) = -(\zeta + \xi_{\mathbf{0}})^T A (\zeta + \xi_{\mathbf{0}}) + \lambda (\zeta^T B_h \zeta - 1), \tag{4.18}$$

where $\lambda \geq 0$ is the Lagrange multiplier. According to the homogenization procedure (see Appendix), Eq.4.18 can be rewritten as:

$$L(\zeta, \lambda) = -\begin{pmatrix} \zeta \\ 1 \end{pmatrix}^T \begin{pmatrix} -A & -A\xi_{\mathbf{0}} \\ sym & -\xi_{\mathbf{0}}{}^T A \xi_{\mathbf{0}} \end{pmatrix} \begin{pmatrix} \zeta \\ 1 \end{pmatrix} + \begin{pmatrix} \zeta \\ 1 \end{pmatrix}^T \begin{pmatrix} \lambda B_h & 0 \\ sym & -\lambda \end{pmatrix} \begin{pmatrix} \zeta \\ 1 \end{pmatrix}. \tag{4.19}$$

As a result, the dual form of Eq. 4.18 is:

$$\begin{array}{rcl} \text{find} & t \in \mathbf{R}, \quad \lambda \geq 0 & \\ \text{minimize:} & -t & \\ \text{subject to:} & \begin{pmatrix} -A+\lambda B_h & -A\xi_0 \\ sym & -\xi_0{}^T A\xi_0 - \lambda - t \end{pmatrix} \succeq 0 \end{array} \tag{4.20}$$

The acquired $\min\{-t\}$ with the condition of the matrix $A \succeq 0$ and $B_h \succeq 0$ is smaller than the global value of the primal problem. The matrix A is obtained by calculating the algebraic value of nodal displacements of the node with the maximum displacements as described in Eq.4.15. The lower-level program is solved as a convex optimization problem, and the upper-level program is realized by the global searching method (In this work, the GA method is applied to do the global searching).

4.2.4 Illustration Example for the 10-bar Truss Structure

The same 10-bar truss structure used in Chapter 3 is examined with the above mentioned RO method. The structural performance constraint is the nodal displacement at node 6, which is $\| u_6 \|^2 = u_{6x}^2 + u_{6y}^2 \leq 5^2$, the uncertainty of the applied load as described by a single ellipsoid, which is $(\xi - \xi_0)^T B_h (\xi - \xi_0) \leq 1$, here the $B_h = \frac{1}{25} I_8$, (I_8 is a unit matrix), and the $\xi_0 = (0,0,0,-1,0,0,0,-1)^T$.

The design variables are the section areas of these bars, and the range of the design variables are: $0.01 \leq a_i \leq 6$, $(i = 1,2,\ldots,10)$.

The corresponding minimum structural weight is 20.819 , and the optimum design is calculated as follows:

Table 4.1: The Acquired Optimum Design with the RO Method

a_1	a_2	a_3	a_4,	a_5
4.352	0.184	3.596	2.632	0.010
a_6	a_7	a_8	a_9,	a_{10}
0.010	0.328	3.458	3.098	0.212

In order to better understand the advantage of the RO method, Fig.4.6 gives the

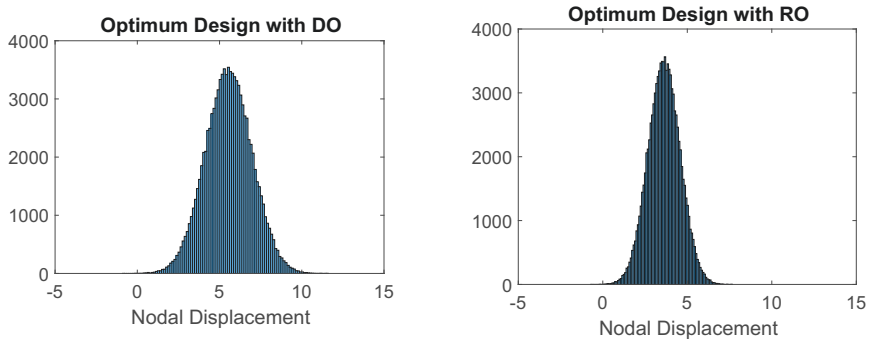

(a) Deterministic Optimization Method (mean= 5.545, var=2.04).

(b) Robust Optimization Method (mean= 3.63, var=0.908).

Figure 4.6: Occurrence Frequency Distribution of Nodal Displacement.

comparison of the occurrence frequency distribution of nodal displacements with the assumption that the loads follow the normal distribution with mean value 1 and standard deviation 0.3. The optimal design acquired by RO method shows better structural performance both on mean value and variance.

4.3 Optimization of Arch Dams with the Robust Optimization (RO) Method

In the sequel, the presented methodology shall be applied to the design of a new arch dam with the following assumptions, provided only for analysis requirements:

- The height of the dam is $140m$,
- 'V' shaped valley.
- The basements on both sides of the valley are assumed to be a rigid foundation.
- The average range of temperature change of air is assumed as $-5.4°C$, the temperature change of the reservoir water is relatively small and assumed

to be $-4.1°C$.

- The water level is assumed as $135m$.

- The lower and upper boundary of the selected design variables for the optimization are assumed according to empirical experiences ([30,35,36]) and are shown in Table 4.2.

Table 4.2: The Upper and Lower Boundaries of Shape Design Variables

$0.5 \leq \alpha \leq 0.9$	$0.3 \leq \beta_1 \leq 0.7$	$0.3 \leq \beta_2 \leq 0.7$
$3 \leq t_1 \leq 10$	$10 \leq t_2 \leq 30$	$15 \leq t_3 \leq 35$
$25 \leq \phi_1 \leq 70$	$25 \leq \phi_2 \leq 70$	$15 \leq \phi_3 \leq 40$
$-2 \leq a_1 \leq 2$	$-2 \leq a_2 \leq 2$	$-2 \leq a_3 \leq 2$

The uncertainty of the applied load is the equivalent nodal force of the load combinations considered in the optimization procedure:

- self-weight
- hydrostatic pressure
- uplift pressure
- temperature load.

The uncertainty of the applied load is expressed as an ellipsoid (see Eq.(4.12), and the range of the uncertainty is assumed to be twice the equivalent nodal force under initial loading conditions. The nominal value of loads and material properties are chosen as initial conditions. According to ([30]), the nominal value of loads and material properties used in the analysis are assumed as given in Table4.3

Table 4.3: Loading Condition and Material Parameters of the Dam Model

Parameters	NominalValue
Air Temperature Variation$(°C)$	5.4
Reservoir Water Temperature Variation$(°C)$	4.1
Water Level (m)	135
Density(kg/m^3)	2400
Young's Modulus(Pa)	$2.1e10$

Table 4.4: Geometrical Parameters of the Optimal Dam Model According to the RO

Height	Thickness(m)	Central Angle$'2\phi'(^\circ)$	Coefficient$'a'$
140	3	123.41	-0.271
120	8.04	117.99	-0.405
105	11.28	112.38	-0.530
90	14.07	105.45	-0.677
75	16.41	97.20	-0.844
55	18.81	84.15	-1.100
35	20.41	68.75	-1.395
20	21.07	55.66	-1.640
0	21.25	36.16	-2.000

Table 4.5: Comparison

	Volume (m^3)	Sum of Displacement (m)	Tensile Stress (MPa)	Von Mises Stress (MPa)
DO	$2.841e+05$	0.01653	1.49	3.15
RO	$4.4173e+05$	0.00987	1.40	2.79

With the conditions as mentioned above, an arch dam model with the RO method and a model with deterministic optimization method are developed to form a comparison (shown in the Fig.4.7). The following Table 4.4 demonstrates the results of the obtained geometrical parameters.

In Fig.4.7 a visual comparison between the different qualities of the two optimized designs can be illustrated. As expected, the RO leads to more conservative designs.

Since the maximum displacement of the arch dam is selected as the performance constraint, the Fig.4.8 and Fig.4.9 show maximum summed displacements of these two arch dam models under the same load situations for deterministic (Fig.4.8) and robust optimization (Fig. 4.9).

Table 4.5 illustrates the details of two optimal arch dams. From the direct comparison, it is demonstrated that the model with RO shows better performance under the same conditions, however, the volume is larger than that acquired through the DO approach.

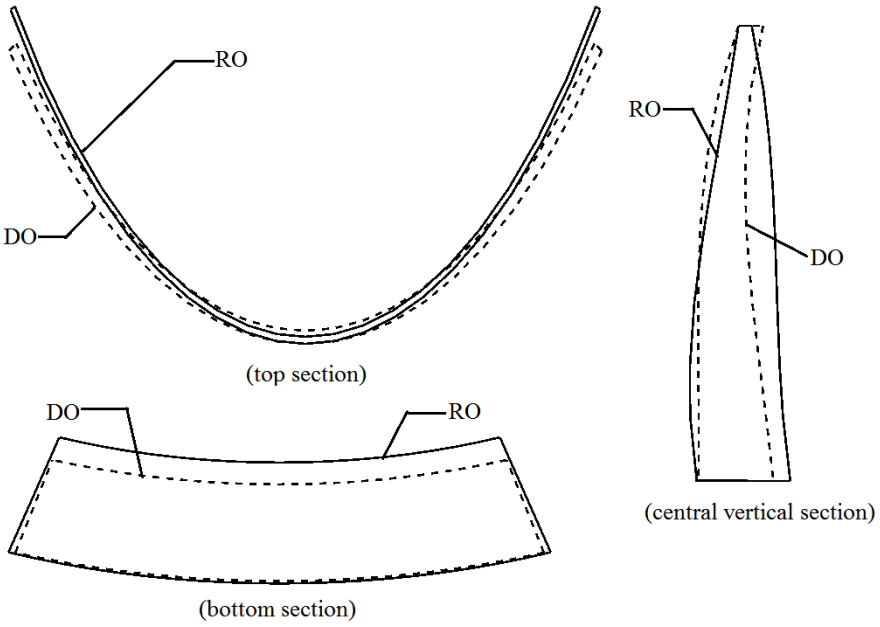

Figure 4.7: Comparison of the Geometries between DO and RO Optimum Design.

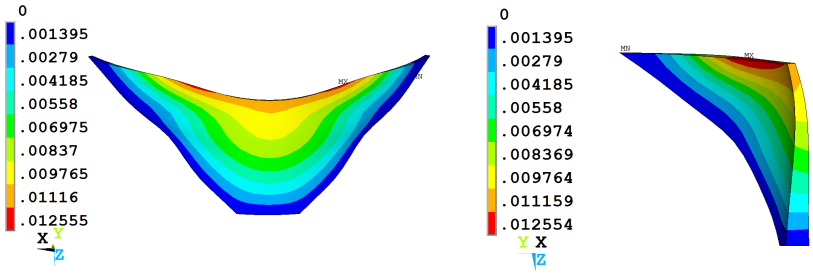

Figure 4.8: The Sum of Displacement (m) of Optimal Arch Dam Based on DO.

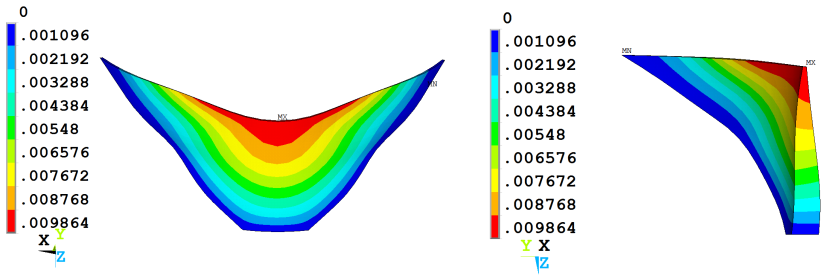

Figure 4.9: The Sum of Displacement (m) of Optimal Arch Dam Based on RO.

Table 4.6: Range of Random Samples

Parameters	Distribution	Variation
Air Temperature Variation($^{\circ}C$)	Uniform	$[4,7]$
Reservoir Water Temperature Variation($^{\circ}C$)	Uniform	$[2,6]$
Water Level (m)	Uniform	$[130,140]$
Density(kg/m^3)	Uniform	$[2200,2600]$
Young's Modulus(Pa)	Uniform	$[1.9e10,2.3e10]$

The question remains regarding the behavior of designed structures under randomly varying loads. Indeed the RO structure behaves more robust, i.e., same variations on the load parameters should lead to changed mean-values and in particular lower variances in the models' responses. Therefore, 200 random load and material property combinations around the nominal values (as shown in Table 4.3) are generated following a range listed in Table 4.6 and the corresponding tensile stresses, von Mises stresses, and the sum of the displacements are recorded. The results are visualized in terms of histograms, see Fig.4.10.

From the Fig.4.10, both mechanical characters of the arch dam realized with RO method show better performances than with the DO methods. The gaps in the tensile stresses and Von Mises stresses are not that clear in comparison to the gap in the sum of displacements, especially the von Mises stresses, it shows little difference between these two dam models. The displacements, however, show a clear difference, and the curve's variation of the RO model is much smaller than the variation of DO model. This situation may be caused by the fact that the sum of displacements are selected as the performance constraint.

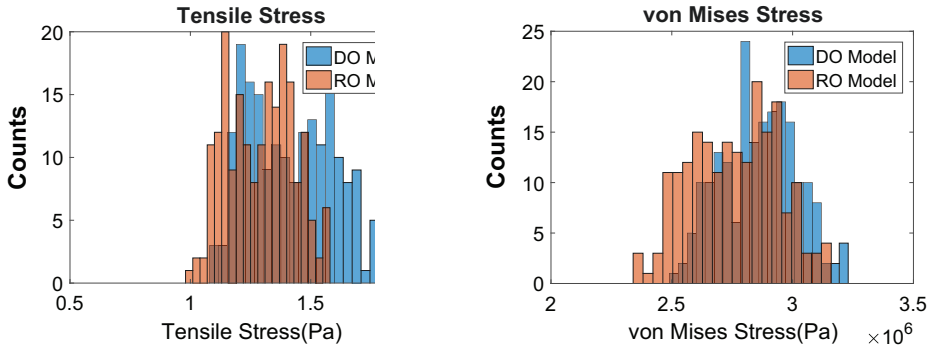

ı von Mises

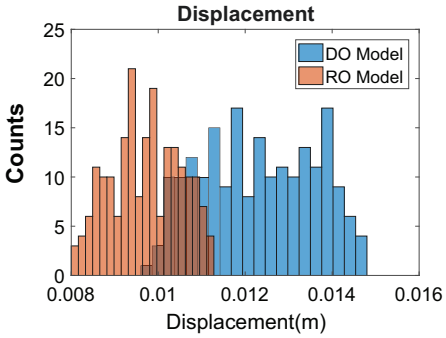

(c) Comparison of the Maximum Sum of Displacements.

Figure 4.10: Comparison of Mechanical Properties between the Arch Dams Acquired with DO Method and RO Method.

Table 4.7: Mean Value of Structural Performance for the Optimal Designs

	Volume (m^3)	Tensile Stress (MP_a)	von Mises Stress (MP_a)	Sum of Displacement (m)
RO	$4.417e5$	1.314	2.816	0.0099
RDO	$3.068e5$	1.466	2.874	0.0122
RBDO	$3.420e5$	1.396	2.973	0.0121
DO	$2.841e5$	1.492	3.304	0.0165

Table 4.8: Standard Deviation of Structural Performance for the Optimal Designs

	Tensile Stress (MP_a)	von Mises Stress (MP_a)	Sum of Displacement (m)
RO	$1.372e5$	$1.546e5$	$7.854e-4$
RDO	$1.271e5$	$1.502e5$	$9.795e-4$
RBDO	$1.893e5$	$1.567e5$	$1.226e-3$
DO	$1.914e5$	$1.586e5$	$1.301e-3$

4.3.1 Comparison of the Optimal Designs of Arch Dams Acquired by the RO, RBDO and RO Method

Both RO, RBDO and RDO methods aim at solving the structural optimization problems, incorporating with the uncertain factors. However, the RO method is based on a non-probabilistic model. The following Fig.4.11-Fig.4.12 show the comparison between the differently optimized arch dams on the structural properties, and the Table 4.7 and Table 4.8 give the conclusions from these structural evaluations.

As can be seen from the figures and tables, the optimal design acquired by RO shows smaller mean values, and the variance is close to the design with RDO. Since the performance constraint in the RO method is displacement, the designed structure performs especially well on it. However, the acquired volume is also much larger than in the two other designs. In other words, the design is acquired by increasing the dam's volume in some way.

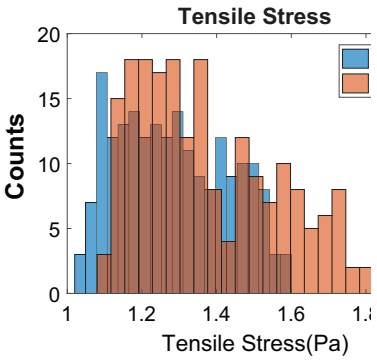

(a) Comparison of Maximum

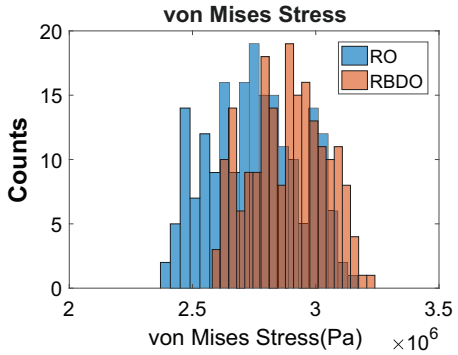

(b) Comparison of Maximum von Mises

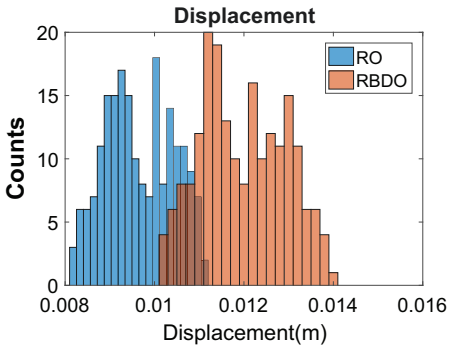

(c) Comparison of the Maximum Sum of Displacements.

Figure 4.11: Comparison of Mechanical Properties between the Arch Dams Acquired with RBDO Method and RO Method.

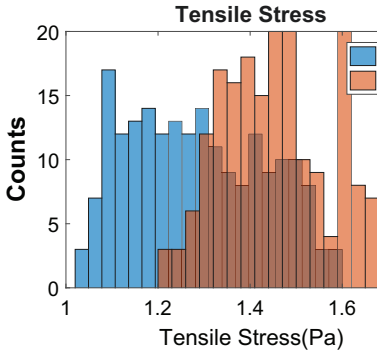

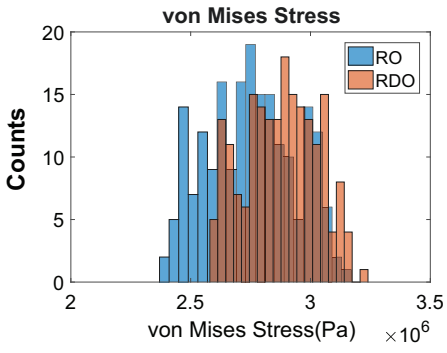

von Mises

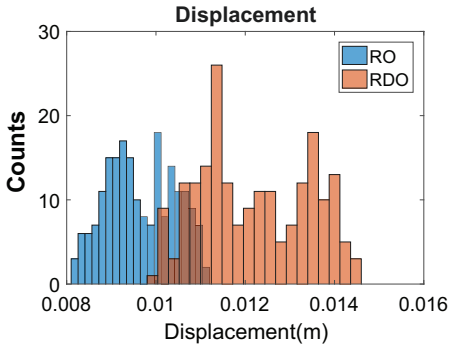

(c) Comparison of the Maximum Sum of Displacements.

Figure 4.12: Comparison of Mechanical Properties between the Arch Dams Acquired with RDO Method and RO Method.

4.4 Conclusion

The task of optimizing an arch-type dam through robust optimization has been solved by the combination of Kriging-based metamodeling and a bi-level semi-defined programming approach, which can be regarded as worst case design optimization. By adopting a 3D Finite Element model of an arch-type dam under load uncertainties, the non-probabilistic robust design is obtained. Comparisons with the results of deterministic optimization show that the RO designs are more robust and will yield more reliable and safe structures. The price to pay is a less effective use of the material. Still, the RO design has visibly improved the efficient use of material than any classical design would propose.

For the further applications of the RO method in engineering designs, some limitations exist and must be solved. The format of the constraints should fulfill specific requirements, which means not all the concerned constraints can be transformed into the required form. Moreover, the analysis is only suitable for simple linear elastic structures. More efforts are still needed to improve the RO method and make it applicable to wider ranges of engineering problems.

Chapter 5

Conclusions

5.1 Summary of Achievements

5.1.1 Comparison of Optimization Methods

Based on the optimal results of the truss structure and the applications into the optimum design of the arch dam, the characteristics of these methods for the arch dam design are concluded as follows:

(a) Deterministic Optimization vs. Uncertainty Based Optimization

The deterministic optimization method is obtained at specific conditions, ignoring that even a small uncertainty in the data can make the optimal solution to the problem completely meaningless. In realistic situations, problems are often unknown in its entirety, giving rise to uncertainties. The reason includes measurement errors, implementation errors, *etc*. With the introduction of uncertainty, the uncertainty based optimization provides the possibility to find an optimal design to cope with the system variations.

(b) Probabilistic Model vs. Non-probabilistic Model

In the probabilistic model, the uncertainties are assumed to obey a known in advance probability distribution. The accuracy of the distribution based on the accuracy of the data information. In most situations, the distribution of the uncertainty data is partially known. This makes the approach of

probability based model less conservative than the non-probabilistic model.

Furthermore, even when the true data obeys some stochastic nature, it is still not easy to identify their distributions in a precise way. Especially for multi-dimensional probability distributions, usually an astronomical number of observations is required. This further increases the difficulty in obtaining the information required to decide on the data distribution. Hence, the probability based model is often forced to operate with oversimplified guesses instead of actual distributions.

The non-probabilistic model in this article adopts the uncertain-but-bounded data model. The possible data information is defined regarding a given perturbation vector varying in a given data set. Compared with the stochastic data model, the data set makes sense without many times specific actions. With the uncertain-but-bounded dataset, we can make predictions on the acceptable probabilistic guarantees.

In the non-probabilistic model, the searching target is directly acquired. Even if the information on the uncertainties is unknown, the results can guarantee the robust properties. In the probability based model, there is no guarantee on the relevance of the stochastic model of uncertainty data. It is difficult to evaluate the influence of the uncertainty information on the whole structural system.

Since the non-probabilistic model remains on the safe side, sometimes the acquired results are too conservative for the design requirements. It will increase more other costs and some unnecessary burden for the structure.

(c) Reliability Based Optimization Design (RBDO) vs. Robust Design Optimization (RDO)

Both reliability-based optimization design and robust design optimization are based on the stochastic model, in which the uncertainty is described by the predefined distributions. However, in the present state of research on these two approaches has revealed the differences of them.

The RBDO method is addressing on offering a quantification of the reliability in the acquired optimum design by minimizing a constrained objective function. The accuracy of the RBDO method hinges on the selected model, data information, *etc*. In the RBDO method, the uncertainty is decided by

a predefined distribution. The availability of detailed statistical inputs is critical to the RBDO. With the introduction of the reliability analysis, the RBDO approach is sensitive to faulty assumptions in the uncertainty inputs. It may lead to results with significant errors in computations of the failure probability if the stochastic model for uncertainty is insufficient.

In the reliability based optimization, the limit state function is used for the calculation of failure probability. In the simulation process, many assumptions are made. It is shown that the changing of any assumptions during the simulation process in reliability analysis, such as material modelings, yield locus, *etc*., would lead to a sizeable mean shift of the simulation response. The mean error will significantly influence the prediction of the failure probability.

The robust design optimization, on the other hand, is less sensitive to model errors when compared with the RBDO approach. For the RDO method, the statistics are less costly to compute for the mean of the objective function, and it becomes more reliable for small sample sizes with limited information on the stochastic inputs.

The objective function of the RDO method is formulated as a multi-criteria optimization problem, in which the minimum standard deviation of this performance is introduced as part of the objective function. The objective function is expressed with a weighted sum of the two design criteria. The weighting factor decides the relative importance of each subpart. Besides, a standard deviation of the original constraint function, which is expressed with a so-called feasibility index, is treated as a constraint condition. With the increase of the feasibility index, the structure shows more feasibility.

The choice of these two methods relies on the real purpose of the optimization study. If the study emphasizes the insensitivity of the structural performance, the RDO method should be adopted. Just minimizing the objective function with the attention on the issue of structural safety in the extreme events favors the use of the RBDO approach. Different selections of methods lead to different optimal designs.

5.2 Outlook

A good structural design not only saves the material, but also provides robust characteristics against all kinds of unexpected situations, and reduces the maintenance costs. In this work, four approaches have been discussed to deal with the uncertainties in the optimization process.

The advantages that exist due to the introduction of uncertainties in the optimization process of the arch dam are highlighted. However, these researches are still far from the expected targets. Further detailed studies must be conducted during future work on the method approach to structural design with uncertainties.

- From the comparison of a non-probabilistic based model and a probabilistic model, we can observe the complementary approaches of how each handles the uncertainties. The stochastic information of uncertainty may work as a guideline for building the uncertain data set for the non-probabilistic model. A further discussion would be considering the combination of these two approaches, to provide a more convenient and efficient result with higher accuracy.

- Comparison with the results of deterministic optimization shows that the RO designs are more robust and will yield more reliable and safer structures. The price to pay is a less effective use of material, yet, the RO design has visibly improved the efficient use of the material.

  For further application of the RO method into engineering designs, there still exists some limitations. The format of the constraints should fulfill specific requirements, which means not all the concerned constraints can be transformed into the required form. Moreover, the analysis is only suitable for simple linear elastic structures. More efforts are still required to improve the RO method and make it applicable to wider ranges of engineering problems.

- Numerical analysis of thermo-hydro- mechanical (THM) coupling problems is an important subject for the arch dam structural safety and stability because of the interactions of these three fields. The thermal expansion and mechanical stress would cause the fractures in the dam body, fluid injection would cause large changes in pressure and temperature, thus affecting

hydraulic properties which would be fractures and pore spaces. Thus the interaction of thermal, hydraulic, and mechanical fields would worsen the structural state, and it is worth well to introduce the THM coupling to the structural analysis.

- So far, the analyses in this work are based on a static model of the arch dam. As we know, the arch dam has outstanding characteristics to withstand earthquakes. However, the seismic analysis of a structure like an arch dam itself is a considerable challenge. It would be even harder to involve uncertainties in the optimization of the arch dam based on a seismic model. To determine a more reliable and efficient way to find the optimum design under uncertainties against the seismic loads would be a challenging but possible in further research.

Appendix A

A.1 Homogenization

Let $\mathbf{Q} \in S^n$, $\mathbf{q} \in \mathbf{R}^n$, and $r \in \mathbf{R}$, then:

$$\begin{pmatrix} \mathbf{x} \\ 1 \end{pmatrix}^T \begin{pmatrix} \mathbf{Q} & \mathbf{q} \\ \mathbf{q}^T & r \end{pmatrix} \begin{pmatrix} \mathbf{x} \\ 1 \end{pmatrix} \succeq 0, \quad \forall \mathbf{x} \in \mathbf{R}^n, \tag{A.1}$$

if and only if:

$$\begin{pmatrix} \mathbf{Q} & \mathbf{q} \\ \mathbf{q}^T & r \end{pmatrix} \succeq 0. \tag{A.2}$$

A.2 S-procedure

For $\mathbf{Q}_i \in S^n$, $\mathbf{q}_i \in \mathbf{R}^n$, $r_i \in \mathbf{R}$, let $f_0(\mathbf{x}), f_1(\mathbf{x}), \ldots, f_m(\mathbf{x})$ be real functions of $\mathbf{x} \in \mathbf{R}^n$ with the form of:

$$f_i(\mathbf{x}) = \begin{pmatrix} \mathbf{x} \\ 1 \end{pmatrix}^T \begin{pmatrix} \mathbf{Q}_i & \mathbf{q}_i \\ \mathbf{q}_i^T & r_i \end{pmatrix} \begin{pmatrix} \mathbf{x} \\ 1 \end{pmatrix} \succeq 0, \quad \forall i = 0, 1, \ldots, m, \tag{A.3}$$

then the implication:

$$f_1(\mathbf{x}) \geq 0, \ldots, f_m(\mathbf{x}) \geq 0, \Rightarrow f_0(\mathbf{x}) \geq 0, \tag{A.4}$$

holds if there exist $\tau_1, \tau_2, \ldots, \tau_m \geq 0$, such that:

$$f_0(\mathbf{x}) \geq \sum_{i=1}^{m} \tau_i f_i(\mathbf{x}) \quad \forall \mathbf{x} \in \mathbf{R}^n. \tag{A.5}$$

A.3 The Lagrange Duality of the lower-level problem

The Lagrange duality of the lower-level problem referring to Chapter.4 is :

$$L(\zeta, \lambda) = -(\zeta + \xi_0)^T A(\zeta + \xi_0) + \lambda(\zeta^T B_h \zeta - 1), \tag{A.6}$$

where λ is the Lagrange multiplier, the corresponding Karush-Kuhn-Tucker(KKT) condition is:

$$\begin{aligned} \nabla_\zeta L(\zeta, \lambda) = -2A(\zeta + \xi_0) + 2\lambda B_h \zeta = 0 \\ \zeta^T B_h \zeta - 1 \leq 0, \quad \lambda \geq 0 \\ (\zeta^T B_h \zeta - 1)\lambda = 0, \end{aligned} \tag{A.7}$$

with the use of homogenization procedure, this can be written as:

$$L(\zeta, \lambda) = -\begin{pmatrix} \zeta \\ 1 \end{pmatrix}^T \begin{pmatrix} -A & -A\xi_0 \\ \text{sym} & -\xi_0^T A \xi_0 \end{pmatrix} \begin{pmatrix} \zeta \\ 1 \end{pmatrix} + \begin{pmatrix} \zeta \\ 1 \end{pmatrix}^T \begin{pmatrix} \lambda B_h & 0 \\ \text{sym} & -\lambda \end{pmatrix} \begin{pmatrix} \zeta \\ 1 \end{pmatrix}. \tag{A.8}$$

The dual function q_d, therefore, is the function of λ.

$$\begin{aligned} q_d(\lambda) &= \inf_{\zeta \in \mathbf{R}^n} L(\zeta, \lambda) = \inf_{\zeta \in \mathbf{R}^n} \begin{pmatrix} \zeta \\ 1 \end{pmatrix}^T \begin{pmatrix} -A + \lambda B_h & -A\xi_0 \\ \text{sym} & -\xi_0^T A \xi_0 - \lambda \end{pmatrix} \begin{pmatrix} \zeta \\ 1 \end{pmatrix} \\ &= \sup\{t \mid L(\zeta, \lambda) \geq t, \forall \zeta \in \mathbf{R}^n\} \\ &\Leftrightarrow \sup\left\{t \mid \begin{pmatrix} -A + \lambda B_h & -A\xi_0 \\ \text{sym} & -\xi_0^T A \xi_0 - \lambda - t \end{pmatrix} \succeq 0\right\}. \end{aligned}$$

References

[1] R. E. Melchers. *Structural Reliability Analysis and Prediction, 2nd edition*. John Wiley & Sons, Inc., USA, 1999. x, xi, 54, 56, 57, 58, 60, 61

[2] S. Sundaresan, K. Ishii, D. R. Houser. A robust optimization procedure with variations on design variables and constraints. *Engineering Optimization*, 24(2):101–117, 1995. xi, 2, 90

[3] S. Boyd and L. Vandenberghe. *Convex Optimization*. Cambridge University Press, New York, 2004. xi, 92, 93

[4] N. Smith. *A History of Dams*. Peter Davies, London, 1971. 1

[5] B. D. Youn and K. K. Choi. A new response surface methodology for reliability-based design optimization. *Computers and Structures*, 82(2-3):241–256, 2004. 2

[6] H. Karadeniz, V. Toğan, T. Vrouwenvelder. An integrated reliability-based design optimization of offshore towers. *Reliability Engineering and System Safety*, 94(10):1510–1516, 2009. 2

[7] H. D. Sherali and V. Ganesan. An inverse reliability-based approach for designing under uncertainty with application to robust piston design. *Journal of Global Optimization.*, 37(1):47–62, 2006. 2, 4, 6, 45

[8] E. Sandgren and T. M. Cameron. Robust design optimization of structures through consideration of variation. *Computers and Structures*, 80:1605–1613, 2002. 2, 5

[9] K. H. Lee and G. J. Park. Robust optimization considering tolerances of design variables. *Cpmputer and Structures*, 79(1):77–86, 2001. 2, 5, 45

[10] K. H. Lee, I. S. Eom, G. J. Park. Robust design for unconstrainrd optimization problems using taguchi method. *AIAA journal*, 34(5):1059–1063, 2001. 2, 45

[11] A. Ben-Tal and L. E. Ghaoui. *Robust Optimization*. MA: Princeton University Press., Princeton and Oxford,, 2009. 2

[12] G. Taguchi. *The System of Experimental Design: Engineering Methods to Optimize Quality and Minimize Cost*. American Supplier Institute, Dearborn, MI, 1987. 2, 78

[13] A. V. Fiacco. *Introduction to Sensitivity and Stability Analysis in Nonlinear Programming*. Academic Press, New York, 1983. 2

[14] J. Sobieski, J. Barthelemy, K. M. Riley. Optimum shape design of arch dams for earthquake loading using a fuzzy inference system and wavelet neural networks. *AIAA Jo11riia*, 20(9):1291–1299, 1982. 2, 13

[15] Proceedings of Design Auromution Conference, ASME Pub. *A RQP based method for estimating parameter sensitivity derivatives*, 1988. 2

[16] G. Sun , G. Li, Z. Gong, X. Cui, X. Yang, Q. Li. Multiobjective robust optimization method for drawbead design in sheet metal forming. *Materials and Design.*, 31(4):1917–1929, 2010. 3, 5, 89

[17] Y. Kanno and I. Takewaki. Sequential semidefinite program for maximum robustness design of structures under load uncertainty. *Journal of optimization theory and Application*, 130(2):265–287, 2006. 3, 6, 89

[18] X. Guo, W. Bai, W. Zhang, X. Gao. Confidence structral robust design and optimization under stiffness and load uncertainties. *Computer Methods in Applied Mechanics and Engineering*, 198(41-44):3378–3399, 2009. 3, 6, 8, 89

[19] A. Ben-Tal and A. Nemirovski. Robust optimization-methodology and applications. *Mathematical Programming*, 92(3):453–480, 2002. 3, 5, 89

[20] A. Ben-Tal and A. Nemirovski. Selected topics in robust convex optimization. *Mathematical Programming.Series B*, 112(1):125–158, 2008. 3

[21] Y. Kanno, M. Ohsaki, N. Katoh. Sequential semidefinite programming for optimization of framed structures under multimodal buckling constraints. *International Journal of Structural Stability and Dynamics*, 1:585–602, 2001. 3

[22] J. L. Serafim. The optimum design of arch dams. *Civil Engineering, ASCE*, 36(2), 1966. 3, 13

[23] M. K. S. Rajan. *Shell Theory Approach for Optimization of Arch Dam Shapes*. PhD thesis, University of California, Berkeley, 1968. 3

[24] G. A. Mohr. Design of shell shape using finite elements. *Computer and Structures*, 10(5):745–749, 1979. 3

[25] R. Sharpe. Design of shell shape using finite elements. *Proc. Institution of Civil Engineers (ICE)*, (7200s):73–98, 1969. 3

[26] R. E. Ricketts and O. C. Zienkiewicz. *Optimization of Concrete Dams*. Quadrant Press, London, England, 1975. 3

[27] K. Wassermann. Three dimensional shape optimizaton of arch dams with prescribed shape function. *Journal of Structural Mechanics*, 11(4):465–489, 1984. 3

[28] A. Fanelli, M. Fanelli, P. Salvaneschi. A neural network approach to the definition of near optimal arch dam shape. *Dam Engineering*, 4(2):123–140, 1993. 3

[29] B. Zhu. Shape optimization of arch dams. *International Water Power and Dam Construction*, 38:43–48, 1987. 3, 40

[30] B. Zhu, B. Rao, J. Jia, Y. Li. Shape optimization of arch dams for static and dynamic loads. *Journal of structural engineering*, 118(11):2996–3015, 1992. 3, 15, 16, 29, 73, 102

[31] J. Pearl. *Heuristics: Intelligent Search Strategies for Computer Problem Solving*. Addison-Wesley Pub. Co., Inc., Reading, MA, United States, 1984. 4

[32] M. Mitchell. *An Introduction to Genetic Algorithms*. MA: MIT Press, Cambridge, 1996. 4

[33] Proceedings of the Sixth International Symposium on Micromachine and Human Science. *A new optimizer using particle swarm theory*, Nagoya, Japan, 1995. 4

[34] A. Afshar, H. O. Bozorg, B. J. Adams, M. A. Mariño. Honey-bee mating optimization (hbmo) algorithm for optimal reservoir operation. *Journal of Franklin Institute*, 344(5):452–462, 2007. 4

[35] S. M. Seyedpoor, J. Salajegheh, E. Salajegheh, S. Gholizadeh. Optimum shape design of arch dams for earthquake loading using a fuzzy inference system and wavelet neural networks. *Engineering Optimization*, 41(5):473–493, 2009. 4, 40, 73, 102

[36] S. Li, L. Ding, L. Zhao, W. Zhou. Optimization design of arch dam shape with modified complex method. *Advances in Engineering Software*, 40(9):804–808, 2009. 4, 13, 40, 102

[37] H. H. Hilton and M. Feigen. Minimum weight analysis based on structural reliability. *Journal of the Aerospace Sciences*, 27(9):641–652, 1960. 4

[38] A. M. Freudenthal and E. J. Gumbel. Safety and the probability of structural failure. *Advances in Applied Mechanics*, 4:117–158, 1956. 4

[39] A. M. Freudenthal and M. Ronay. Second order effects in dissipative media. *The Royal Society*, 294:14–50, 1966. 4

[40] C. A. Cornell. Bounds on the reliability of structural systems. *Journal of the Structural Division*, 93(1):171–200, 1967. 4

[41] D. E. Kinser and F. Moses. Optimum structural design with failure probability constraints. *AIAA Journal*, 5(6):1152–1158, 1967. 4

[42] F. Moses and J. D. Stevenson. Reliability-based structural design. *Journal of the Structural Division*, 96(2):221–244, 1970. 4

[43] B. D. Youn and K. K. Choi. A new response surface mezhodology for reliability-based design optimizatiom. *Computure and Sturctures*, 82(2-3):241–256, 2004. 4, 45

[44] H. Karadeniz, V. Toğan, T. Vrouwenvelder. An integrated reliability-based design optimization of offshore towers. *Reliability Engineering and System Safety*, 94(10):1510–1516, 2009. 4, 45

[45] M. Zhang. *Structural Reliability Analysis: Methods and Procedures*. Science Press Ltd, Beijing, China, 2009. 4

[46] A. M. Hasofer and N. Lind. An exact and invariant first-order reliability format. *Journal of Engineering Mechanics*, 100:111–121, 1974. 4

[47] C. G. Bucher and U. Bourgund. A fast and efficient response surface approach for structural reliability problems. *Structural Safety*, 7(1):57–66, 1990. 4

[48] W. T. Liu and F. Mose. A sequential response surface method and its application in the reliability analysis of aircraft structural systems. *Structural Safety*, 16(1-2):39–46, 1994. 4

[49] L. D. Liaw and R. I. Devries. Reliability-based optimization for robust design. *International Journal of Vehicle Design*, 25(1-2):64–77, 2001. 4

[50] L. P. Chao, M. V. Gandhi, B. S. Thompson. A design for manufactoring methodology for incorporating manufacturing uncertainty in the robust design of fibrous laminated composite structures. *J Composite Mat*, 27(2):175–194, 1993. 5

[51] W. Chen, J. K. Allen, K. Tsui, F. Mistree. A procedure for robust design: minimizing variations caused by noise factors and control factors. *Journal of Mechanical Design*, 118(4):478–485, 1996. 5

[52] A. L. Soyster. Convex programming with set-inclusive constraints and applications to inexact linear programming. *Operations Research*, 21(5):1154–1157, 1973. 5

[53] G. Taguchi. *Taguchi on Robust Technology Development: Bringing Quality Engineering Upstream*. ASME Press, New York, 1993. 5, 78

[54] Y. Ben-Haim and I. E. Elishakoff. *Convex Models of Uncertainty in Applied Mechanics*. Elsevier, New York, 1990. 5, 88

[55] C. P. Pantelides and S. Ganzerli. Design of trusses under uncertain loads using convex models. *Journal of Structural Engineering*, 124(3):318–329, 1973. 5

[56] I. Elishakoff, R. T. Haftka, J. Fang. Structural design under bounded uncertainty optimization with anti-optimization. *Computers and Structures*, 53(6):1401–1405, 1994. 5

[57] M. Lombardi and R. T. Haftka. Anti-optimization technique for structural design under load uncertainties. *Computer Methods in Applied Mechanics and Engineering*, 157(1-2):19–31, 1998. 5

[58] G. Calafiore and L. E. Ghaouib. Ellipsoidal bounds for uncertain linear equations and dynamical systems. *Automatica*, 40(5):773–787, 2004. 5

[59] R. Jin, X. Du, W. Chen. The use of metamodeling techniques for optimization under uncertainty. *Structural and Multidisciplinary Optimization*, 25(2):99–116, 2003. 6, 29

[60] K. H. Lee and G. J. Park. Robust optimization in discrete design space for constrained problems. *AIAA journal*, 40:774–780, 2002. 6

[61] Chair of Risk, Safety & Uncertainty Quantification. *UQLab user manual: Structural Reliability,Report UQLab-V0.9-107*, ETH Zurich, 2015. 6

[62] B. Echard, N. Gayton, M. Lemaire. Structural design under bounded uncertainty optimization with anti-optimization. *Structural Safety*, 33(2):145–154, 2011. 6, 61

[63] L. A. Schmit and B. Farshi. Some approximation concepts for structural synthesis. *AIAA J.*, 12(1):692–699, 1974. 29

[64] G. A. Fenton and D. V. Griffiths. *Risk Assessment in Geotechnical Engineering*. John Wiley & Sons, Inc., New Jersey,, 2008. 29, 74

[65] C. E. Rasmussen and C. K . I. Williams. *Gaussian Processes for Machine Learning*. the MIT Press, Cambridge, 2006. 29

[66] E. H. Vanmarcke. *Random Fields: Analysis and Synthesis.* The MIT Press, Cambridge, 1984. 33

[67] Proc. 2nd Int. Conf. on Vulnerability, Risk Analysis and Management (ICVRAM2014). *UQLab: A framework for uncertainty quantification in Matlab*, Liverpool, United Kingdom, 2014. 33, 76

[68] C. Guo and X. Yang. A programming of genetic algorithm in matlab7.0. *Modern Applied Science*, 5(1):p230, 2011. 35

[69] R. Malhotra, N. Singh, Y. Singh. Genetic algorithms: Concepts, design for optimization of process controllers. *Computer and Information Science*, 4(2):39, 2011. 35

[70] A. R. Parkinson, R. J. Balling, J. D. Hedengren. *Optimization Methods for Engineering Design*. Brigham Young University, Provo, Utah, 2013. 40

[71] F. P. Bernardo and P. M. Saraiva. Robust optimization framework for process parameter and tolerance design. *AIChE Journal*, 44(9):2007–2017, 1998. 45

[72] M. Yu, L. He, L. Song. Twin shear stress theory and its generalization. *SCIENTIA SINICA (Series A)*, 82(28):1174–1183, 1985. 51

[73] A. Parkinson, C. Sorensen, N. Pourhassan. A general approach for robust optimal design. *Transactions of the ASME*, 115:74–80, 1993. 79, 89

Academic Curriculum Vitae

Tan, Fengjie

Institute of Structural Mechanics
Bauhaus-University Weimar
Marienstrasse 15, 99423 Weimar, Germany
Email: fengije.tan@uni-weimar.de

Education

- Ph.D student: Institute of Structural Mechanics, Bauhaus-University Weimar, Germany, 2014-2018.
- M.Sc: Master of Civil Engineering, School of Civil Engineering, Tongji University, China, 2011-2014.
- B.S: Bachelor of Civil Engineering, School of Civil Engineering, Beijing Jiaotong University, China, 2007-2011.

Publications

- Li, N., Tang, B., Tan, F., Xie, L. *Slope stability analysis o earth rock dams based on unified strength criterion by genetic algorithm*. Rock and Soil Mechanics, 34(1):243-249, 2013.
- Li, N. and Tan, F. *Contact searching for higher order and lower order elements based on face-face model*. Journal of Shenyang University of Technology,36(3):328-333, 2014.
- Tan, F., Lahmer, T., Siddappa,M. *Section optimization and reliability analysis of arch-type dams including coupled mechanical-thermal and hydraulic fields*. Proceedings, IKM, Weimar, Germany,2015.
- Tan, F., and Lahmer, T. *Shape optimization based design of arch-type dams under uncertainties*,Engineering Optimization. 50(9): 1470-1482.
- Tan, F., and Lahmer, T. *Shape design of Arch Dam under Load uncertainty with Robust Optimization Method*,Frontiers of Structural and Civil Engineering, Accepted, 2018.